# Cooperative wireless communications in the presence of limited feedback

Stefan Cerovic

▶ **To cite this version:**

Stefan Cerovic. Cooperative wireless communications in the presence of limited feedback. Library and information sciences. Université Paris Saclay (COmUE), 2019. English. NNT : 2019SACLC079 . tel-02330710

**HAL Id: tel-02330710**
**https://theses.hal.science/tel-02330710**

Submitted on 24 Oct 2019

**HAL** is a multi-disciplinary open access archive for the deposit and dissemination of scientific research documents, whether they are published or not. The documents may come from teaching and research institutions in France or abroad, or from public or private research centers.

L'archive ouverte pluridisciplinaire **HAL**, est destinée au dépôt et à la diffusion de documents scientifiques de niveau recherche, publiés ou non, émanant des établissements d'enseignement et de recherche français ou étrangers, des laboratoires publics ou privés.

université PARIS-SACLAY

CentraleSupélec

NNT : 2019SACLC079

Thèse de doctorat

# Cooperative wireless communications in the presence of limited feedback

Thèse de doctorat de l'Université Paris-Saclay
préparée à CentraleSupélec

École doctorale n°580 Sciences et technologies de l'information et de la communication (STIC)
Spécialité de doctorat : réseaux, information et communications

Thèse présentée et soutenue à Gif-sur-Yvette, le 25 Septembre 2019, par

**M. STEFAN CEROVIĆ**

Composition du Jury :

| | |
|---|---|
| M. Samson Lasaulce<br>Directeur de recherche, CNRS | Président |
| M. Didier le Ruyet<br>Professeur, CNAM | Rapporteur |
| Mme Karine Amis<br>Professeur, IMT Atlantique | Rapporteur |
| M. Raymond Knopp<br>Professeur, Eurecom | Examinateur |
| M. Antoine O. Berthet<br>Professeur, CentraleSupélec | Directeur de thèse |
| M. Raphaël Visoz<br>Ingénieur de recherche, Orange Labs | Co-encadrant de thèse |

*In memory of my father.*

# Abstract

A constant need for improved quality of wireless services has pushed the wireless technology and development of wireless networks to the point where they have became an integral part of our modern society. Exploiting an innovative concept such as cooperative communications is one possible avenue for answering the increasingly challenging demands from users, which is the main subject of this thesis. Its principle idea is to allow devices to share their available resources in power and/or bandwidth in order to mutually improve their transmission and reception.

Cooperation techniques have been studied for Multiple Access Multiple Relay Channel (MAMRC), consisted of at least two sources which communicate with a single destination with the help of at least two nodes which perform relaying functions (relaying nodes). A relaying node can be either a dedicated relay, which does not have its own message to transmit, or a source itself, which does have its own message and that can relay the messages of the other sources in some cases. All relaying nodes are assumed to operate in half-duplex mode, while all the channels experience slow (quasi-static) fading. Time Division Multiplexing is assumed. First, the link adaptation algorithm is performed at the scheduler which is located at the destination. Sources transmit in turns in consecutive time slots during the first transmission phase. The second phase consists of a limited number of time slots for retransmissions. In each time slot, the destination schedules a node (being a source or a relay) to transmit redundancies, implementing a cooperative Hybrid Automatic Repeat reQuest (HARQ) protocol. Bidirectional limited control channels are available from sources and relays towards the destination to implement the necessary control signaling of HARQ protocols.

In the first part of the thesis, the focus is on design of centralized scheduling (node selection) strategies for the second phase. The scheduling decisions are made based on the knowledge of the correctly decoded source sets of each node, with the goal to maximize the average spectral efficiency under the given constraint of fairness. A scheduled node uses Joint Network and Channel Coding on its decoded source set.

An information outage analysis is conducted and Monte-Carlo (MC) simulations are performed, which show that these strategies outperform the state of the art one based on the minimization of the probability of the common outage event after each time-slot.

In the second part of the thesis, a slow-link adaptation algorithm is proposed which aims at maximizing the average spectral efficiency under individual QoS targets for a given modulation and coding scheme (MCS) family. The defined utility metric is conditional on the node selection strategy that is used in the second phase. Channel Distribution Information is reported to the destination in order to derive the source rates on a long-term basis, which is adapted to the scenario of fast changing radio conditions. Discrete source rates are first determined using the "Genie-Aided" assumption, which is followed by an iterative rate correction algorithm. The resulting scheduling and link adaptation algorithm yields performance close to the exhaustive search approach as demonstrated by MC simulations. In addition, a fast-link adaptation algorithm is proposed, adapted to the scenario where the CSI of all links is reported to the destination.

In the third part of the thesis, performances of three different cooperative HARQ protocols are compared, with the goal to identify the one which offers the best trade-off between performance and complexity. Incremental Redundancy (IR) HARQ with Single and Multi User encoding are considered, as well as the Chase Combining HARQ with Single User encoding. MC simulations demonstrate that IR-HARQ with Single User encoding offers the best trade-off between performance and complexity for a small number of sources in our setting. Additionally, a practical encoding and decoding scheme is proposed for a scenario where relaying nodes implement Single User encoding, and its performance has been evaluated using MC simulations. The encoding/decoding scheme is based on a turbo code in conjunction with the proposed link adaptation algorithm. The algorithm operates with a family of practical MCSs, where Circular Buffer is implemented to form transmission messages with desired coding rate.

**Keywords**: Centralized scheduling, node selection, slow-link adaptation, iterative rate correction, Multi-Source Multi-Relay Wireless Network, spectral efficiency, chase combining, incremental redundancy, HARQ, turbo code.

# Résumé

Le besoin permanent d'une qualité améliorée des services sans-fil a poussé les réseaux sans-fil à devenir une partie intégrante de notre société moderne. Etant un moyen possible pour répondre aux demandes de plus en plus exigeantes des utilisateurs, le concept innovant des communications coopératives fut le sujet principal de cette thèse. Cette technique consiste à permettre aux terminaux de partager leurs ressources disponibles de puissance et/ou de bande passante afin d'améliorer mutuellement leurs communications (transmission et réception).

Les techniques de coopération ont été étudiées pour un canal multi-accès multi-relais (MAMRC) composé d'au moins deux sources qui communiquent avec une seule destination à l'aide d'au moins deux nœuds qui exécutent la fonctionnalité de relayage (nœuds de relayage). Un nœud de relayage peut être soit un relais dédié, qui ne possède pas son propre message à transmettre, soit une source elle-même, qui possède son propre message et qui peut, dans certains cas, relayer les messages des autres sources. Tous les nœuds de relayage sont supposés fonctionner en mode semi-duplex et tous les canaux subissent un évanouissement lent (quasi-statique). Le multiplexage par répartition dans le temps est supposé. Tout d'abord, l'algorithme d'adaptation de lien est exécuté par l'ordonnanceur situé à la destination. Durant la première phase de transmission, les sources transmettent chacune à leur tour leur message respectif pendant des intervalles de temps dédiés chacun à une source. La deuxième phase se compose d'un nombre limité d'intervalles de temps consacrés pour les retransmissions. Dans chaque intervalle de temps, la destination planifie un nœud (que ce soit source ou relais) pour transmettre les redondances, mettant en œuvre un protocole coopératif d'Hybrid Automatic Repeat reQuest (HARQ). Des canaux de contrôle limités bidirectionnels sont disponibles depuis les sources et les relais vers la destination afin de permettre la signalisation nécessaire pour les protocoles HARQ.

Dans la première partie de la thèse, l'accent est mis sur la conception d'une stratégie d'ordonnancement centralisé (sélection des nœuds) nécessaire pour la deuxième phase de transmission. Les décisions d'ordonnancement sont prises en fonction

de la connaissance des ensembles de sources correctement décodées par chaque noeud et ayant comme objectif de maximiser l'efficacité spectrale moyenne sous une contrainte d'équité. Le nœud planifié utilise le codage conjoint du réseau et du canal sur son ensemble de sources décodées. L'analyse de la probabilité de coupure de l'information ainsi que les simulations Monte-Carlo (MC) montrent que ces stratégies sont plus performantes que celles de l'état de l'art basées sur la minimisation de la probabilité de coupure commune après chaque intervalle de temps.

Dans la seconde partie de la thèse, un algorithme d'adaptation de lien lent est proposé afin de maximiser l'efficacité spectrale moyenne sous contrainte de vérification d'une qualité de service individuelle cible pour une famille donnée de schémas de modulation et de codage (MCS). La métrique utilitaire définie dépend de la stratégie de sélection de nœud utilisée dans la deuxième phase. L'information sur la distribution des canaux est transmise à la destination afin d'en déduire les débits des sources à long terme tout en s'adaptant au scénario de l'évolution rapide des conditions radio. Les débits des sources discrets sont déterminés en utilisant l'approche "Genie-Aided" suivie d'un algorithme itératif de correction de débit. Les simulations MC montrent que l'algorithme d'ordonnancement et d'adaptation de lien proposé permet d'obtenir des performances proches de celles de la recherche exhaustive. De plus, un algorithme d'adaptation de lien rapide est proposé, adapté au scénario dans lequel le CSI de tous les liens est signalé à la destination.

Dans la troisième partie de la thèse, les performances de trois différents protocoles HARQ coopératifs sont comparées dans le but d'identifier celui qui offre le meilleur compromis entre la performance et la complexité. L'HARQ à redondance incrémentale (IR) avec codage mono et multi-utilisateur est pris en compte ainsi que l'HARQ type Chase Combining avec codage mono-utilisateur. Les simulations MC montrent que le IR-HARQ avec codage mono-utilisateur offre le meilleur compromis entre performance et complexité pour le scénario considéré avec un faible nombre de sources. En outre, un schéma pratique de codage et de décodage est proposé pour un scénario où les nœuds de relayage utilisent le codage mono-utilisateur et sa performance est évaluée par des simulations MC. Le schéma de codage/décodage est basé sur un code turbo ainsi que sur l'algorithme d'adaptation de lien proposé. Cet algorithme fonctionne avec une famille de MCS pratiques, où Circular Buffer est implémenté afin de générer les messages de transmission avec le débit de codage souhaité.

**Mots-Clés**: Ordonnancement centralisé, sélection de nœud, adaptation de lien lente, correction itérative du débit, réseaux sans-fil multi-source multi-relais, efficacité spectrale, chase combining, redondance incrémentale, HARQ, code turbo.

# Acknowledgment

It would not be possible to complete my Ph.D. journey without the selfless help and huge support of different people, who I would like to kindly thank by using this opportunity. Firstly, I would like to express my sincere gratitude to Professor Antoine O. Berthet for accepting to be my supervisor, for his support, responsiveness and all the useful discussions that we have had during the last three years. The rigorousness of his work, as well as his passion for the research have been inspirational to me. Besides, I was very privileged to have Doctor Raphaël Visoz as my co-supervisor, who I cannot thank enough. Exchanges of the ideas and discussions that we have had almost on a daily basis were essential for my progress. His human qualities, as well as his pedagogy and patience have made working with him a real pleasure, which allowed me to learn so much from the unique combination of his scientific expertise and his awareness of the needs from an industry standpoint.

I am deeply grateful to all the jury members for taking interest in my work. I was honoured to have Professor Samson Lasaulce as the jury president, Professor Didier Le Ruyet and Professor Karine Amis as reviewers, who I especially thank for their valuable review of my manuscript, and Professor Raymond Knopp as an examiner. Their relevant comments and questions during the Ph.D. defense have further opened my eyes in this field and will serve as a solid basis for my future work.

I could hardly imagine better team atmosphere to work in than the one which I have had in RAP team (formerly known as RIDE) in Orange Labs, where I have spent the majority of my time. I have been warmly welcomed since the day one, and I would like to thank to all its current and former members for their support and pleasant discussions that we have had, both technical and less formal ones. I am truly grateful to the team manager Pierre Dubois for his continuous support and understanding during the whole duration of my Ph.D., including the most difficult moments of my personal life, and for having the confidence in me. Particular thanks go to my Ph.D. colleagues Rita and Thomas for their support

and help which came in many forms over the years, and for all the fun moments that we have spent together. I am also very thankful to Louis Madier for helping me at the beginning of my Ph.D. to grasp this challenging subject more easily, and for all the advices and ideas that he has shared with me.

It is hard to put into words the importance of my family: my late father Zoran to whom I dedicate this thesis, mother Mira, brothers Danilo and Nikola, and my wife Marija. Your unconditional love, support, and belief in me have driven me forward during all this time (and much earlier), so this thesis is also yours. Thank you for everything. Particular understanding and patience was needed by my wife, for which I am eternally grateful.

# Contents

**Abstract** i

**Résumé** iii

**Acknowledgment** v

**Acronyms** ix

**Notations** xiii

**List of Figures** xiv

**List of Tables** xvi

**1 Introduction** 1
- 1.1 Cooperative communications . . . . . 1
- 1.2 Motivation and scope of the thesis . . . . . 11
- 1.3 Thesis contributions and outline . . . . . 14

**2 System Model** 19

**3 Node Selection Strategies** 25
- 3.1 Performance metric and outage events . . . . . 25
- 3.2 Cooperative HARQ retransmission strategies . . . . . 28
- 3.3 Novel HARQ control information exchange procedure . . . . . 31
- 3.4 Numerical results . . . . . 33

**4 Link Adaptation Algorithms** 39
- 4.1 Slow-link adaptation algorithm . . . . . 39
- 4.2 Fast-link adaptation algorithm . . . . . 47
- 4.3 Numerical results . . . . . 50

**5 Cooperative HARQ Protocols** **65**
5.1 Outage definitions of different cooperative HARQ protocols . . . . . 65
5.2 Practical coding scheme design . . . . . 72

**6 Conclusion and Perspective** **89**
6.1 Conclusion . . . . . 89
6.2 Perspectives . . . . . 91

**Appendices** **94**
A Sub-block interleaver . . . . . 95
B Mutual information calculation for discrete i.i.d. inputs . . . . . 96

**List of Publications** **99**

**Bibliography** **101**

# Acronyms

| | |
|---|---|
| **AF** | Amplify-and-Forward |
| **APP** | A Posteriori Probability |
| **ARQ** | Automatic Retransmission ReQuest |
| **AWGN** | Additive White Gaussian Noise |
| **BC** | Broadcast Channel |
| **BCJR** | Bahl Cocke Jeinek Raviv |
| **BER** | Bit Error Rate |
| **BGFNC** | Binary Galois Field Network Code |
| **BI-XOR** | Bit-Interleaved XOR |
| **BLER** | BLock Error Rate |
| **BPSK** | Binary Phase-Shift Keying |
| **CBR** | Coded Bi-directional Relaying |
| **CC** | Chase Combining |
| **CDI** | Channel Distribution Information |
| **CF** | Compress-and-Forward |
| **CoF** | Compute-and-Forward |
| **CRC** | Cyclic Redundancy Check |
| **CSI** | Channel State Information |
| **DDF** | Dynamic Decode-and-Forward |

| | |
|---|---|
| **DF** | Decode-and-Forward |
| **DMT** | Diversity-Multiplexing Trade-off |
| **DP** | Dynamic Programming |
| **D-SDF** | Dynamic Selective Decode-and-Forward |
| **EM** | ElectroMagnetic |
| **FEC** | Forward Error Correction |
| **HARQ** | Hybrid Automatic Repeat reQuest |
| **IAB** | Integrated Access and Backhaul |
| **IR** | Incremental Redundancy |
| **JNCC** | Joint Network-Channel Coding |
| **JNCD** | Joint Network Channel Decoding |
| **LDPC** | Low Density Parity Check |
| **LLR** | Log-Likelihood Ratio |
| **LTE** | Long-Term Evolution |
| **MABC** | Multiple Access Broadcast |
| **MAC** | Multiple Access Channel |
| **MAF** | Multiple-access Amplify-Forward |
| **MAMRC** | Multiple Access Multiple Relay Channel |
| **MAP** | Maximum a Posteriori |
| **MARC** | Multiple Access Relay Channel |
| **MC** | Monte-Carlo |
| **MCS** | Modulation and Coding Scheme |
| **MDP** | Markov Decision Process |
| **MDS** | Maximum Distance Separable |
| **MRC** | Maximum Ratio Combining |

**NBGFNC** Non-Binary Galois Field Network Code

**NOMA** Non-Orthogonal Multiple Access

**NOMARC** Non-Orthogonal Multiple Access Relay Channel

**NOMAMRC** Non-Orthogonal Multiple Access Multiple Relay Channel

**NR** New Radio

**OMA** Orthogonal Multiple Access

**OMAMRC** Orthogonal Multiple Access Multiple Relay Channel

**PCCC** Parallel Concatenated Convolutional Code

**PMF** Probability Mass Function

**PNC** Physical-Layer Network Coding

**QAM** Quadrature Amplitude Modulation

**QMF** Quantize-Map-and-Forward

**QPSK** Quadrature Phase Shift Keying

**RBC** Relay Broadcast Channel

**RC** Relay Channel

**RCLDPC** Rate Compatible Low-Density Parity-Check

**RCTC** Rate-Compatible Turbo Codes

**RSC** Recursive Systematic Convolutional

**SC** Selection Combining

**SDF** Selective Decode-and-Forward

**SI** Self-Interference

**SIC** Self-Interference Cancellation

**SISO** Soft-In Soft-Out

**SNCC** Separate Network-Channel Coding

**SNCD** Separate Network-Channel Decoding

**SNR** Signal-to-Noise Ratio

**TDBC** Time Division Broadcast

**TWRC** Two-Way Relay Channel

# Notations

| | |
|---|---|
| $\mathbb{C}$ | Set of complex numbers |
| $\mathcal{S}$ | A finite countable set |
| $\mathbf{x}$ | A vector |
| $\mathbf{X}$ | A matrix |
| $\mathbb{E}\{.\}$ | The expected value |
| $\lceil . \rceil$ | The ceiling function |
| $[P]$ | The Iverson bracket having the value 1 if condition $P$ is satisfied, and 0 otherwise |
| $\emptyset$ | The empty set |
| $\lvert\mathcal{S}\rvert$ | Cardinality of set $\mathcal{S}$ |
| $\Pr\{\mathcal{E}\}$ | Probability of event $\mathcal{E}$ |
| log | Logarithmic function |
| exp | Exponential function |
| $\mathcal{A} \cup \mathcal{B}$ | Union of sets $\mathcal{A}$ and $\mathcal{B}$ |
| $\mathcal{A} \cap \mathcal{B}$ | Intersection of sets $\mathcal{A}$ and $\mathcal{B}$ |
| $\mathcal{A} \setminus \mathcal{B}$ | Difference of sets $\mathcal{A}$ and $\mathcal{B}$ |
| $\mathcal{A} \subseteq \mathcal{B}$ | Set $\mathcal{A}$ is a subset of set $\mathcal{B}$ |

# List of Figures


2.1 Orthogonal Multiple Access Multiple Relay Channel (OMAMRC) with feedback. . . . . 20
2.2 Transmission of a frame: the initial, the first and the second phase. . . 21
2.3 Control information exchange procedure at the beginning of each time-slot in the second phase. . . . . 23

3.1 Control information exchange procedure at the beginning of each time-slot in the second phase. . . . . 32
3.2 Average spectral efficiency of different strategies for symmetric rates equal to $R = 1[b.c.u]$, and symmetric links scenario. . . . . 34
3.3 Average spectral efficiency of different strategies with slow link adaptation and symmetric link scenario. . . . . 35
3.4 Average spectral efficiency of different strategies for asymmetric rates $[R_{s_1} = 3, R_{s_2} = 2.5, R_{s_3} = 2]$[b.c.u], and asymmetric link scenario. . . . 37

4.1 "Genie-Aided" assumption, where all the sources except for source $s_1$ are assumed decoded correctly at the destination. . . . . 42
4.2 Average spectral efficiency that corresponds to different slow-link adaptation algorithms s.t. $BLER^{(1)}_{\text{QoS}}$ target. . . . . 53
4.3 Allocated rates to sources for different slow-link adaptation algorithms s.t. $BLER^{(1)}_{\text{QoS}}$ target. . . . . 54
4.4 Average spectral efficiency that corresponds to the proposed slow-link adaptation algorithm for different scenarios s.t. $BLER^{(1)}_{\text{QoS}}$ target. . . . 55
4.5 Convergence analysis of the proposed slow-link adaptation algorithm s.t. $BLER^{(1)}_{\text{QoS}}$ target. . . . . 56
4.6 Average spectral efficiency that corresponds to different slow-link adaptation algorithms s.t. $BLER^{(2)}_{\text{QoS}}$ target. . . . . 57
4.7 Allocated rates to sources for different slow-link adaptation algorithms s.t. $BLER^{(2)}_{\text{QoS}}$ target. . . . . 58
4.8 The highest individual BLock Error Rate (BLER) among sources for different slow-link adaptation algorithms s.t. $BLER^{(2)}_{\text{QoS}}$ target. . . . . 59

4.9 Average spectral efficiency that corresponds to the proposed slow-link adaptation algorithm for different scenarios s.t. $BLER^{(2)}_{\mathrm{QoS}}$ target. . . . 60
4.10 Average spectral efficiency that corresponds to different fast-link adaptation algorithms. . . . 61
4.11 Average number of iterations needed by the iterative rate correction algorithm for fast-link adaptation to converge. . . . 62
4.12 Average spectral efficiency that corresponds to the proposed fast-link adaptation algorithm for different scenarios. . . . 63

5.1 Allocated rates to sources for different Hybrid Automatic Repeat reQuest (HARQ) protocols for asymmetric link configuration in (3,3,1)-OMAMRC. 69
5.2 Average spectral efficiency obtained by using different HARQ protocols for asymmetric link configuration in (3,3,1)-OMAMRC. . . . 70
5.3 Average spectral efficiency obtained by using different HARQ protocols for asymmetric link configuration in (4,3,1)-OMAMRC. . . . 71
5.4 Average spectral efficiency obtained by using different HARQ protocols for asymmetric link configuration in (5,3,1)-OMAMRC. . . . 72
5.5 Average spectral efficiency obtained by using different HARQ protocols for symmetric link configuration and different OMAMRC. . . . 73
5.6 Turbo code encoding scheme. . . . 75
5.7 Link adaptation using circular buffer technique. . . . 76
5.8 Demodulation, demultiplexing and deinterleaving at the receiver. . . . 78
5.9 Turbo code decoding scheme. . . . 84
5.10 BER performance of proposed turbo coding scheme for $\mathrm{MCS}_1$ and $\mathrm{MCS}_8$. 86
5.11 Allocated MCSs to different sources as a function of $\gamma$, in terms of corresponding spectral efficiencies. . . . 87
5.12 Total average spectral efficiency obtained for (3,3,1)-MAMRC with 3 retransmissions and no user co-operation. . . . 88

# List of Tables

5.1 Average SNR of the links between all sources. . . . . 68
5.2 Candidate MCSs. . . . . 85

A.1 Inter-column permutation pattern for sub-block interleaver. . . . . 96

# 1 | Introduction

## 1.1 Cooperative communications

Over the past two decades, wireless networks have progressively became an integral part of our modern society. An ever-increasing demand for higher quality and availability of wireless services, as well as a constant need for new ones, have led to rapid enhancement of wireless technologies and growth of their serving areas. Mobile cellular networks are probably the most noteworthy example of wireless networks, number of their unique users expecting to reach 75% of the global population by the year 2020. Today, ubiquitous connectivity along with minimum quality of service provided is anticipated in such networks: users want to have the access to the offered services whatever the location and the time, while having very high data rates, small response time etc. Although convenient for their use, wireless networks impose quite big challenges by their nature when it comes to their design. Random effects resulting from the wireless propagation environment, mutual interference between different users, scarce frequency spectrum, limited number of antennas and computational capabilities of devices are only some of them. One possible avenue for overcoming those challenges is to allow devices to share their available resources in power and/or bandwidth, as well as their antennas, in order to mutually enhance their transmission and reception.

### 1.1.1 Single Relay Channel and Relaying Protocols

The approach of sharing available resources in power and/or bandwidth has given rise to the concept of *cooperative communications*, which is the main focus of this thesis. In scientific community, this research topic has been present for several decades, and is still very active to the present date. It remains very promising to increase the spectral and power efficiency of future wireless networks, as well as their coverage. Fundamental principles and general problems of cooperative

communications are introduced by van der Meulen [1, 2], where the three-terminal Relay Channel (RC) is studied (consisted of a source, a relay and a destination), and for which upper and lower bounds on the capacity are given. A relay channel was also studied by Satō[3], where the outer bounds for capacity are derived. Probably the most remarkable work on relaying, even until today, is published by Cover and El Gammal in 1979, [4]. The key idea is that the relay can use the overheard transmission from the source to form its own transmission that aids in decoding at the destination. It is assumed that the relay operates in *half-duplex* mode, meaning that it cannot receive and transmit either (i) at the same time, or (ii) in the same frequency band. The capacity is established for degraded, reversely degraded and feedback relay channels, where the min-cut max-flow capacity upper bound was used, defined in [5] (see also [6, 7]). Moreover, the achievable lower bound, as well as a tight upper bound to the capacity of the general relay channel are derived. Most of these results have still not been surpassed up until today. Structurally different random coding schemes presented in this work have given rise to two well-known relaying protocols: Decode-and-Forward (DF), and Compress-and-Forward (CF). In DF relaying protocol (referred to as "cooperation scheme" in [4]), the relay decodes the source message and cooperates with the source to help the destination in decoding. In CF relaying protocol (referred to as "observation scheme" in [4]), which is also known as Observe-and-Forward [8], Estimate-and-Forward or Quantize-and-Forward [9], the relay transmits an estimate (or quantized version) of its observation of the source signal to the destination. The idea is that relays use source coding proposed in [10, 11] in order to exploit side information at the destination. An extension of the CF coding scheme for the relay channel, targeted for general multi-message noisy networks, was presented in [12]. Finally, in [4], cooperation and observation schemes were combined in a single coding scheme in order to maximize the achievable rates.

Partial Decode-and-Forward relaying protocol is a variant of DF protocol where the relay decodes only a part of the transmitted source's message, and forward it to the destination instead of decoding the whole message [4, 13]. DF and CF belong to the category of nonlinear (regenerative) relaying protocols. Other commonly used protocols in literature that belong to the same category are Compute-and-Forward (CoF) [14 – 16] and Quantize-Map-and-Forward (QMF) [17]. CoF relaying protocol can be used in networks consisted of more than one source, where the relays decode linear equations of the transmitted messages using the noisy linear combinations provided by the channel. QMF can be seen as another "network generalization" of CF, where each relay quantizes the received signal at the noise level and maps it to a random Gaussian codeword for forwarding, and the final destination decodes the source's message based on the received signal. On the other hand, the most famous example of the category of linear relaying protocols is

certainly Amplify-and-Forward (AF) [8], where the relay simply transmits a scaled version of the received signal. This relaying protocol can be viewed as repetition coding from two separate transmitters, except that the relay transmitter amplifies its own receiver noise.

Single relay channel (with single source and single destination) has further been analysed in [13, 18 – 27]. Generally speaking, it is not trivial to extend relaying to wireless media. Error-prone communication links due to *fading* and *noise* constitute a first issue to cope with. The second issue is *signal superposition* at the relays and destination, which comes as a natural consequence of the *broadcast property*, and substantially complicates the design, analysis and optimization of cooperative protocols. For wireless (Rayleigh fading) relay channels new capacity bounds are given in [18, 19, 24, 25], while semideterministic relay channel is studied in [13]. Other contributions include power allocation strategies [19, 25], and some results on *full-duplex* relaying [18, 19]. Full-duplex relays are able to transmit and receive at the same time and in the same frequency band. However, due to practical constraints, that assumption is considered unrealistic even today, so most of research papers still consider half-duplex relays only. Some novel information-theoretic random coding schemes are proposed in [26, 27], which can be seen as an extension of work in [4]. In [18, 19, 22, 24, 25], some of the earlier mentioned relaying protocols have been compared in terms of performance, where no decisive conclusion can be made as different protocols can be regarded as the most suitable for different scenarios.

### 1.1.2 Multiple Relay Channel

Natural extension of the previous model is a multiple relay channel, consisted of more than one relay, single source and single destination (also known as a relay network), which has also grabbed a significant attention of the research community, e.g. in [6, 18, 23, 24, 28 – 31]. Rather than using conventional forms of space diversity with physical arrays, the basic principle here is to exploit space diversity using a collection of distributed antennas belonging to multiple terminals, thus forming a "virtual array" through distributed transmission and signal processing [32, 33]. In [6], it is demonstrated that the max-flow min-cut interpretation for the capacity expressions given in [4] can also be found for fairly general classes of discrete memoryless relay networks. Novel achievable rates and capacity upper bounds along with corresponding information-theoretic coding schemes are presented in [18, 23], where different types of discrete memoryless and fading channels were considered. New relaying protocols such as Non-orthogonal Amplify-and-Forward, Dynamic Decode-and-Forward (DDF) [24], and *Opportunistic relaying* [28] are introduced

and evaluated in terms of achieved Diversity-Multiplexing Trade-off (DMT) [34]. The authors in [29] have studied large Gaussian relay networks and identified the scenarios where the upper and lower bound on the capacity coincide in the limit as the number of relays tends to infinity. The power efficiency of sensory and ad-hoc networks is studied in [30], with relaying protocol similar to AF being used. In [31], multiple parallel relay channel is studied where relays operate in full-duplex mode and cannot communicate between themselves. There, generalized AF, DF, generalized Partial DF and "linear relaying" protocols have been compared in terms of achievable rates for different network geometries and number of relays.

### 1.1.3 User Cooperation

Cooperation in wireless multihop networks has been the subject of intensive research and abundant literature since the early 2000s. Sendonaris et al. have introduced the concept of *user cooperation* (also known as "cooperative diversity" in [8, 32, 33]) as a new method to create diversity in the uplink of a cellular system [35, 36] and show its benefit under some of the various performance metrics used in time-varying fading environments, namely outage probability [37], capacity-versus-outage [38], diversity gain, multiplexing gain, and the diversity-multiplexing trade-off. Amongst the following key contributions in this research area are those of Laneman et al. [8, 32, 33] addressing the performance of several relaying protocols in wireless environments. Another interesting relaying protocol coined "coded cooperation" has been proposed and analysed in detail in [39–43]. Its main principle is to integrate cooperation into channel coding by partitioning the codewords of each mobile (source) and transmitting portions of each codeword through independent fading channels. Additionally, it is demonstrated in which scenarios does it outperform DF and AF with repetition coding.

### 1.1.4 Multiple Access Relay Channel

Another important class of relay channels is Multiple Access Relay Channel (MARC) consisted of multiple sources which do not cooperate, single relay and single destination. This model might fit a situation where the sources are too weak to cooperate (like in sensor networks for example), but they can send their data to more powerful nodes that form a "backbone" network [18]. MARC is introduced in [44], where the capacity upper bound is derived for both Gaussian and discrete memoryless channel, and the achievable rates were given for Gaussian MARC. Novel coding schemes and tighter capacity bounds were proposed in [45] for DF, CF and AF relaying protocols, as well as in [18] for DF relaying protocol and

different wireless channels. In [46], MARC was studied in the context of three-tier hierarchical wireless sensor networks where the capacity bounds were given for both scenarios with half and full duplex relays, together with DF, partial DF and CF relaying protocols. New linear relaying protocol named Multiple-access Amplify-Forward (MAF) was proposed and analysed in [46], where it is shown that it achieves the optimal diversity-multiplexing trade-off at high multiplexing gains. DDF relaying protocol has also been studied for this type of channel [47 – 49], where the relays cooperate as soon as they correctly decode all the packets of the sources. DMT has been studied, where it was shown that DDF is optimal at low multiplexing gain, while the outage events have been defined for the scenario of fixed transmission rates.

### 1.1.5 Relay Broadcast Channel

Relay Broadcast Channel (RBC), composed of a source, a relay and two destinations (sinks), is introduced as the natural counterpart of the MARC in [18] and analysed for the same scenarios. In [50], the same channel is referred to as *Dumb Relay Broadcast Channel*, for which the capacity region is found, as well as for the *Partially Cooperative Relay Broadcast Channel*, both being considered as the extensions of a two user degraded broadcast channel. In Partially Cooperative RBC, one user serves both as a user and a relay for the other user (there is no additional relay). In Fully Cooperative RBC [51], both users serve as relays for each other. New capacity regions for both Gaussian and discrete memoryless variants of Fully and Partially Cooperative RBC with DF were proposed in [52, 53], for the cases where the feedback channel is either available or not. The extension to the case of multiple receivers is provided in [54], while new coding schemes (decoding in particular) for Partially Cooperative RBC and corresponding achievable rate regions were proposed in [55]. In [56], the Multiple Access Channel (MAC) - Broadcast Channel (BC) duality known for conventional one hop Gaussian channel was found to be applicable to multiple hop communication over AF relay networks where direct channel is not available between a source and a destination. For two-hop parallel AF relay MAC, assuming a sum power constraint across all relays, the optimal relay amplification factors were found, as well as the resulting optimal rate regions.

### 1.1.6 Network Coding

Network coding, initially proposed by Ahlswede et al. in [57] for the graphical networks, is a powerful paradigm where intermediate nodes in a network are allowed not only to store and route but also to perform algebraic operations on the

incoming data flows. A graphical network is a weighted directed acyclic/cyclic graph modelling physically separated point-to-point communication links in the absence of noise and interference. The max-flow min-cut upper bound on the capacity of single or multi-packets multi-cast graphical networks is provably achieved by network coding under the condition that all the destinations should decode all the packets. The proof of achievability is done using random network coding (possibly nonlinear). An important class of network codes are *linear* network codes, characterized by a simple implementation of encoding and decoding in practice. There, a block of data is treated as a vector over a certain base field, and it is allowed to the node to apply a linear transformation to that vector before passing it on [58]. In [58, 59], linear network codes are shown to achieve the same max-flow capacity as random network codes for a multicast network consisted of a source and multiple sinks (with lossless links). However, in [60] it is shown for multicast graphical networks where each destination does not demand all of the source's messages that there are no linear solutions. In [61, 62], it is proved that a distributed random linear network coding approach asymptotically achieves capacity, as given by the max-flow min-cut bound of [57], in multisource multicast networks. A general bound on the success probability of such codes for arbitrary networks is also given, showing that the error probability decreases exponentially with code length.

The principle of network coding has given rise to the relaying protocol called Physical-Layer Network Coding (PNC) [63, 64], which makes use of a broadcast nature of wireless networks by dealing with ElectroMagnetic (EM) signal reception and modulation at the physical layer. A critical process at the relay is to transform the superimposed channel-coded packets received from the two end nodes (plus noise) to the network-coded combination of the source packets.

### 1.1.7 Two-Way Relay Channel

Two-Way Relay Channel (TWRC) has also captured significant interest of the research community [65 – 79], especially since it is regarded as a primary example of the use of *network coding* in wireless networks [80]. In TWRC, two users exchange independent informations in the presence of one relay, which applies network coding on received messages [65]. Such a channel has been recognized as an important building block in many practical systems, such as wireless sensor networks and satellite communication systems. In the first set of contributions, full-duplex relays were considered in the restricted TWRC, i.e. the encoders of both terminals do not cooperate and the transmitted symbols at one terminal do not depend on its past received symbols [66 – 68]. Multiple access by two terminals and broadcast transmission by the relay occur simultaneously. The achievable rate regions were

provided in [66], and different relaying protocols were compared. The conclusion of that work is that when the relay is close to one of the transmitters, it is best to use a combined decode/compress-and-forward scheme. In [67], the coding scheme and achievable rate region for TWRC and Three-Way Broadcast Channel were provided, relying on the technique of random binning together with network coding. The lattice list decoding at the end terminals in combination with the random binning technique (CoF relaying protocol) for TWRC was studied in [68]. For half-duplex relays, Coded Bi-directional Relaying (CBR), also known as Time Division Broadcast (TDBC) protocol, was introduced in [69] as a way to overcome half-duplex constraint of traditional non-cooperative schemes based on time sharing approaches, where four time slots are required to accomplish information exchange between the two sources via the relay [70]. TDBC is a three-phase relaying protocol, where in the first two phases (time-slots) the communicating nodes transmit their messages in succession, while in the third phase the relay jointly encodes and broadcasts their messages, where a priori known information at receivers is exploited for decoding. Both scenarios where the direct link between two communicating nodes is available or not were considered in [69]. Even more spectrally efficient protocol, coined Multiple Access Broadcast (MABC) protocol [77], is consisted of two phases only, where in the first one the two communicating nodes transmit simultaneously, and in the second one the relay jointly encodes and broadcasts their messages. Due to a half-duplex constraint, communicating nodes cannot exploit the direct link between them. Capacity region and information-theoretic coding schemes for MABC were presented in [71 – 74] for DF and CF relaying protocols, as well as a practical code which relies on well-developed single user codes. Lattice codes and lattice decoding for MABC were considered in [76], while in [75] the authors have presented MABC as a way to overcome half-duplex constraint, and have extended the analysis to the case where $N$ communicating pairs exchange information through $K$ relays, using "Orthogonal-and-forward" protocol. In [77, 78], TDBC and MABC protocols were compared for DF, AF, CF, mixed DF/CF and CoF relaying protocols in terms of achievable rates for different Signal-to-Noise Ratio (SNR) and relay geometries. Finally, in [79] the achievable rates for novel MABC with Joint Decode-and-Forward and MABC with Denoise-and-Forward relaying protocols were proposed, and compared with classical TDBC with DF and TDBC with AF relaying protocols.

### 1.1.8 Multiple Access Multiple Relay Channel

The $(M, L, 1)$-Multiple Access Multiple Relay Channel (MAMRC) consists of $M$ statistically independent sources which transmit their packets to a single common destination with the help of $L$ independent dedicated relays, $M$ and $L$ being

arbitrary integers. The term "dedicated" means that the relays devote all their resources to help and do not have packets of their own to transmit. Only the assumption of a unique destination makes this network topology a reduced version of the most general multiterminal setting. The graphical $(M, L, 1)$-MAMRC is formally a multi-packet multicast single-destination graphical network and as such its capacity is known and achieved through linear network coding. However, the capacity region of the general $(M, L, 1)$-MAMRC is still unknown [18].

In wireless MAMRC networks, the type of Multiple Access is assumed to be either Orthogonal (OMA), or Non-Orthogonal (NOMA) [81], where the orthogonality may refer to time, frequency or code space. For slow-fading $(M, L, 1)$-MAMRC with half-duplex relays, DF type of relaying protocols seem promising, especially under NOMA. Selective Decode-and-Forward (SDF) [32] is an interesting variant of DF relaying protocol, where relays are not obliged to wait to successfully decode all the sources in the network before switching from *listening* to *transmitting* phase. Even though SDF is an energy efficient protocol where there is no error propagation from the relays to the destination, other relaying protocols mentioned in the section 1.1.1 are shown to outperform it in some scenarios, but rigorous fair comparisons still have to be done for the slow fading half-duplex $(M, L, 1)$-MAMRC. In [82], Dynamic Selective Decode-and-Forward (D-SDF) has been proposed, which combines the advantages of both Selective DF, previously studied by the same authors in [83 – 85], and Dynamic DF. Namely, the condition for switching from *listening* to *transmitting* phase at relays may vary during the time, which is advantageous especially in the scenario of asymmetric link quality of source-to-relay links, where one source having bad quality of links towards relays will not keep them from helping other sources.

When it comes to practical code design, the design of channel and network codes may be done *separately* or *jointly*, which is referred to as Separate Network-Channel Coding (SNCC) or Joint Network-Channel Coding (JNCC), respectively. For SNCC, a channel coding is performed first using a capacity-approaching code, and then network coding is performed on a block level treating links either as correct or erased, using an algebraic block code with good erasure correcting capabilities. Separate Network-Channel Decoding (SNCD) is also performed sequentially: first (soft-input hard output) channel decoding, then network decoding (hard input algebraic decoding). For JNCC, the channel and network redundancy are exploited jointly, where the network code is part of the overall channel code applying on all sources' packets. Nevertheless, the network and the channel code may be designed separately in order to obtain the desired structural properties of the global channel code. At the receivers (destination and relays), channel decoding and network decoding are also fused in a single global code decoding process, referred to as Joint Network Channel Decoding (JNCD).

The cooperative protocols SDF/SNCC/SNCD and SDF/JNCC/JNCD for the $(M, L, 1)$-MAMRC have been analyzed from an information outage perspective in [86] and [83, 87], respectively. For the slow fading half-duplex $(M, L, 1)$-Orthogonal Multiple Access Multiple Relay Channel (OMAMRC) different linear SNCC have been proposed, designed either over the binary Galois field or high-order Galois fields [88 – 90]. In particular, Xiao and Skoglund have proved that a necessary and sufficient condition for SNCC/SNCD to achieve the full diversity order is to impose on Non-Binary Galois Field Network Codes (NBGFNCs) to be Maximum Distance Separable (MDS) [90]. JNCC schemes (together with JNCD) have been first investigated for slow fading half-duplex $(2, 1, 1)$-OMAMRC in [91, 92]. They are based on linear binary Low Density Parity Check (LDPC) codes or turbo codes [93] and borrow ideas from network coding and distributed turbo coding [41, 94]. Similar ideas have been independently presented in [95] for the slow fading half-duplex 2-user cooperative MAC. Provably full-diversity JNCC for the slow fading half-duplex $(2, 1, 1)$-OMAMRC has been proposed in [96] based on the concept of root-check LDPC codes for nonergodic block-fading channels [97]. SDF/JNCC/JNCD has been introduced for the slow fading half-duplex $(2, 1, 1)$-Non-Orthogonal Multiple Access Relay Channel (NOMARC) in [98]. In [89], the Authors put forward a SNCC scheme for the slow fading half-duplex $(M, L, 1)$-OMAMRC based on *random* NBGFNCs and non-binary irregular LDPC codes. Perfect Source-to-Relay (S-R) links are assumed and a sub-optimal Soft-In Soft-Out (SISO) network decoder is described, referred to as *selection updating decoder*. Other competing SDF/JNCC approaches for the slow fading half-duplex $(M, L, 1)$-OMAMRC and the slow fading half-duplex $(M, L, 1)$-Non-Orthogonal Multiple Access Multiple Relay Channel (NOMAMRC) have been propounded in [99] and [85], respectively. Particular attention has been paid to the linear Binary Galois Field Network Codes (BGFNCs) that are derived from the binary image of Non-Binary Galois Field Network Codes. The channel coding is consisted of: (i) the encoding of sources' packets using turbo codes, followed by (ii) the generation of extra parity bits by using punctured convolutional codes at the relays. By using the principle of multiple turbo codes [100], sources that have been helped by at least one relay can potentially benefit from an extended codebook (from the destination perspective). Mohamad *et al.* have then proposed Bit-Interleaved XOR (BI-XOR) based JNCC class of joint network channel binary codes, which are simple in design and close to full diversity with high probability. For the decoding part, JNCD is performed by combining the received information from both sources and relays, for example, by an iterative exchange of extrinsic information on a global factor graph [101] whose constraint nodes include the encoding constraints at the sources and at the relays.

For DDF protocols, the switching point between listening and transmitting phase

is not fixed, so a different approach needs to be adopted. Rateless codes, also known as fountain codes, have attracted considerable interest among coding and communication theorists, since their introduction in [102, 103]. Such codes do not have a fixed or predetermined rate at the transmitter. In theory, a source can generate as many encoding symbols as needed to enable a destination to decode the message. In fact, in rateless schemes, the receiver keeps accumulating mutual information, rather than energy, from the source. In [104], rateless codes where used to implement DDF relaying in non-orthogonal multiple access relay channel. The sources keep transmitting until the destination correctly decodes their messages, while the relay is activated only when it can correctly decode all the sources' messages. In most practical communication scenarios, however, the receivers cannot wait infinitely until correct decoding of all sources' messages and, after a certain period, an error event should be declared (outage event). This imposes a minimum coding rate on the practical fountain codes. On the other hand, if the receivers try to decode the sources' messages at each new received symbol they will consume a lot of energy, hence they wait the accumulation of certain number of symbols to initiate the decoding process. To circumvent these limitations, one can instead resort to the concept of rate compatible error-correcting codes. A rate-compatible code family is a set of codes with different rates, where higher rate codes are embedded into lower rate codes [105]. One method to construct rate-compatible codes is to employ puncturing: First, a low-rate mother code is generated, and then codes of higher rates are obtained by puncturing different number of bits at different positions from the mother code. In [82], the Authors focus on families of Rate-Compatible Turbo Codes (RCTC) [106 – 108], but Rate Compatible Low-Density Parity-Check (RCLDPC) codes could have been considered as well [109]. The optimization of the mother code and optimization of the puncturing patterns are usually carried out separately.

### 1.1.9 Cooperative HARQ

The concept of cooperation does not restrict to the physical layer and extends to the link layer as well, through concepts like cooperative Automatic Retransmission ReQuest (ARQ), packet combining, or crosspacket channel coding. ARQ is an error-controlling method which can help to improve the performance of the upper-layer protocols (like TCP) significantly at the expense of an increased delay [110]. It relies on the use of control channels, using which the receiver can send a request to the transmitter to repeat the message in the case of error in decoding. When Forward Error Correction (FEC) is used in conjunction with an ARQ protocol, it is called hybrid error control or HARQ [111]. The two most famous HARQ combining strategies are Chase Combining (CC) [112], where the retransmissions

are identical copies of the original transmission (known also as repetition coding), and Incremental Redundancy (IR), where the retransmissions consist of new parity bits from the channel encoder [113].

Research in relay networks with *limited feedback* has made significant progress in the past few years, most of contributions considering a network consisted of single source, single relay and single destination [114 – 125]. In [114] and [115], the performance of different HARQ protocols have been studied, where both repetition and IR strategies have been analysed for retransmission rounds. Energy efficiency and Energy-Delay Tradeoff were studied in [116] and [117] for basic ARQ with space-time coding and IR-HARQ, respectively. Novel HARQ strategies which dynamically switch between AF/CF and DF relaying protocol are evaluated from spectral and energy efficiency perspectives in [118]. CC-HARQ, IR-HARQ and HARQ Type I were compared in terms of energy efficiency with proper circuitry consumption taken into account in [120]. In [121], the delay-limited throughput is defined which takes into account the delay constraints, and evaluated for IR-HARQ where the relay performs space-time coding. The effective capacity is defined and analysed in [122], while the efficient power allocation between different transmission time-slots is studied in [123, 124]. The optimal initial transmission rate for IR-HARQ with DF relaying protocol was analysed as a function of relay location and experienced SNR in [125], but no rate allocation algorithm has been proposed.

Another set of contributions deals with the networks composed of multiple sources or multiple relays. The advantage of using relay selection schemes over distributed space-time block coded transmissions in user co-operation networks is shown in [126, 127], where for a given user, other users in the network serve as relaying nodes. In [128], for the same type of network simple closed-form upper bounds on outage probability are derived for the proposed schemes, where it is shown that the full spatial diversity is achieved. In [129], the advantage of using network coding is demonstrated for multi-user relay channel consisted of two sources, one relay and the destination, with the feedback channel available from both the relay and the destination. Optimal transmission power allocation for multi-hop networks with ARQ has been studied either individually in [110], or jointly with relay selection in [130].

## 1.2 Motivation and scope of the thesis

In this thesis, we study centralized scheduling and link adaptation strategies for cooperative HARQ protocols in Multiple Access Multiple Relay Channel (MAMRC).

In practice, some of the typical wireless communication scenarios where MAMRC is present include:

- Wireless sensor networks, where sensors cooperatively pass the data to the central node (user co-operation), possibly using intermediate nodes with better computing and communication capabilities (relays, see e.g. [46]);
- Cellular networks, where mobile terminals of the users in good propagation conditions (relays) can help the base station (destination) in decoding of the messages of mobile terminals of users (sources) that are in bad propagation conditions. Alternatively, relays could be dedicated devices with the fixed location, or placed on moving trains, buses etc.
- Scenario of Integrated Access and Backhaul (IAB) in New Radio (NR) [131], where the radio resources are shared between access and backhaul links, e.g. very dense deployment of NR cells without the need for densifying the transport network proportionally (where the IAB-nodes are relays).
- Relay assisted D2D communications;
- etc.

It is assumed in our work that all the links in the network are subject to slow-fading and Additive White Gaussian Noise (AWGN). Time Division Multiplexing is assumed, where transmissions of the sources are divided into frames consisted of time-slots, during which orthogonal transmissions occur, i.e. OMAMRC is considered. During a frame, channel gains are assumed to be constant (due to slow-fading assumption). Orthogonality is the simplest way to deal with interference. Although NOMA is known to be more optimal for slow fading channels from the information-theoretic point of view, due to required complexity of the receiver design such an approach is still not being used in practice. At least two sources communicate with a single destination with the help of at least two relaying nodes. A relaying node can be either a dedicated relay, which does not have its own message to transmit, or a source itself, which does have its own message and that can relay the messages of the other sources in some cases (user co-operation). Relaying nodes are half-duplex, hence their inability to simultaneously receive and transmit information flows in the same frequency band is conveniently encompassed by OMA. Even though several approaches have been proposed to combat the half-duplex constraint as we were able to see in the previous section (see e.g. [70]), the vast majority of contributions dealing with relaying and network coding assumes OMA and half-duplex relays. Channel State Information (CSI) is available at the receiver of each direct link.

Even for the advanced relaying protocols in MAMRC networks with no feedback such as D-SDF (see [82]), the level of cooperation that could be achieved is limited due to the half-duplex constraint. Namely, a relay might prefer to cooperate with a limited amount of (successfully decoded) sources for a longer duration instead of waiting too long to get a better chance to cooperate with *all* the sources. We refer to this problem as the "switching problem". Other then using full-duplex relays, this problem could be solved by introducing feedback control channels in both directions. Based on the exchanged control information the destination could decide for each individual time-slot the node to transmit, all the other nodes remaining silent or being in the "listening" mode. Thus, on the one side we assume that a broadcast control channel of limited rate from destination to source and relay nodes is present (limited feedback channel). On the other side, a unicast forward coordination control channel of limited rate is available from each individual source and relay towards the destination (except if sources do not perform user co-operation, in which case there are no unicast forward coordination control channels from them towards the destination). So, in our work we suppose that a frame is split into two phases. During the first phase, each source transmits in turn its message in consecutive time-slots. During the second phase (retransmission phase) the destination schedules a relay or a source to transmit in each time slot, i.e. HARQ protocol is being used. One of the main challenges of this thesis is to find an optimal node selection (scheduling) strategy that the destination should adopt, as well as the algorithm which chooses the initial rates for sources, having the goal to maximize the average spectral efficiency under individual QoS targets. The SDF relaying protocol is retained, where the relaying nodes are allowed to cooperate only with the sources which they were able to decode, but they are not obliged to wait to successfully decode them all before becoming active, as they can obviously be triggered by the destination at any moment. Both CC and IR HARQ protocols are considered, i.e. the retransmission message is consisted either of the exact same bits as the original message, or of the additional parity bits.

On the subject of scheduling strategies for cooperative MAMRC networks the contributions are not very numerous, e.g. [132 – 135]. In [132], the information outage probability is derived for MAMRC with AF relaying protocol and Selection Combining (SC) technique, where in each time-slot the best source-relay pair is selected to transmit. A similar scheme has been analysed in [133], with the difference that at first all sources transmit in turn in order to assure fairness, just as in the first phase in our work. In another work Maximum Ratio Combining (MRC) is considered instead of SC for the similar set-up [134], where for each source the destination decides if the relay having the best quality of the channel towards itself should transmit or not using AF relaying protocol. There, the quality of source-to-relay channels is not taken into account, and just as in [132] and [133], the

relays are not assumed to perform network coding. MAMRC with SNCC/SNCD, which is known to be suboptimal to JNCC/JNCD, is studied in [135] with an assumption of perfect source-to-relay links and where classical DF protocol is used. In [136], SNCC/SNCD with DF has also been considered , where an outage analysis is done for a proposed relay ordering algorithm that is based on finite field network coding. In [137], an information outage analysis of SDF with JNCC/JNCD for the slow-fading ($M$,$L$,1)-MAMRC with control channels used by IR-HARQ protocol is conducted. The scheduling (node selection) strategies proposed in the latter work, applicable only for the symmetric rate scenario, are far from being optimal in terms of long-term aggregate throughput, even tough the number of retransmissions is minimized.

None of the previously mentioned approaches deals with the problem of the optimal and efficient rate allocation. Most of the papers that deal with the rate allocation problem in the combination with HARQ techniques consider a single source, a single or eventually multiple relays, and a single destination. In [138] a presence of a fixed infra-structured relay is considered, and it is shown that large gains in throughput and coverage area can be obtained when the source and the relay are allowed to use different spectral efficiencies, where the simple SC technique is used. A scenario of a single ad-hoc relay with no direct link available from the source to the destination where the repetition coding is adopted, i.e. CC-type of HARQ, is studied in [139]. There, a rate allocation strategy of both the source and the relay is proposed under the outage probability constraint and both finite and infinite allowed number of retransmissions constraint. In [140], a rate adaptation problem is presented as Markov Decision Process (MDP) where Dynamic Programming (DP) is employed for optimization, in a single relay scenario with the feedback available from both the relay and the destination to the source. IR-HARQ technique is adopted in that work, and the advantage in terms of average throughput and the outage probability compared with the non-adaptive HARQ is demonstrated, where the analysis is also extended to multiple relay scenario. Joint power and rate optimization for multihop relay network (where multiple relays are serially connected from the source to the destination) with the IR-HARQ technique being used is investigated in [141]. It is shown that the proposed scheme outperforms both IR-HARQ scheme with fixed power and rate and CC-HARQ scheme in terms of long-term average transmission rate.

## 1.3 Thesis contributions and outline

The remainder of this thesis is organized as follows. In **Chapter 2** we detail the common system model assumptions that are adopted throughout the whole thesis.

The main contributions of this thesis are described in three different chapters, which we briefly outline in the following.

In **Chapter 3**, we investigate centralized scheduling strategies for cooperative IR retransmissions in the slow-fading half-duplex time-slotted $(M, L, 1)$-MAMRC. The goal of the proposed strategies is to maximize the normalized average spectral efficiency under the given fairness constraint, which is defined using the information theory outage analysis tool. As the destination cannot make an optimal scheduling decision based only on available CSI of direct links towards itself, the HARQ mechanism occurs at the beginning of each time-slot in the second phase, where control information is exchanged between relays and the destination. The destination transmits common ACK/NACK messages, while the relaying nodes transmit the information about their decoding sets, where the particular attention is paid in order for the amount of control information which is exchanged to be as small as possible. A scheduled relay retransmission uses Joint Network and Channel Coding on its correctly decoded source messages (cooperative retransmission). Monte-Carlo simulations show that these strategies outperform the state of the art one based on the minimization of the probability of the common outage event after each time-slot. Moreover, the average spectral efficiency reached with these strategies is close to the upper-bound, calculated by the exhaustive search approach over all possible node sequence activations. The same conclusion remains valid for both symmetric and asymmetric source rate scenarios.

This chapter has led to the following publication:

- S. Cerovic, R. Visoz, L. Madier, A. O. Berthet, "Centralized scheduling strategies for cooperative harq retransmissions in multi-source multi-relay wireless networks", in *Proc. IEEE ICC'18*, Kansas City, MO, USA, May 2018.

and patent filling:

- S. Cerovic, R. Visoz, "Optimized control channel design for Orthogonal Multiple Access Multiple Relay Channel", *Patent n:201564FR01*, France, 2018.

In **Chapter 4**, we propose a slow-link adaptation algorithm for the same slow-fading half-duplex orthogonal time-slotted $(M, L, 1)$-MAMRC, where during the second phase, one of the proposed node selection strategies from chapter 3 is adopted. The proposed algorithm aims at maximizing the average spectral efficiency after a fixed number of retransmissions under individual QoS targets for a given modulation

and coding scheme family. Such an algorithm can be applied in the scenario where the Channel Distribution Information (CDI) of all links (e.g., average SNR of all links) is reported to the destination on a long-term basis in order to derive the (slow) rate allocation of the sources. This kind of scenario typically corresponds to fast varying radio conditions, e.g., for high mobility conditions. Additionally, we propose a slightly modified version of the same algorithm coined fast-link adaptation algorithm, adapted to the scenario where the CSI of all links is reported to the destination. This scenario could be of interest when the channel states change slowly and can be assumed to be constant during tens of frames. Otherwise, the acquisition of the CSI of each link would be too costly in terms of feedback overhead. To reduce the algorithm's complexity, the discrete rates are first determined by using the "Genie-Aided" assumption which consists in considering for a given source that all other sources are known to the relaying nodes and the destination. In a second step, an iterative rate correction algorithm is applied. The resulting scheduling and link adaptation algorithms offer a tractable complexity under practical knowledge of channel states and yield performance close to the corresponding exhaustive search approaches as demonstrated by Monte-Carlo simulations.

This chapter has led to the following publication:

- S. Cerovic, R. Visoz, "Slow-link adaptation algorithm for Multi-Source Multi-Relay Wireless Networks with Cooperative Retransmissions", *to be submitted*.

and patent fillings:

- S. Cerovic, A. Mohamad, R. Visoz, "Centralized scheduling and user cooperation for improved Incremental Retransmission in the uplink", *Patent n:201362FR01*, France, 2017.
- S. Cerovic, R. Visoz, "Iterative Rate Allocation for Slow-Link Adaptation with Cooperative HARQ Retransmissions in Multi-Source Multi-Relay Wireless Networks", *Patent n:201534FR01*, France, 2018.

In **Chapter 5**, we investigate the performance of three different cooperative HARQ protocols for slow-fading half-duplex $(M, L, 1)$-MAMRC. The first one consists in sending incremental redundancies (IR) on all the messages from the scheduled node decoding set (Multi-User encoding), while the second one sends IR for a single source (Single User encoding) chosen randomly. The latter is particularly attractive since its implementation can reuse state-of-art rate compatible punctured codes such as low density parity check codes or turbo codes. The third one is of the Chase Combining (CC) type, where the selected node repeats the transmission

(including modulation and coding scheme) of one source chosen randomly from its decoding set. In that case, Maximal Ratio Combining technique is used at the destination on all the transmissions related to a given source. We can expect that such a protocol behaves poorly in general compared to the IR-type of HARQ. Both considered Single User cooperative HARQ protocols can be considered to have a similar complexity in terms of the code construction (state of the art rate compatible punctured codes), which is lower than in the case of Multi-User encoding and joint iterative decoding. As a result, the HARQ protocol comparison comes down to a performance comparison where information theory outage analysis is particularly relevant. On the other hand, we also design a practical encoding and decoding scheme for the scenario where relaying nodes implement Single User encoding and evaluate its performance using Monte-Carlo (MC) simulations. The proposed scheme is based on a slow-link adaptation algorithm propounded in chapter 4 which operates with a family of practical Modulation and Coding Schemes (MCSs), a node selection strategy proposed in chapter 3 and multi-rate turbo encoder/decoder based on Circular Buffer technique.

This chapter has led to the following publication:

- S. Cerovic, R. Visoz, L. Madier, "Efficient Cooperative HARQ for Multi-Source Multi-Relay Wireless Networks", *2018 14th International Conference on Wireless and Mobile Computing, Networking and Communications (WiMob)*, Limassol, Greece, Oct. 2018.

Finally, in **Chapter 6** we draw conclusions and discuss some perspectives on future work.

# 2 | System Model

In this chapter, we take a detailed look on system model assumptions that are common for the three following chapters.

An $(M, L, 1)$-OMAMRC is investigated under slow-fading assumption. $M$ sources, belonging to the set $\mathcal{S} = \{s_1, \ldots, s_M\}$, transmit independent messages $\mathbf{u}_s \in \mathbb{F}_2^{K_s}$ of $K_s$ information bits towards a common destination. The number of information bits of a source message depends on the selected MCS by the destination. Alternatively, MCS of a source is predetermined and fixed before any transmission occurs. $L$ relays, that operate in half-duplex mode and that belong to the set $\mathcal{R} = \{r_1, \ldots, r_L\}$, help the destination in decoding the sources' messages. They overhear the messages from sources due to the broadcast property of wireless medium, and apply SDF relaying protocol. Relays do not have their own messages to transmit. Additionally, if not stated otherwise, we assume that user-cooperation is performed, i.e. when not transmitting, sources listen to other sources and relays transmissions and help the decoding at the destination by applying the SDF relaying protocol (see Fig. 2.1). Moreover, HARQ protocol is used, which is either of type Incremental Redundancy, or Chase Combining. In the case of IR-type of HARQ protocol, two types of encoding are considered: Single User encoding and Multi-User encoding (JNCC), depending on the number of sources that the node performing the relaying functions will help during its transmission. We define the set of all source and relay nodes as $\mathcal{N} = \mathcal{S} \cup \mathcal{R}$.

CSI is available only at the receiver side of each link and is assumed perfect. Hence, the destination only has the perfect knowledge of CSI of source-to-destination (S-D) links, $\mathbf{h}_{\mathrm{S,D}} = [h_{s_1,d}, \ldots, h_{s_M,d}]$, and of relay-to-destination (R-D) links $\mathbf{h}_{\mathrm{R,D}} = [h_{r_1,d}, \ldots, h_{r_L,d}]$. On the other hand, the CSI of source-to-source (S-S), source-to-relay (S-R) and relay-to-relay (R-R) links are unknown to it.

Transmission of source messages is split into frames, where during one frame exactly one message from each source is sent, as well as the retransmissions related to those messages. Slow (block) fading is assumed, where within an integer multiple of the frame duration the radio-links between the different nodes are considered

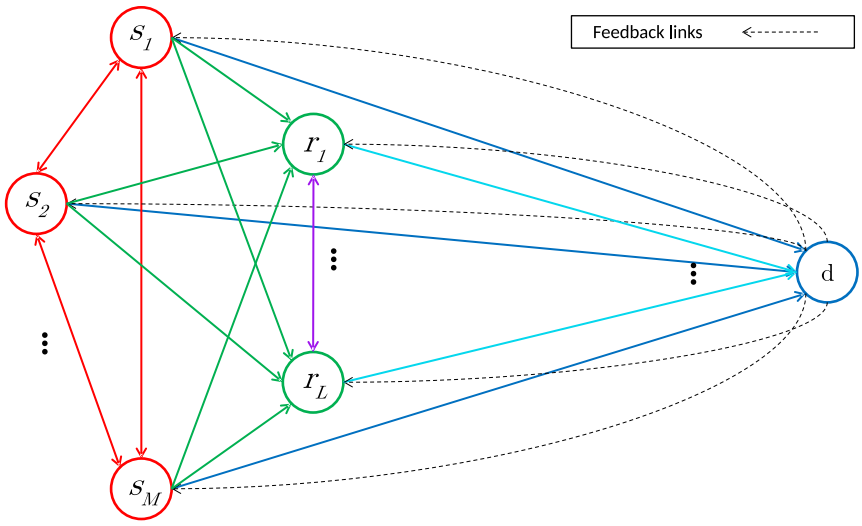


**Figure 2.1:** Orthogonal Multiple Access Multiple Relay Channel (OMAMRC) with feedback.

to be fixed. If not stated otherwise, it will be assumed that radio channels are fixed during one frame exactly. From one realization to another the radio channels change independently. In the case where the source rates are not predetermined, we consider that before any communication occurs, during the "initial phase", a link adaptation algorithm is performed (see Fig. 2.2). There, a scheduler, located at the destination, applies an algorithm in order to choose the MCS for each source. Two different scenarios are considered, where either CDI or CSI of S-S, S-R and R-R links are used as the required input to the algorithm. In both cases, all channel information are conveyed over unicast forward coordination control channels (from sources and relays towards the destination) that are assumed to be errorless. The scheduling decision is transmitted to all nodes using the errorless limited feedback broadcast control channel. In the following, we describe in more detail two considered scenarios and corresponding required inputs for the link adaptation algorithms.

**Slow-link adaptation**: link adaptation algorithm which is based on **CDI** of each link in the network. This kind of scenario typically corresponds to fast varying radio conditions, e.g., for high mobility conditions, when the acquisition of CSI of each link in the network at the destination may reveal too costly in terms of feedback overhead. Furthermore, we consider that during a certain number of frames $N_f >> 1$ (e.g. few hundred), the probability distribution of the quality of each link remains constant. That means that the quality of the given link in the given frame represents one realization of the associated probability distribution (obviously, radio channels change from one frame to another in this scenario). Hence,

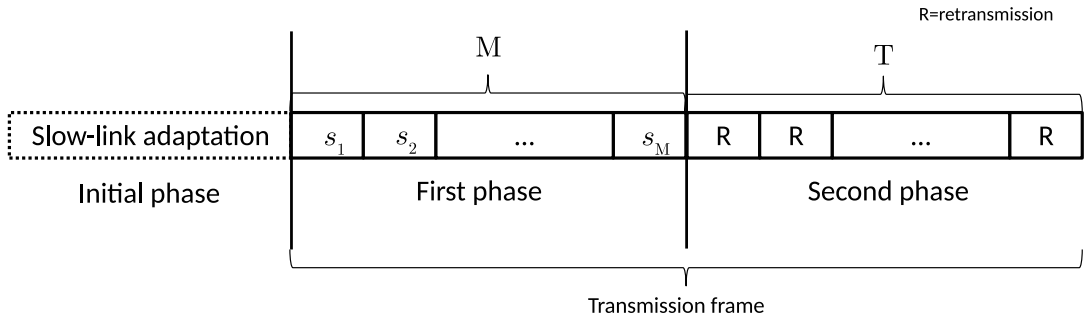


**Figure 2.2:** Transmission of a frame: the initial, the first and the second phase.

CDI (e.g., average SNR of corresponding links) is reported to the destination in order to derive the source rates on a long-term basis, where the destination can track the CDI of S-D and R-D links by itself. It follows that the initial phase occurs once every few hundred frames, once the CDI of network links change. Between two occurrences of the initial phase, the sources' rates are kept fixed.

**Fast-link adaptation**: link adaptation algorithm which is based on **CSI** of each link in the network. This scenario could be of interest when the channel states change slowly and can be assumed to be constant during tens of frames. Hence, CSI of all links are reported to the destination, and the initial phase is repeated each time the CSI of different links in the network change.

Our main focus is on the slow-link adaptation algorithm.

Transmission of one frame is split into maximum of $M + T$ ($T \geq L$ being a system design parameter, which depends on the latency requirements) time-slots, grouped into two transmission phases. During the first phase consisting of the first $M$ time slots, each source transmits in turns its message. Each time-slot is made of $N_1$ channel uses, whereby time resource is shared equally between sources. In that phase when one source transmits, relays and all other sources listen and try to decode the message of that source. A Cyclic Redundancy Check (CRC) is appended to each source message (before applying the selected MCS which consists of channel coding, interleaving and modulation operations) in order to allow the relaying nodes and the destination to detect any decoding error on the source messages. During the second phase sources, if they are selected, act as relays, i.e. they can cooperate with other sources, in order to help the destination to successfully decode the messages from all the sources (user co-operation). Otherwise, if user co-operation is not used, or if sources were not able to decode any message from other sources, once they are selected they simply send additional parity bits for their own message or retransmit it, depending on if IR or CC type of HARQ is used, respectively . At the beginning of each time-slot during the second phase (called

also " retransmission round" in the following), the exchange of control information occurs between the destination at the one hand, and sources and relays on the other hand, so the destination can select one node (relay or a source) to transmit in that round. In general, we assume that the control exchange procedure similar to the one described in [137] takes place. Its main steps are illustrated on Fig. 2.3, and are explained in the following for the case of retransmission round $t$:

1. The destination broadcasts a common ACK bit using the feedback broadcast control channel to all the sources and relays nodes if it succeeded in decoding all the source messages after round $t-1$. Otherwise it broadcasts a common NACK.

2. If NACK bit was sent by the destination, each node $n \in \{s_1, \ldots, s_M, r_1, \ldots, r_L\}$ transmits the information about the set of its successfully decoded sources after round $t-1$ (also called the "decoding set" in the following, denoted by $\mathcal{S}_{n,t-1}$ on the figure) using dedicated unicast forward coordination control channels. Otherwise, if an ACK bit was sent, a new frame begins and the sources transmit new messages while the relays and destination empty their memory.

3. Using some node selection (scheduling) strategy, the destination makes a scheduling decision about the node $\hat{a}_t$ to select for transmission. Its decision is broadcasted using the feedback broadcast control channel.

4. Selected node transmits its message $u_{\hat{a}_t}$. If Multi-User encoding is used (and if user co-operation is used in the case that a source is selected), it performs JNCC with the messages of the sources that it was able to decode. Otherwise, it sends additional redundancy bits on the randomly selected message from its decoding set or its exact original bits, depending on if IR or CC-HARQ is used, respectively. Note that a priori, the decoding set of a source is itself.

Note that the end of the first phase is considered as the end of the round zero. The non-selected nodes in a given retransmission round can benefit from the transmission of the scheduled node as well, and update their decoding sets accordingly. The number of retransmission rounds used in the second phase $T_{used} \in \{1, \ldots, T\}$ depends on the success of the decoding process at the destination. It is assumed that all nodes transmit with the same power, where each node is equipped with one antenna only. In the rest of the paper, the following notations are used:

- $x_{a,k} \in \mathbb{C}$ is the coded modulated symbol for channel use $k$, sent from node $a \in \mathcal{S} \cup \mathcal{R}$, whose power is normalized to unity.

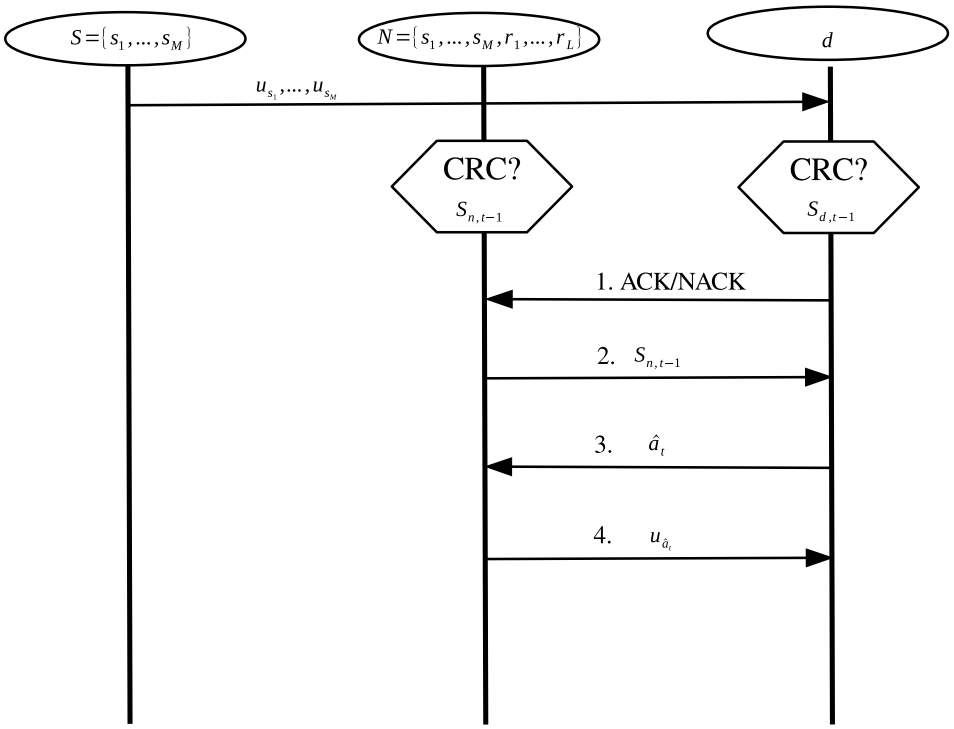


**Figure 2.3:** Control information exchange procedure at the beginning of each time-slot in the second phase.

- $y_{a,b,k}$ is a received signal at node $b \in \mathcal{S} \cup \mathcal{R} \cup \{d\} \setminus \{a\}$, originating from node $a$ described previously.
- $\gamma_{a,b}$ is the average signal-to-noise ratio SNR that captures both path-loss and shadowing effects.
- $h_{a,b}$ are the channel fading gains, which are independent and follow a zero-mean circularly symmetric complex Gaussian distribution with variance $\gamma_{a,b}$.
- $n_{a,b,k}$ are independent and identically distributed AWGN samples, which follow a zero-mean circularly-symmetric complex Gaussian distribution with unit variance.

Using the previous notation, the received signal at node $b$, originating from node $a$ can be represented as:

$$y_{a,b,k} = h_{a,b}x_{a,k} + n_{a,b,k}, \tag{2.1}$$

where $k$ denotes a current channel use. During the first phase, $a \in \mathcal{S}$ and $k \in \{1, \ldots, N_1\}$. During the second phase, $a \in \mathcal{S} \cup \mathcal{R}$ and $k \in \{1, \ldots, N_2\}$. During both phases $b \in \mathcal{S} \cup \mathcal{R} \cup \{d\} \setminus \{a\}$.

# 3 | Node Selection Strategies

In this chapter, we investigate different node selection (scheduling) strategies for $(M, L, 1)$-MAMRC under system model assumptions described in chapter 2.

## 3.1 Performance metric and outage events

Let us define the initial transmission rate of source $s$ as $R_s = K_s/N_1$ in bits per complex dimension or bits per channel use [b.c.u]. We can define a long-term transmission rate $\bar{R}_s$ per source as the fraction of the number of transmitted bits over the total number of channel uses spent, for a number of frames that tends to infinity:

$$\bar{R}_s = \frac{R_s}{M + \alpha \mathbb{E}(T_{\text{used}})}, \tag{3.1}$$

where we take into account the average number of retransmission rounds used in the second phase: $\mathbb{E}(T_{\text{used}}) = \sum_{t=1}^{T} t \Pr\{T_{\text{used}} = t\}$ , and where $\alpha = N_2/N_1$ is the ratio between the available number of channel uses in each time-slot of the second phase and the number of available channel uses in each time-slot of the first phase. Obviously, this definition is suited for the scenario where the source rates are kept fixed during multiple frames, where radio channels change from one frame to another. Those rates can be selected using some slow-link adaptation algorithm, which is the subject of our study in the next chapter.

The total average spectral efficiency (in the following we will omit the word "total" for simplicity), can be defined as the sum of the individual average spectral efficiencies:

$$\eta = \sum_{i=1}^{M} \bar{R}_{s_i} (1 - \Pr\{\mathcal{O}_{s_i,T}\}), \tag{3.2}$$

where $\mathcal{O}_{s,T}$ is the event that source $s$ is not decoded correctly at the destination after round $T$, called the "individual outage event of source $s$ after round $T$" in the following.

In this chapter, our goal is to maximize the average spectral efficiency by applying the proper centralized scheduling strategy of the sources. It is understood that the node selection within our centralized scheduling strategies should be fair in the sense that the node selection should not depend on the initial rates of the sources. As a result, the maximization of the average spectral efficiency under this fairness constraint is equivalent to the maximization of the normalized average spectral efficiency defined as:

$$\bar{\eta} = \sum_{i=1}^{M} \frac{1}{M + \alpha \mathbb{E}(T_{\text{used}})} (1 - \Pr\{\mathcal{O}_{s_i,T}\}). \tag{3.3}$$

Note that it is equivalent to the maximization of the average spectral efficiency in case of symmetric initial rates, i.e., $\bar{R}_{s_i} = R$ for all $i \in \{1, \ldots, M\}$.

Since the destination does not have the CSI of all links in the network, it cannot take an optimal scheduling decision, no matter the criterion of optimization. Each relaying node (relay and source which performs user co-operation) at the beginning of each retransmission round transmits its decoding set to the destination, which can be considered as a partial knowledge of the CSI of S-S, S-R and R-R links. In general, the individual outage event of source $s$ after round $t$, $\mathcal{O}_{s,t}(a_t, \mathcal{S}_{a_t,t-1}|\mathbf{h}_{\text{dir}}, \mathcal{P}_{t-1})$, depends on selected node in that round $a_t \in \mathcal{N}$ and associated decoding set $\mathcal{S}_{a_t,t-1}$. It is conditional on the knowledge of $\mathbf{h}_{\text{dir}}$ and $\mathcal{P}_{t-1}$, where $\mathcal{P}_{t-1}$ denotes the set collecting the nodes $\hat{a}_k$ which were selected in rounds $k \in \{1, \ldots, t-1\}$ prior to round $t$ together with their associated decoding sets $\mathcal{S}_{\hat{a}_k,k-1}$, and the decoding set of the destination $\mathcal{S}_{d,t-1}$ ($\mathcal{S}_{d,0}$ is the destination's decoding set after the first phase). Similarly, we define the "common outage event after round $t$" $\mathcal{E}_t(a_t, \mathcal{S}_{a_t,t-1}|\mathbf{h}_{\text{dir}}, \mathcal{P}_{t-1})$ as the event that at least one source is not decoded correctly at the destination at the end of round $t$. The probability of the individual outage event of source $s$ after round $t$, $\mathcal{O}_{s,t}(a_t, \mathcal{S}_{a_t,t-1}|\mathbf{h}_{\text{dir}}, \mathcal{P}_{t-1})$, for candidate node $a_t$ can be formulated as $\mathbb{E}\{[\mathcal{O}_{s,t}(a_t, \mathcal{S}_{a_t,t-1}|\mathbf{h}_{\text{dir}}, \mathcal{P}_{t-1})]\}$, where $\mathbb{E}\{.\}$ is the expectation operator, and $[P]$ is the Iverson bracket having the value 1 if condition $P$ is satisfied, and 0 otherwise. In the same way we can define the probability of the common outage event: $\mathbb{E}\{[\mathcal{E}_t(a_t, \mathcal{S}_{a_t,t-1}|\mathbf{h}_{\text{dir}}, \mathcal{P}_{t-1})]\}$. In the rest of the thesis, in order to simplify the notation, the dependency on $\mathbf{h}_{\text{dir}}$ and $\mathcal{P}_{t-1}$ is omitted.

In this chapter, we assume that Multi User encoding/decoding (JNCC/JNCD) framework is used with IR type of HARQ. Therefore, in each round $k$ of the second phase, the transmitted sequence of selected node $\hat{a}_k$ (if it is a relay or a source which performs user co-operation), and the transmitted sequences of the sources in $\mathcal{S}_{\hat{a}_k,k-1}$ form a joint codeword on the messages of the sources in $\mathcal{S}_{\hat{a}_k,k-1}$.

If the decoding set at the destination after round $t-1$ is given by $\mathcal{S}_{d,t-1}$, we define the set of non-successfully decoded sources at the destination as $\bar{\mathcal{S}}_{d,t-1} = \mathcal{S} \setminus \mathcal{S}_{d,t-1}$.

First, we want to analytically define the common outage event $\mathcal{E}_{t,\mathcal{B}}(a_t, \mathcal{S}_{a_t,t-1})$ after round $t$ for a candidate node $a_t$ of some subset $\mathcal{B}$ of the set of non-successfully decoded sources at the destination $\mathcal{B} \subseteq \bar{\mathcal{S}}_{d,t-1}$. Since in a given round the transmitted incremental redundancies potentially contain multiple source messages, the destination has no choice but to decode the source messages jointly, i.e., considering the received transmissions as part of a joint codeword on all the source messages. As a result, we resort to Multiple Access Channel (MAC) framework, where the event $\mathcal{E}_{t,\mathcal{B}}(a_t, \mathcal{S}_{a_t,t-1})$ is true if the vector of rates of sources contained in $\mathcal{B}$ lies outside of the corresponding MAC capacity region.

We can express this event as:

$$\mathcal{E}_{t,\mathcal{B}}(a_t, \mathcal{S}_{a_t,t-1}) = \bigcup_{\mathcal{U}\subseteq\mathcal{B}} \Big\{ \sum_{s\in\mathcal{U}} R_s > \sum_{s\in\mathcal{U}} I_{s,d} + \sum_{l=1}^{t-1} \alpha I_{\hat{a}_l,d}[\mathcal{C}^{\text{com}}_{\hat{a}_l}] + \alpha I_{a_t,d}[\mathcal{C}^{\text{com}}_{a_t}] \Big\}, \quad (3.4)$$

where $I_{a,b}$ denotes the mutual information between the nodes $a$ and $b$, and where $\mathcal{C}^{\text{com}}_{\hat{a}_l}$ and $\mathcal{C}^{\text{com}}_{a_t}$ have the following definitions:

$$\begin{aligned} \mathcal{C}^{\text{com}}_{\hat{a}_l} &= \Big\{ \{\mathcal{S}_{\hat{a}_l,l-1} \cap \mathcal{U} \neq \emptyset\} \wedge \{\mathcal{S}_{\hat{a}_l,l-1} \cap \mathcal{I} = \emptyset\} \Big\}, \\ \mathcal{C}^{\text{com}}_{a_t} &= \Big\{ \{\mathcal{S}_{a_t,t-1} \cap \mathcal{U} \neq \emptyset\} \wedge \{\mathcal{S}_{a_t,t-1} \cap \mathcal{I} = \emptyset\} \Big\}. \end{aligned} \quad (3.5)$$

In (3.5), the sources that belong to $\mathcal{I} = \bar{\mathcal{S}}_{d,t-1} \setminus \mathcal{B}$ are considered as interference, with $\wedge$ standing for the logical and. Since IR-type of HARQ is used, in (3.4) we basically compare the sum-rate of sources contained in each subset $\mathcal{U} \subseteq \mathcal{B}$ with the accumulated mutual information at the destination. The accumulated mutual information is split into three summations, which originate from:

- The direct transmissions from sources contained in $\mathcal{U}$ towards the destination during the first phase: $\sum_{s\in\mathcal{U}} I_{s,d}$.
- The transmission of the previously activated nodes during the second phase: $\sum_{l=1}^{t-1} \alpha I_{\hat{a}_l,d}[\mathcal{C}^{\text{com}}_{\hat{a}_l}]$. Node $\hat{a}_l$ for $l = \{1, \ldots, t-1\}$ is involved in the calculation only if it was able to successfully decode at least one source from the subset $\mathcal{U}$ (since JNCC is used), but at the same time not from the set $\mathcal{I}$ (if the second condition was not true the signal would represent an interference). Multiplication by $\alpha$ serves as a normalization before adding two mutual information originating from two different phases, where the transmission uses $N_1$ and $N_2$ channel uses, respectively.
- The transmission of the candidate node $a_t$ during the second phase: $\alpha I_{a_t,d}[\mathcal{C}^{\text{com}}_{a_t}]$, under the same conditions as for the previously activated nodes.

If one or more MAC inequalities associated to the sum-rate of sources in different sets $\mathcal{U}$ is not respected, the common outage event of the set $\mathcal{B}$ is proclaimed.

By similar reasoning, the individual outage event of source $s$ after round $t$ for candidate node $a_t$ can be defined as:

$$\mathcal{O}_{s,t}(a_t, \mathcal{S}_{a_t,t-1}) = \bigcap_{\mathcal{I}\subset\bar{\mathcal{S}}_{d,t-1}} \bigcup_{\mathcal{U}\subseteq\bar{\mathcal{I}}:s\in\mathcal{U}} \left\{ \sum_{s\in\mathcal{U}} R_s > \sum_{s\in\mathcal{U}} I_{s,d} + \sum_{l=1}^{t-1} \alpha I_{\hat{a}_l,d}[\mathcal{C}^{\text{ind}}_{\hat{a}_l,s}] + \alpha I_{a_t,d}[\mathcal{C}^{\text{ind}}_{a_t,s}] \right\}, \tag{3.6}$$

where $\bar{\mathcal{I}} = \bar{\mathcal{S}}_{d,t-1} \setminus \mathcal{I}$, and $\mathcal{C}^{\text{ind}}_{\hat{a}_l,s}$ and $\mathcal{C}^{\text{ind}}_{a_t,s}$ have the following definitions:

$$\begin{aligned} \mathcal{C}^{\text{ind}}_{\hat{a}_l,s} &= \Big\{ \{s \in \mathcal{S}_{\hat{a}_l,l-1} \cap \mathcal{U}\} \wedge \{\mathcal{S}_{\hat{a}_l,l-1} \cap \mathcal{I} = \emptyset\} \Big\}, \\ \mathcal{C}^{\text{ind}}_{a_t,s} &= \Big\{ \{s \in \mathcal{S}_{a_t,t-1} \cap \mathcal{U}\} \wedge \{\mathcal{S}_{a_t,t-1} \cap \mathcal{I} = \emptyset\} \Big\}. \end{aligned} \tag{3.7}$$

## 3.2 Cooperative HARQ retransmission strategies

The practical approach of the selection strategies described in [137], which are based on the minimization of the probability of the common outage event after each round in the second phase, seems as a good idea at first sight for the maximization of the average spectral efficiency (referred to as "long-term aggregate throughput" in that work). Indeed, since $\Pr\{\mathcal{O}_{s,T}\} \leq \Pr\{\mathcal{E}_T\}$ for each $s \in \mathcal{S}$, and since $\Pr\{\mathcal{E}_t\} \leq \Pr\{\mathcal{E}_{t-1}\}$, the individual outage probabilities of all sources are being lowered as well, while the average number of retransmission rounds in the second phase is minimized. Note that $\Pr\{\mathcal{O}_{s,T}\}$ and $\mathbb{E}(T_{\text{used}})$ are in the expression of the average spectral efficiency. However, the individual outage probabilities are not minimized in that way (even tough they are lowered), which can be very costly in the case where the quality of each link in the network is bad. In such a scenario, we can end up easily in the case where neither of the sources is being decoded correctly at the end of the round $T$. Hence, it may be more useful to dedicate the retransmission rounds to the successful decoding of a subset of sources. As shown in Section 3.4, it has a positive impact on the average spectral efficiency. Another drawback of the proposed strategies in [137] is that they are applicable only to the symmetric source rate scenario.

In the following, we propose three different node selection strategies.

### 3.2.1 Strategy 1: Node selection based on the number of newly decoded sources

The idea of this strategy is to go exhaustively through all node selection alternatives and try to find the node activation that maximizes the number of decoded sources at the destination at the end of round $t$. The derivation of the number of decoded sources is performed only for the nodes for which $\bar{\mathcal{S}}_{d,t-1} \cap \mathcal{S}_{a_t,t-1} \neq \emptyset$. The destination chooses the node which brings the highest number of newly decoded sources, which is equivalent to the maximization of the cardinality of the decoding set of the destination. When there are multiple nodes that bring the same number of decoded sources at the destination, the selected node is the one having the highest mutual information between itself and the destination.

The reasoning for that comes from the nature of (3.6), where if we want to minimize the probability of the individual outage event of given source $s$, we need to maximize the right-hand side of all the inequalities that are in (3.6). Obviously, the choice of the candidate node $a_t$ only affects $\alpha I_{a_t,d}[\mathcal{C}_{a_t,s}]$ in (3.6). The problem is that in general, there is not a single node $a_t$ that simultaneously maximizes $\alpha I_{a_t,d}[\mathcal{C}_{a_t,s}]$ for each possible $s$, $\mathcal{I}$ and $\mathcal{U}$. However, for a given $s$, $\mathcal{I}$ and $\mathcal{U}$, the optimal selection process is equivalent to the choice of the candidate node $a_t$ with the highest $I_{a_t,d}$, for which $\mathcal{C}_{a_t,s} = 1$. Therefore, our intuitive approach for the node selection is:

$$\hat{a}_t = \underset{a_t \in \mathcal{A}'_t}{\operatorname{argmax}} \{I_{a_t,d}\}, \tag{3.8}$$

where $\mathcal{A}'_t$ is the set of candidate nodes that maximizes the decoding set of the destination after the round $t$.

Our method for determining the decoding set of the destination for the selected candidate node $a_t$ is based on multiple checks of common outage events associated to the subsets of $\bar{\mathcal{S}}_{d,t-1}$. Before proceeding to the algorithm, let us recall the sufficient and necessary conditions for a set of sources to be the decoding set of the destination. They are: (i) The $|\mathcal{S}_d|$-user MAC is not in common outage and (ii) For all the subsets $\mathcal{S}'_d$ that include $\mathcal{S}_d$ ($\mathcal{S}_d \subset \mathcal{S}'_d$), the $|\mathcal{S}'_d|$-user MAC is in outage.

Let us denote with $\mathcal{B}_j^{(i)}$ the $j$-th subset of cardinality $i$ of the $\bar{\mathcal{S}}_{d,t-1}$, where $j \in \{1, \ldots, \binom{|\bar{\mathcal{S}}_{d,t-1}|}{i}\}$ (as there are total of $\binom{|\bar{\mathcal{S}}_{d,t-1}|}{i}$ subsets of cardinality $i$ in the $\bar{\mathcal{S}}_{d,t-1}$). Furthermore, let us denote with $v(a_t)$, where $a_t \in \mathcal{N}$, the number of newly decoded sources at the destination after round $t$ comparing to round $t-1$, by choosing the node $a_t$. The step-by-step algorithm of this strategy is described in Alg. 1.

### 3.2.2 Strategy 2: Node selection based on the highest mutual information

In this strategy, the similar intuitive approach is used as in strategy 1 for the case where multiple nodes can provide the destination with the same number of newly decoded sources. The difference here is that in round $t$, each node that was able to decode at least one source from the set $\bar{\mathcal{S}}_{d,t-1}$ is a candidate node. That is to say, the selection criterion has the following form:

$$\hat{a}_t = \underset{a_t \in \mathcal{S} \cup \mathcal{R}}{\operatorname{argmax}} \{ I_{a_t,d} [\bar{\mathcal{S}}_{d,t-1} \cap \mathcal{S}_{a_t,t-1} \neq \emptyset] \}. \tag{3.9}$$

Obviously, this strategy offers much less computational complexity compared with the previous one.

### 3.2.3 Strategy 3: Node selection based on the highest product of the mutual information and the cardinality of the decoding set

The biggest drawback of the strategy 2 is that a node with small cardinality of the set $|\mathcal{S}_{a_t,t-1}|$ may be chosen. So we propose a modification of that strategy where in each round the destination selects the node $a_t$ with the highest product of $I_{a_t,d} \cdot |\mathcal{S}_{a_t,t-1}|$. Such product could potentially be a good joint indicator of both the amount of the mutual information $I_{a_t,d}$, and the cardinality of the decoding set $|\mathcal{S}_{a_t,t-1}|$.

### 3.2.4 The exhaustive search approach for the best possible activation sequence

Conditional on the knowledge of the CSI of all links in the network, we can find the optimal activation sequence of nodes with respect to normalized average spectral efficiency by using the exhaustive search approach. Since the maximum number of rounds is $T$ and for each round there are $M + L$ possible candidate nodes, the number of possible activation sequences is equal to $(M + L)^T$. For each possible activation sequence, we can check how many sources the destination can decode at any given round. Finally, in order to determine which activation sequence is optimal, the following procedure is used:

- Out of all activation sequences leading to the correct decoding of all the sources at the destination, select the one(s) which necessitates the lowest number of rounds. If there are several activation sequence candidates, choose one of them randomly.

- If no activation sequence leads to the correct decoding of all sources until $T$, then choose the one which is associated with the highest cardinality of the decoding set at $T$. If there are still several activation sequence candidates (which brings the same $|\mathcal{S}_{d,T}|$), choose one of them randomly.

This kind of procedure is computationally very expensive. In addition, we should stress that the knowledge of the CSI of all links would incur extremely large feedback overhead. Thus this strategy has no interest in practice. It is used in Section 3.4 as an upper bound yielding the optimal node selection strategy in case of full CSI knowledge.

## 3.3 Novel HARQ control information exchange procedure

For the node selection strategy 2 proposed in subsection 3.2.2, which offers low complexity and promising performance (which is going to be confirmed in section 3.4), the HARQ mechanism described in chapter 2 incurs unnecessary control overhead on the unicast control channels from the sources and relays towards the destination. Such unicast control signaling is more costly than the control signaling from the destination to the sources and relays, since it is conveyed over the broadcast channel. We propose a novel control information exchange procedure that relies on the specificities of the scheduling rule used in the adopted node selection strategy. The control signaling from the sources and relays towards the destination on the unicast control channels is reduced at the price of increasing the amount of signaling on the broadcast control channel from the destination to sources and relays.

At the beginning of retransmission round $t$ during the second phase, we propose the following control information exchange procedure for the HARQ mechanism, illustrated on Fig. 3.1:

1. The destination broadcasts $M$ bits that indicate its decoding set $\mathcal{S}_{d,t-1}$ after round $t-1$ over the feedback broadcast control channel.

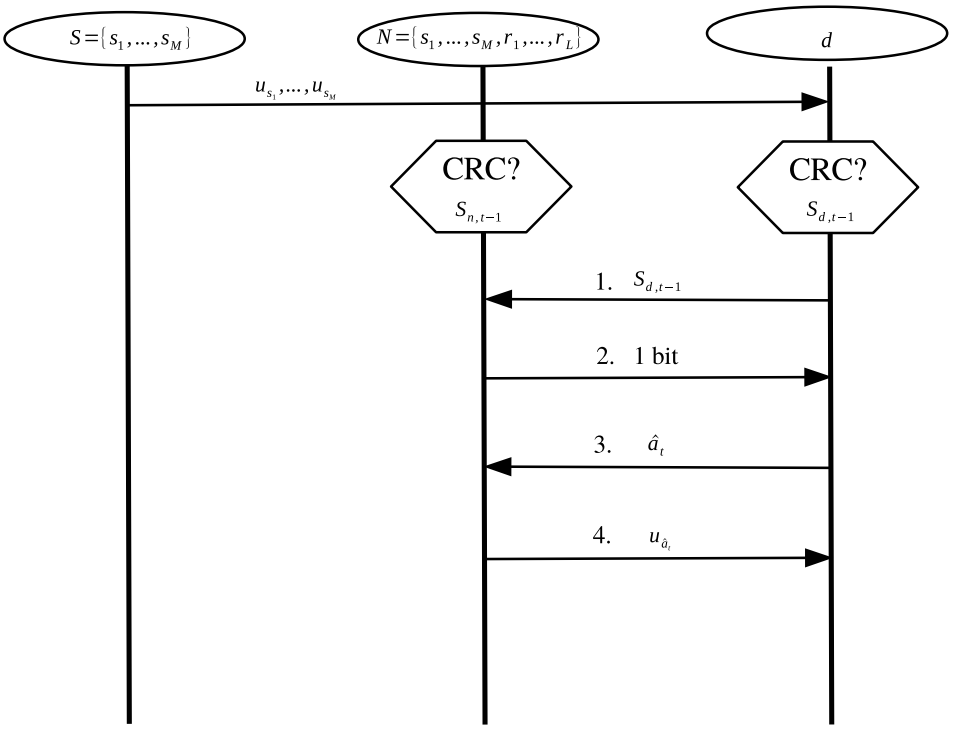


**Figure 3.1:** Control information exchange procedure at the beginning of each time-slot in the second phase.

2. If the decoding set of the destination consists of all source messages, a new frame begins and the sources transmit new messages while the relays and destination empty their memory buffers. Otherwise, each source that perform user co-operation (cooperating source) and each relay which was able to decode at least one source message that is not included in the decoding set of the destination sends 1 bit on a dedicated unicast forward coordination control channel. Each cooperating source or relay which did not decode any message needed by the destination, i.e., any message that is not included in the decoding set of the destination after round $t-1$, remains silent.

3. Using node selection strategy 2, the destination can make the scheduling decision about the node to select for transmission. Its decision is broadcasted using the feedback broadcast control channel.

4. Selected node transmits. It performs Multi User encoding with the messages of the sources that it was able to decode.

## 3.4 Numerical results

In this section, we want to evaluate the performance of the three proposed selection strategies in terms of the average spectral efficiency by performing Monte-Carlo (MC) simulations. Two different selection strategies are used as benchmark. The first one, referred to as "Reference 1" in the figure legends, is the strategy 1 from [137], which is described in section 3.2. The second one uses the exhaustive search approach to find the optimal node selection strategy. It is described in section 3.2.4, and referred to as "Upper-bound" in the figure legends.

We focus on the (3,3,1)-OMAMRC, with $T = 3$ and $\alpha = 0.5$. Independent Gaussian distributed channel inputs is assumed (with zero mean and unit variance), in which case $I_{a,b} = \log_2(1 + |h_{a,b}|^2)$. Some other formulas could be also used for calculating $I_{a,b}$ taking into account, for example, discrete entries, finite length of the codewords, non-outage achieving JNCC/JNCD architectures etc. They would not have any impact on the basic concepts of this work [142]. Without loss of generality, we assume in this section that sources do not perform user co-operation.

In the first part of simulations, we assume a symmetric rate scenario where $R_s = R = 1$ [b.c.u] for all $s \in \mathcal{S}$. All the links in the network are symmetric, i.e., $\gamma_{a,b} = \gamma$, $\forall a \in \mathcal{S} \cup \mathcal{R}$, $\forall b \in \mathcal{R} \cup \{d\}$, and $a \neq b$. Fig. 3.2 shows the average spectral efficiency as a function of $\gamma$ for different strategies.

In the range of low SNR, "Reference 1" strategy is significantly worse in terms of the average spectral efficiency than all the other strategies. Indeed, the minimization of the common outage probability at each round often leads to smaller number of correctly decoded source messages than for the other strategies. Note that the asymptotic limit of the average spectral efficiency for boundless capacity links in the network is equal to $\eta = \sum_{s \in \mathcal{S}} R_s / M$, since in that regime $\mathbb{E}(T_{\text{used}}) \to 0$ and $\Pr\{\mathcal{O}_{s,T}\} \to 0$, $\forall s \in \mathcal{S}$. The three strategies proposed in this paper perform close to each other. Strategy 1 is the best one, and strategy 3 is the worst. We can conclude that strategies 2 and 3 represent a good trade-off between computational complexity and performance. Finally, all the proposed strategies are much closer to the theoretical upper-bound than "Reference 1" strategy, confirming the validity of our intuitive approach.

The same comparison is made keeping a symmetric link scenario in Fig. 3.3. However, here the initial rates are chosen from a discrete Modulation and Coding Scheme (MCS) family whose rates belong to {0.5,1,1.5,2,2.5,3,3.5} [b.c.u]. The initial rates are chosen to maximize the average spectral efficiency with respect to the average SNR (slow link adaptation). Here, the slow link adaptation is very simple since the rates of the sources and the SNR are equal. The slow link

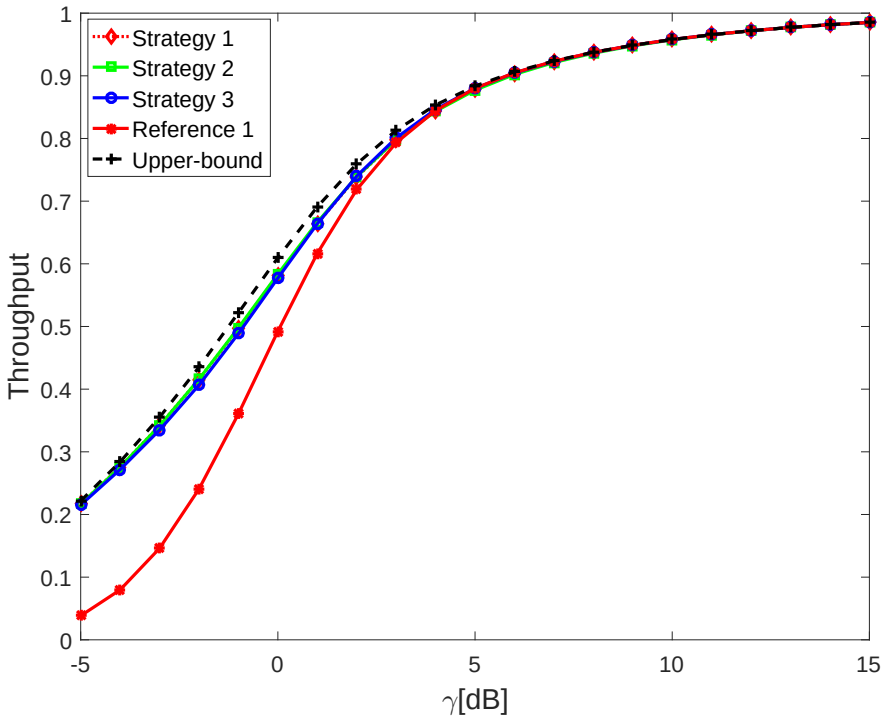


**Figure 3.2:** Average spectral efficiency of different strategies for symmetric rates equal to $R = 1[b.c.u]$, and symmetric links scenario.

adaptation for "Reference 1" is illustrated by the black dotted line that corresponds each to a given initial rate (the same for each source) ranging from 0.5 to 3.5 [b.c.u]. It simply takes the envelope of these curves. The gain of the proposed strategies (within the framework of slow link adaptation) compared with "Reference 1" is approximately 1 dB.

Finally, in the second part of the simulations, we want to illustrate the application of the proposed strategies in an asymmetric source rate scenario, where the initial rates are set to $[R_{s_1} = 3, R_{s_2} = 2.5, R_{s_3} = 2]$ [b.c.u] as an example. Average SNR of all links in the network are also set to be asymmetric and in the range: $\gamma_{a,b} \in \{-10\text{dB}, \ldots, 15\text{dB}\}$. This time, the average spectral efficiency, shown on the Fig. 3.4, is a function of $\Delta_\gamma$, which is added to each individual link simultaneously with respect to the starting asymmetric link configuration. Obviously, "Reference 1" strategy is left out from the simulations. We observe that the performance of the proposed strategies remains close to the upper-bound.

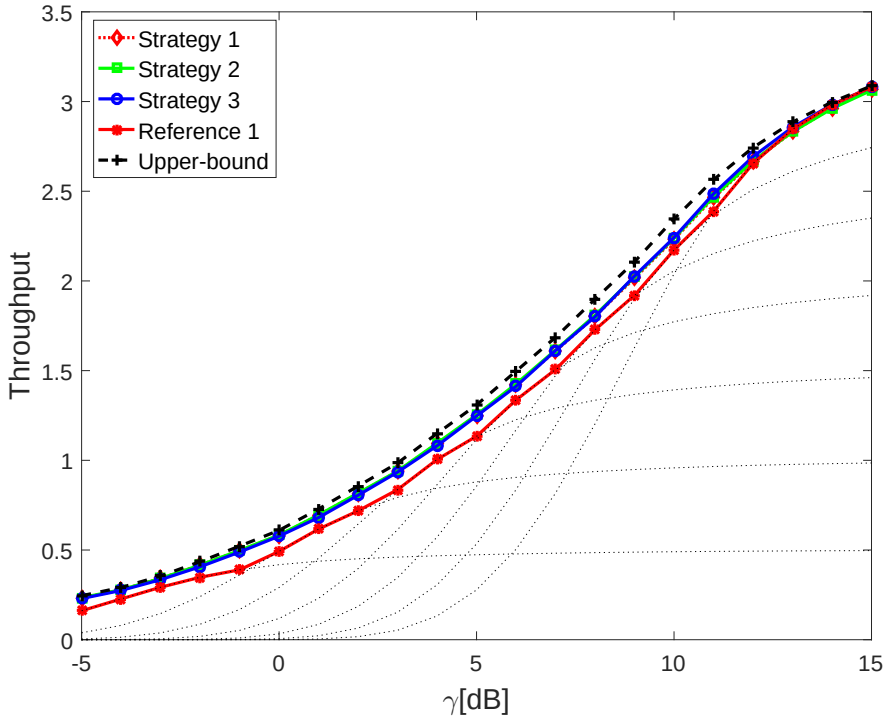


**Figure 3.3:** Average spectral efficiency of different strategies with slow link adaptation and symmetric link scenario.

**Algorithm 1** Node selection process of strategy 1.

$v(a'_t) \leftarrow 0$, $\forall a'_t \in \mathcal{N}$. ▷ Initialization.
$\max_v \leftarrow 0$. ▷ We track the maximum $v(a_t)$.
**for** $n \leftarrow 1$ **to** $|\mathcal{N}|$ **do**
    $a_t \leftarrow \mathcal{N}(n)$. ▷ Pick a new candidate node.
    **if** $\bar{\mathcal{S}}_{d,t-1} \cap \mathcal{S}_{a_t,t-1} = \emptyset$ **then**
        **continue**. ▷ $v(a_t) = 0$ remains.
    **end if**
    found $\leftarrow 0$. ▷ Indicator that we found $v(a_t)$.
    **for** $i \leftarrow |\bar{\mathcal{S}}_{d,t-1}|$ **to** $1$ **do**
        **for** $j \leftarrow 1$ **to** $\binom{|\bar{\mathcal{S}}_{d,t-1}|}{i}$ **do**
            Calculate $\mathcal{E}_{t,\mathcal{B}_j^{(i)}}(a_t, \mathcal{S}_{a_t,t-1})$ (using (3.4)).
            **if** $\mathcal{E}_{t,\mathcal{B}_j^{(i)}}(a_t, \mathcal{S}_{a_t,t-1}) = 0$ **then**
                $v(a_t) \leftarrow i$.
                **if** $v(a_t) > \max_v$ **then**
                    $\max_v = v(a_t)$.
                **end if**
                found $\leftarrow 1$.
                **break**.
            **end if**
        **end for**
        **if** found $= 1$ **then**
            **break**.
        **end if**
    **end for**
**end for**
$\mathcal{A}'_t \leftarrow \emptyset$. ▷ Set of candidate nodes with maximum $v(a_t)$.
**for** $n \leftarrow 1$ **to** $|\mathcal{N}|$ **do**
    $a_t \leftarrow \mathcal{N}(n)$.
    **if** $v(a_t) = \max_v$ **then**
        $\mathcal{A}'_t \leftarrow \mathcal{A}'_t \cup \{a_t\}$.
    **end if**
**end for**
$\hat{a}_t \leftarrow \text{argmax}_{a_t \in \mathcal{A}'_t}\{I_{a_t,d}\}$.

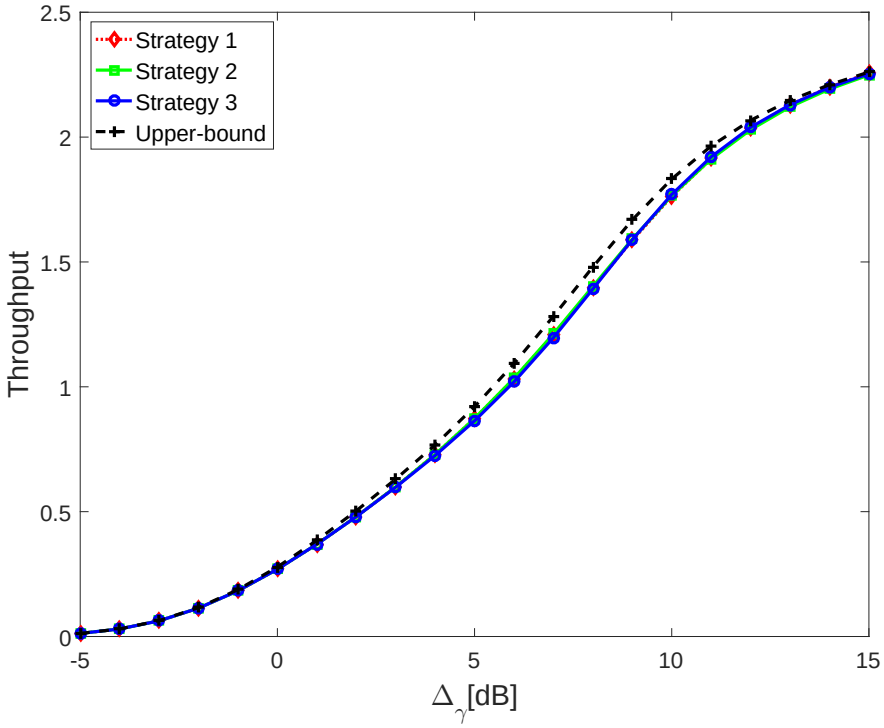


**Figure 3.4:** Average spectral efficiency of different strategies for asymmetric rates $[R_{s_1} = 3, R_{s_2} = 2.5, R_{s_3} = 2]$[b.c.u], and asymmetric link scenario.

# 4 | Link Adaptation Algorithms

In this chapter, for the $(M, L, 1)$-MAMRC under system model assumptions described in chapter 2, we propose a slow-link adaptation (rate allocation) algorithm that aims at maximizing the average spectral efficiency after a fixed number of $T$ retransmissions, under the QoS constraint on the individual average BLER for each source $s_i$, where $i \in \{1, \ldots, M\}$. Additionally, we propose a fast-link adaptation algorithm where in each frame the goal is to maximize the spectral efficiency after a fixed maximum number of $T$ retransmissions. In both cases the defined utility metric is conditional on the node selection strategy that is used in the second phase. The proposed algorithms try to accurately allocate the rates for different choices of the node selection strategy.

## 4.1 Slow-link adaptation algorithm

### 4.1.1 Problem formulation

Let us remind ourselves of the definition of the average spectral efficiency for the scenario of fast changing radio conditions and fixed source rates during multiple frames, stated in chapter 3, and used as the performance metric in this chapter:

$$\eta^{\text{sla}} = \sum_{i=1}^{M} \frac{R_s}{M + \alpha \mathbb{E}(T_{\text{used}})} (1 - \Pr\{\mathcal{O}_{s_i,T}\}), \tag{4.1}$$

where $\mathcal{O}_{s,T}$ has the same definition as in chapter 3. The individual outage probability $\Pr\{\mathcal{O}_{s,t}\}$ stands in practice for the average BLER of source $s$ after $t$ retransmissions. In the following, we denote it either $\Pr\{\mathcal{O}_{s,t}\}$ or $BLER_{s,t}$.

In MAMRC network, the knowledge of instantaneous CSI of all the links allows link adaptation algorithm to allocate the rates of sources in the most accurate way (fast-link adaptation). Since the number of channels in such a network grows

exponentially with the number of sources and relays, frequent changes of the channel states (e.g. in high mobility scenario) can incur excessive amount of control signaling on forward coordination control channels. In that case, fast-link adaptation is deemed impractical, and slow-link adaptation is a more suitable solution. The idea of slow-link adaptation is to adapt the rates of sources to Channel Distribution Information (CDI) of all links, which remain constant during longer periods of time.

Let the source $s$ transmit with the rate $R_s$, and let us denote the average BLER after $T$ rounds with $BLER_{s,T}(R_s)$. In the point-to-point link scenario, the individual throughput of the source $s$ is given by $\eta_s = \bar{R}_s \times (1 - BLER_{s,T}(R_s))$. In order to maximize it, the usual practice would be to find the optimal pair $(R_s, BLER_{s,T}(R_s))$. In the MAMRC setup however, $BLER_{s,T}$ depends on the vector of rates $(R_{s_1}, \ldots, R_{s_M})$. The same holds for fast-link adaptation, except that $BLER_{s,T}$ is replaced by $[\mathcal{O}_{s,T}]$ which takes either the value 0 or 1. The reason for the dependence of $BLER_{s,T}$ on all sources' rates lies in the fact that the decoding set of the selected node in the given round depends on all the rates, which influences the probability of non-successful decoding of the message of the source $s$. Hence, in theory, all $(R_{s_1}, \ldots, R_{s_M})$ need to be optimized jointly in order to reach the optimal solution.

In order to be precise with the notation, we distinguish hereafter $R_{s_i}$, the rate of source $s_i$ after the optimization, and $R_i$, one possible value of $R_{s_i}$ taken from the set of possible rates $\{\hat{R}_1, \ldots, \hat{R}_{n_{\text{MCS}}}\}$, where $n_{\text{MCS}}$ is the number of different MCSs.

In general, the optimization problem that is needed to be solved under the given individual QoS constraints for slow-link adaptation is given by (4.2). It should be noted that $\Pr\{\mathcal{O}_{s,T}\}$ is conditional on the node activation sequence.

$$\begin{aligned}(R_{s_1}, \ldots, R_{s_M}) = \underset{(R_1,\ldots,R_M)\in\{\hat{R}_1,\ldots,\hat{R}_{n_{\text{MCS}}}\}^M}{\text{argmax}} & \sum_{i=1}^{M} \frac{R_i}{M + \alpha\mathbb{E}(T_{used})}\Big(1 - \Pr\{\mathcal{O}_{s_i,T}\}\Big), \\ & \text{subject to } \Pr\{\mathcal{O}_{s_i,T}\} \leq BLER_{\text{QoS},s_i},\ \forall i \in \{1, \ldots, M\}.\end{aligned} \tag{4.2}$$

Solution for a given problem is analytically intractable to the knowledge of the authors. Namely, it is hard to predict what is the decoding set of each node in a given round, as it depends on the rates of sources, which we are trying to find in the first place. The same conclusion holds even in the case where the node activation sequence is pre-determined and known in advance.

Nevertheless, in this chapter we are interested in case where some optimized node scheduling strategy is used, i.e., the node activation sequence cannot be known in

advance. We retain here the scheduling strategy 2 from chapter 3, which tries to "optimally" select a node in each time-slot of the second phase in order to maximize the number of correctly decoded messages at the destination. More precisely, in each retransmission round the destination selects the node with the highest mutual information between itself and that node, among all nodes which were able to decode at least one source from the set of non-successfully decoded sources at the destination. We will refer to this strategy as the "optimized" node selection strategy in the following.

One way to find the solution of a problem given by 4.2 would be to exhaustively check all $n_{\mathrm{MCS}}^{M}$ possible combinations of allocated rates, and to choose the one which maximizes the average spectral efficiency subject to individual QoS constraints. Obviously, such an approach is computationally very expensive.

### 4.1.2 Solution of the optimization problem based on "Genie-Aided" assumption

In order to reduce the complexity, we can resort to an approach that is based on "Genie-Aided" assumption, where all the sources $s \in \mathcal{S} \backslash s_i = \{s_1, s_2, \ldots, s_{i-1}, s_{i+1}, \ldots, s_M\}$ except the one for which we want to allocate the rate, $s_i$, are assumed to be decoded correctly at the destination and relaying nodes (by "relaying nodes" we consider both relays and sources which perform user co-operation). In that way we decouple the problem, as the dependence of the decoding set of potentially selected cooperating nodes on sources other than the considered one is avoided. From a viewpoint of a source $s_i$, the multiple access multiple relay network reduces to (1,$L+M-1$,1) multiple relay network. An example is given on Fig. 4.1 for $s_i = s_1$, where the sources $\{s_2, \ldots, s_M\}$ are symbolically denoted by $\{r_{L+1}, \ldots, r_{L+M-1}\}$, as they only serve as relays. Under such an assumption, when "optimized" node selection strategy is used in the second phase, the sequence of selected nodes does not correspond to the one where "Genie-Aided" assumption is not made, and which is quite impossible to predict. Indeed, since source $s_i$ is the only one which is not decoded correctly at the destination, all the scheduling decisions are oriented towards helping him exclusively, which results in an allocated rate higher than the optimal one. Possibly a better approximation of the realistic node selection sequence while evaluating rate $R_{s_i}$ is a random node activation sequence, and that approach is adopted in the rest of the chapter.

Hence, although the initial rates found under "Genie-Aided" assumption are not the exact solutions of the maximization problem (4.2), they can serve as a good starting point for finding close to the optimal solution. Indeed, even though we always consider that only one source is not decoded correctly, which is not a realistic

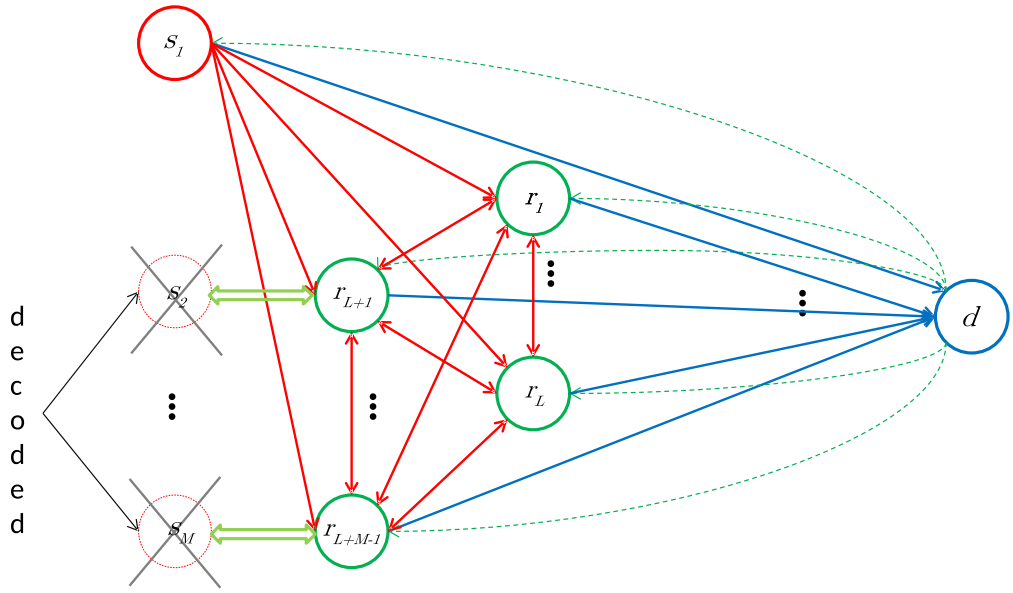


**Figure 4.1:** "Genie-Aided" assumption, where all the sources except for source $s_1$ are assumed decoded correctly at the destination.

assumption, and that node activation sequence is purely random, we take into account the quality of all the links which can potentially help the transmission of a given source in the calculation. Not surprisingly, this approach gives a more accurate solution if the prior knowledge of the activation sequence is available.

In this chapter, in the slow-link adaptation scenario we assume that the channel statistics of each link follows a centered circularly complex Gaussian distribution. Since the links are independent from each other, the average SNR of each link is sufficient as an input to trace back the statistics of each link. Given the simplified, $(1,L+M-1,1)$ network, the problem of finding the maximum rate $R_{s_i}$ for the source $s_i$ subject to $BLER_{\mathrm{QoS},s_i}$ constraint has the following form:

$$R_{s_i}^{\mathrm{sla}} = \underset{R_i \in \{\hat{R}_1,\ldots,\hat{R}_{n_{\mathrm{MCS}}}\}}{\operatorname{argmax}} \left\{ \frac{R_i}{M+\alpha\mathbb{E}(T_{used})} \Big( 1 - \int \Big[ R_i > I_{s_i,d} + \sum_{l=1}^{T} \alpha I_{\hat{a}_l,d}[s_i \in \mathcal{S}_{\hat{a}_l,l-1}] \Big] P(\mathbf{H}) \mathrm{d}\mathbf{H} \Big) \right\}$$
$$\text{subject to } \Pr\{\mathcal{O}_{s_i,T}\} \leq BLER_{\mathrm{QoS},s_i}, \tag{4.3}$$

where $P(\mathbf{H})$ is the joint probability of channel realizations of all the links in the network.

A detailed step-by-step algorithm in which a rate is allocated to source $s_i$ under "Genie-Aided" assumption with CDI available at the destination (slow-link adaptation) is given by Algo. 2. In the algorithm, each possible candidate rate from the set $\{\hat{R}_1, \ldots, \hat{R}_{n_{\text{MCS}}}\}$ is considered one after another in the first "for loop" on $j$. The second "for loop" allows to average out the individual BLER, or $\Pr\{\mathcal{O}_{s,T}\}$, for the given rate $R_j$ over Nb_MC realizations of all channels. The averaging is done according to statistics given by average SNRs of all links. Hence, inside the loop *cnt* the quality of each channel is known, since they result from the random realization of all channels. Therefore, in order to calculate (4.3), it is sufficient to use the Monte-Carlo (MC) simulations approach, where the integral is replaced by the sum:

$$\begin{aligned}&\int \left[R_i > I_{s_i,d} + \sum_{l=1}^{T} \alpha I_{\hat{a}_l,d}[s_i \in \mathcal{S}_{\hat{a}_l,l-1}]\right] P(\mathbf{H})\mathrm{d}\mathbf{H} \\ &= \frac{1}{\text{Nb\_MC}} \sum_{cnt=1}^{\text{Nb\_MC}} \left[R_i > I_{s_i,d}(\mathbf{H}_{cnt}) + \sum_{l=1}^{T} \alpha I_{\hat{a}_l,d}(\mathbf{H}_{cnt})[s_i \in \mathcal{S}_{\hat{a}_l,l-1}]\right].\end{aligned}$$

Note that the variable *out* from Algo. 2 basically corresponds to:

$$out = \left[R_i > I_{s_i,d}(\mathbf{H}_{cnt}) + \sum_{l=1}^{T} \alpha I_{\hat{a}_l,d}(\mathbf{H}_{cnt})[s_i \in \mathcal{S}_{\hat{a}_l,l-1}]\right].$$

### 4.1.3 Iterative rate correction algorithm for allocated rates

In the case of "optimized" node selection strategy used in the second phase, one of the main causes for the inaccuracy of the link adaptation algorithm under GA assumption is the absence of knowledge of the exact sequence of node activation. The latter depends in practice on all sources' rates. For that reason, we propose the application of an algorithm with the goal to correct those rates. The main idea of this algorithm is inspired by the "iterative water-filling algorithm", and its main steps are given in Algo. 3. Without loss of generality and for the sake of notation simplicity, we assume that the steps between the rates of the considered MCS family are the same and denoted $\Delta$, i.e., $\Delta = \hat{R}_{i+1} - \hat{R}_i, \forall i \in \{1, \ldots, n_{\text{MCS}} - 1\}$.

At the beginning, all the sources' rates are initialized using the output of the algorithm based on GA assumption with a random node selection: $R_{s_1}(0), \ldots, R_{s_M}(0)$ (note that some other node selection strategy could be used under GA assumption to obtain the initial point). In the given iteration $t$, all the sources' rates are

**Algorithm 2** Slow-link adaptation algorithm based on "Genie-Aided" assumption for source $s_i$ s.t. $BLER_{\mathrm{QoS},s_i}$ target.

**for** $j \leftarrow 1$ **to** $n_{\mathrm{MCS}}$ **do** ▷ Number of candidate rates.
  Pick sequentially $R_j \in \{\hat{R}_1, \ldots, \hat{R}_{n_{\mathrm{MCS}}}\}$.
  $out \leftarrow 0$. ▷ Counter of iterations leading to outage.
  $\bar{T}_{used} \leftarrow 0$. ▷ Accumulated nb. of rounds used in the 2. phase.
  **for** $cnt \leftarrow 1$ **to** Nb_MC **do** ▷ Max. number of MC sim.
    Draw $\mathbf{H}_{cnt}$ based on $P(\mathbf{H})$.
    Calculate $I_{a,b}(\mathbf{H}_{cnt})$ for $\forall a \in \mathcal{N}, \forall b \in \{\mathcal{N} \cup \{d\} \setminus \{a\}\}$.
    **if** $R_j \leq I_{s_i,d}$ **then**
      $\mathcal{S}_{d,0} \leftarrow \mathcal{S}_{d,0} \cup \{s_i\}$.
      **continue**. ▷ $out$ and $\bar{T}_{used}$ do not change.
    **end if**
    **for** $t \leftarrow 1$ **to** $T$ **do** ▷ For each round we do:
      Random node selection by the scheduler: $\hat{a}_t$.
      $C_1 \leftarrow I_{s_i,\hat{a}_t} + \sum_{k=1}^{t-1} \alpha I_{\hat{a}_k,\hat{a}_t}[s_i \in \mathcal{S}_{\hat{a}_k,k-1}]$. ▷ Accumulated mutual information between $s_i$ and $\hat{a}_t$.
      **if** $R_j \leq C_1$ **then** ▷ Check if $\hat{a}_t$ has decoded $s_i$.
        $\mathcal{S}_{\hat{a}_t,t-1} \leftarrow \mathcal{S}_{\hat{a}_t,t-1} \cup \{s_i\}$.
      **end if**
      $C_2 \leftarrow I_{s_i,d} + \sum_{k=1}^{t} \alpha I_{\hat{a}_k,d}[s_i \in \mathcal{S}_{\hat{a}_k,k-1}]$.
      **if** $R_j \leq C_2$ **then** ▷ Check if the dest. has decoded $s_i$.
        $\mathcal{S}_{d,t} \leftarrow \mathcal{S}_{d,t} \cup \{s_i\}$.
        $T_{used} \leftarrow t$. ▷ Nb. of rounds used for the current MC iteration.
        **break**. ▷ $out$ does not change.
      **end if**
      **if** $t = T$ **then**
        $out \leftarrow out + 1$.
        $T_{used} \leftarrow T$.
      **end if**

28: **end for**
29: $\bar{T}_{used} \leftarrow \bar{T}_{used} + T_{used}$.
30: **end for**
31: $P^{out}_{s_i,R_j} \leftarrow \frac{out}{\text{Nb\_MC}}$ ▷ The average outage prob. of $s_i$ with $R_j$.
32: $\mathbb{E}(T_{used,R_j}) \leftarrow \frac{\bar{T}_{used}}{\text{Nb\_MC}}$ ▷ The avg. nb. of rounds used in the 2. phase.
33: **end for**
34: Choose the maximum supported rate $R_{s_i}$ for source $s_i$:
$R_{s_i} \leftarrow \text{argmax}_{R_j \in \{\hat{R}_1,\ldots,\hat{R}_{n_{\text{MCS}}}\}} \left\{ \frac{R_j}{M+\alpha\mathbb{E}(T_{used,R_j})} \left(1 - P^{out}_{s_i,R_j}\right) \right\}$,
subject to $P^{out}_{s_i,R_j} \leq BLER_{\text{QoS},s_i}$.

updated in a cyclic fashion. The rate of source $s_i$ is a function of the sources' rates updated in the same iteration prior to source $s_i$ (sources with index $i' < i$), and the rates updated for the last time in the previous iteration, $t-1$ (sources with index $i'' > i$).

The principle of the update function for source $s_i$ is to, starting from the rate calculated in the previous iteration $R_{s_i}(t) = R_{s_i}(t-1)$, check whether the average spectral efficiency $\eta_{\text{current}}$ increase or decrease by increasing it to the first higher candidate rate $R_{s_i}(t) + \Delta$. Additionally, we check if the condition that each individual BLER is below the corresponding target, $BLER_{\text{check}}$, is true. If both conditions are met, we continue to increase the rate $R_{s_i}(t)$ and to check those conditions until we arrive to the case where in $SW$ consecutive points at least one of those conditions is not met (when we proclaim the event $finished\_increasing$ to be true in Algo. 3 in order to proceed). The last value of rate $R_{s_i}$ which led both conditions to be true is kept, and the algorithm proceed to the next source. In Algo. 3, variable *max_throughput* is used to store the value of the maximum average spectral efficiency that could be obtained, found until that moment, while variables $[R_1^{\text{opt}}, \ldots, R_M^{\text{opt}}]$ are the rates that reach it. In the case where one of the conditions is not met when we increase rate $R_{s_i}$ for the first time, we go in the other direction, meaning that we keep decreasing rate $R_{s_i}$ to the first lower candidate rate $R_{s_i}(t) - \Delta$ as long as we don't arrive to $SW$ consecutive points where at least one of those conditions is not met (when $finished\_decreasing$ becomes true). Variable *check_lower_rates* is simply used to restrain the algorithm from going into the direction of decreasing the rate of a given source in the case where its first increase leads to the augmentation of the average spectral efficiency and to $BLER_{\text{check}}$ being true. Of course, whenever we increase or decrease rate $R_{s_i}(t)$ we always keep in mind the minimum and the maximum candidate source rate. We adopt the rule where even if the lowest available candidate rates lead to at least one individual $BLER_{s_i}$ higher than $BLER_{\text{QoS},s_i}$, those same rates are allocated

**Algorithm 3** Iterative rate correction for slow-link adaptation algorithm under the QoS constraints on individual BLER targets $BLER_{\mathrm{QoS},s_i}, \forall i \in \{1,\ldots,M\}$.

$t \leftarrow 0$. ▷ Counter of iterations.
Set the candidate rates: $\{\hat{R}_1,\ldots,\hat{R}_{n_{\mathrm{MCS}}}\}$.
Rate initialization under GA assumption with the random node selection: $R_{s_1}(0),\ldots,R_{s_M}(0)$.
Calculate $\eta(R_{s_1}(0),\ldots,R_{s_M}(0))$.
$max\_throughput \leftarrow \eta(R_{s_1}(0),\ldots,R_{s_M}(0))$.
**while** $(|R_{s_i}(t) - R_{s_i}(t-1)| > 0$, for any $i \in \{1,\ldots,M\})$ **do** ▷ e.g. $R_{s_1}(-1) = 0$
    $t \leftarrow t+1$.
    **for** $i \leftarrow 1$ **to** $M$ **do**
        $count\_SW \leftarrow 0$ ▷ Counter of adjacent rates that result in smaller $\eta$ or $BLER_{\mathrm{check}} = 0$.
        $R_{s_i}(t) \leftarrow R_{s_i}(t-1)$. ▷ We start with the rate from the previous iteration.
        $finished\_increasing \leftarrow 0$. ▷ Aux. variable, to stop increasing the rate.
        $finished\_decreasing \leftarrow 0$. ▷ Aux. variable, to stop decreasing the rate.
        **while** $\Big((R_{s_i}(t) < \hat{R}_{n_{\mathrm{MCS}}})$ **and** $(finished\_increasing = 0)\Big)$ **do**
            $R_{s_i}(t) \leftarrow R_{s_i}(t) + \Delta$. ▷ Increase to the first higher candidate rate.
            Calculate $\eta_{\mathrm{current}} \leftarrow \eta(R_{s_1}(t),\ldots,R_{s_i}(t),R_{s_{i+1}}(t-1),\ldots,R_{s_M}(t-1))$.
            $BLER_{\mathrm{check}} \leftarrow \Big[BLER_{s_i} \leq BLER_{\mathrm{QoS},s_i}, \forall i \in \{1,\ldots,M\}\Big]$.
            **if** $\Big((\eta_{\mathrm{current}} > max\_throughput)$ **and** $BLER_{\mathrm{check}}\Big)$ **then**
                $check\_lower\_rates \leftarrow 0$. ▷ No need to decrease the rates.
                $max\_throughput \leftarrow \eta_{\mathrm{current}}$. ▷ Maximum throughput updated.
                $[R_1^{\mathrm{opt}},\ldots,R_M^{\mathrm{opt}}] \leftarrow [R_{s_1}(t),\ldots,R_{s_i}(t),R_{s_{i+1}}(t-1),\ldots,R_{s_M}(t-1)]$.
            **else** ▷ If conditions are not met.
                $count\_SW \leftarrow count\_SW + 1$. ▷ We increase the counter.
                **if** $\Big((count\_SW = SW)$ **or** $(R_{s_i}(t) = \hat{R}_{n_{\mathrm{MCS}}})\Big)$ **then**
                    $R_{s_i}(t) \leftarrow R_{s_i}(t) - count\_SW \times \Delta$.
                    $finished\_increasing \leftarrow 1$; ▷ We reverse $R_{s_i}$ to one which gives max $\eta$.
                **end if**
            **end if**
        **end while**

29: **if** $(check\_lower\_rates = 0)$ **then**
30: **continue** ▷ No need to decrease the rate.
31: **end if**
32: $count\_SW \leftarrow 0.$ ▷ We reset $count\_SW$.
33: **while** $\Big((R_{s_i}(t) > \hat{R}_1)$ **and** $(finished\_decreasing = 0)\Big)$ **do**
34: $R_{s_i}(t) \leftarrow R_{s_i}(t) - \Delta.$ ▷ Decrease to the first lower candidate rate.
35: Calculate $\eta_{\text{current}} \leftarrow \eta(R_{s_1}(t), \ldots, R_{s_i}(t), R_{s_{i+1}}(t-1), \ldots, R_{s_M}(t-1)).$
36: $BLER_{\text{check}} \leftarrow \Big[BLER_{s_i} \leq BLER_{\text{QoS},s_i}, \forall i \in \{1, \ldots, M\}\Big].$
37: **if** $\Big((\eta_{\text{current}} > max\_throughput)$ **and** $BLER_{\text{check}}\Big)$ **then**
38: $max\_throughput \leftarrow \eta_{\text{current}}.$ ▷ Maximum throughput updated.
39: $[R_1^{\text{opt}}, \ldots, R_M^{\text{opt}}] \leftarrow [R_{s_1}(t), \ldots, R_{s_i}(t), R_{s_{i+1}}(t-1), \ldots, R_{s_M}(t-1)].$
40: **else**
41: $count\_SW \leftarrow count\_SW + 1.$ ▷ We increase the counter.
42: **if** $\Big((count\_SW = SW)$ **or** $(R_{s_i}(t) = \hat{R}_1)\Big)$ **then**
43: $R_{s_i}(t) \leftarrow R_{s_i}(t) + count\_SW \times \Delta.$
44: $finished\_decreasing \leftarrow 1.$ ▷ We reverse $R_{s_i}$ to one which gives max $\eta$.
45: **end if**
46: **end if**
47: **end while**
48: **end for**
49: **end while**

to all sources. In the most standard case where $SW = 1$ and where there are no constraints on individual BLERs, this kind of procedure translates to the rule where we keep increasing (or decreasing) the rate of a given source as long as the average spectral efficiency increases, before proceeding to the next source.

The complexity of the proposed iterative rate correction algorithm is much smaller than in the case of the exhaustive search approach algorithm. In the later, the calculation of each individual BLER is performed ${n_{\text{MCS}}}^M$ times, while in the proposed algorithm, in one iteration the same calculation is performed at most $n_{\text{MCS}} \times M$ times (the worst possible case in theory, which is highly unlikely).

## 4.2 Fast-link adaptation algorithm

For the scenario where the source rates are adapted to the instantaneous link conditions, we use the similar reasoning for a design of a two-step, fast-link

adaptation algorithm, as in the case of the slow-link adaptation algorithm. For that reason, in the following, our main focus will be set on its differences compared with the slow-link adaptation one.

### 4.2.1 Problem formulation

In this scenario, the goal is to maximize the spectral efficiency for each new instance of the channels in the network. Hence, the number of rounds used in the second phase $T_{used}$ directly figures in the expression of the spectral efficiency, while the individual outage event $\mathcal{O}_{s_i,T}$ is either true or not (there is no reason to consider its probability):

$$\eta^{\text{fla}} = \mathbb{E}\left\{\sum_{i=1}^{M} \frac{R_{s_i}}{M + \alpha T_{\text{used}}}(1 - [\mathcal{O}_{s_i,T}])\right\}. \tag{4.4}$$

where $R_s$, $T_{\text{used}}$ and $\mathcal{O}_{s_i,T}$ are random variables depending on the CSI and the scheduling strategy, having the same definition as in section 4.1.

In the definition of the optimization problem that is needed to be solved, we again replace $\Pr\{\mathcal{O}_{s_i,T}\}$ with $[\mathcal{O}_{s_i,T}]$ and $\mathbb{E}(T_{used})$ with $T_{used}$, since link adaptation is performed for each new instance of the channels:

$$(R_{s_1}, \ldots, R_{s_M}) = \underset{(R_1,\ldots,R_M)\in\{\hat{R}_1,\ldots,\hat{R}_{n_{\text{MCS}}}\}^M}{\text{argmax}} \sum_{i=1}^{M} \frac{R_i}{M + \alpha T_{used}}\Big(1 - [\mathcal{O}_{s_i,T}]\Big). \tag{4.5}$$

Obviously, since we do not consider the probabilities of the individual outage events there can be no QoS constraints, i.e. $BLER_{\text{QoS},s_i} = 1$ for $\forall i \in \{1, \ldots, M\}$.

### 4.2.2 Solution of the optimization problem based on "Genie-Aided" assumption

Under the "Genie-aided" assumption for fast-link adaptation, where all the sources except for source $s_i$ are considered to be successfully decoded by the destination, the problem of finding its optimal rate $R_{s_i}$ simplifies to the following:

$$R_{s_i}^{\text{fla}} = \underset{R_i\in\{\hat{R}_1,\ldots,\hat{R}_{n_{\text{MCS}}}\}}{\text{argmax}} \left\{\frac{R_i}{M + \alpha T_{used}}\Big(1 - \Big[R_i > I_{s_i,d} + \sum_{l=1}^{T} \alpha I_{\hat{a}_l,d}[s_i \in \mathcal{S}_{\hat{a}_l,l-1}]\Big]\Big)\right\}. \tag{4.6}$$

The fast-link adaptation algorithm under the "Genie-Aided" assumption is given by Algo. 4. The main difference in comparison with the slow-link adaptation algorithm

is the absence of the averaging of the individual outage probability over Nb_MC realizations of all channels. For that reason, variables $\bar{T}_{used}$, $P^{out}_{s_i,R_j}$ and $\mathbb{E}(T_{used,R_j})$ are not used, just as "for" loop on *cnt*. Variable *out* in this case simply takes the value 0 or 1. Additionally, instead of drawing the channels $\mathbf{H}_{cnt}$, it is assumed that $\mathbf{H}$ is already known at the destination due to available CSI information of all channels.

**Algorithm 4** Fast-link adaptation algorithm based on "Genie-Aided" assumption for source $s_i$.

**for** $j \leftarrow 1$ **to** $n_{\text{MCS}}$ **do** ▷ Number of candidate rates.
  Pick sequentially $R_j \in \{\hat{R}_1, \ldots, \hat{R}_{n_{\text{MCS}}}\}$.
  $out \leftarrow 0$.
  $T_{used}$
  Calculate $I_{a,b}(\mathbf{H})$ for $\forall a \in \mathcal{N}, \forall b \in \{\mathcal{N} \cup \{d\} \setminus \{a\}\}$.
  **if** $R_j \leq I_{s_i,d}$ **then**
    $\mathcal{S}_{d,0} \leftarrow \mathcal{S}_{d,0} \cup \{s_i\}$.
    **continue**. ▷ *out* and $T_{used}$ do not change.
  **end if**
  **for** $t \leftarrow 1$ **to** $T$ **do** ▷ For each round we do:
    Random node selection by the scheduler: $\hat{a}_t$.
    $C_1 \leftarrow I_{s_i,\hat{a}_t} + \sum_{k=1}^{t-1} \alpha I_{\hat{a}_k,\hat{a}_t}[s_i \in \mathcal{S}_{\hat{a}_k,k-1}]$. ▷ Acc. mut. inf. between $s_i$ and $\hat{a}_t$.
    **if** $R_j \leq C_1$ **then** ▷ Check if $\hat{a}_t$ has decoded $s_i$.
      $\mathcal{S}_{\hat{a}_t,t-1} \leftarrow \mathcal{S}_{\hat{a}_t,t-1} \cup \{s_i\}$.
    **end if**
    $C_2 \leftarrow I_{s_i,d} + \sum_{k=1}^{t} \alpha I_{\hat{a}_k,d}[s_i \in \mathcal{S}_{\hat{a}_k,k-1}]$.
    **if** $R_j \leq C_2$ **then** ▷ Check if the dest. has decoded $s_i$.
      $\mathcal{S}_{d,t} \leftarrow \mathcal{S}_{d,t} \cup \{s_i\}$.
      $T_{used} \leftarrow t$. ▷ Nb. of rounds used for the current MC iteration.
      **break**. ▷ *out* does not change.
    **end if**
    **if** $t = T$ **then**
      $out \leftarrow 1$.
      $T_{used} \leftarrow T$.
    **end if**
  **end for**
**end for**
Choose the maximum supported rate $R_{s_i}$ for source $s_i$:
$R_{s_i} \leftarrow \text{argmax}_{R_j \in \{\hat{R}_1,\ldots,\hat{R}_{n_{\text{MCS}}}\}} \left\{ \frac{R_j}{M+\alpha T_{used}} \left(1 - out\right) \right\}$.

### 4.2.3 Iterative rate correction algorithm for allocated rates

Iterative rate correction algorithm in the case of of available CSI at the destination (fast-link adaptation) relies on the similar idea as the one used for slow-link adaptation case. Obviously, the biggest difference is the absence of verifications of the individual BLER conditions. Also, the parameter $\eta_{\text{current}}$ now simply denotes the spectral efficiency, as there is no averaging being done. This scenario has actually motivated the introduction of parameter $SW$ (whose name is inspired by the term "sliding window") and checks on multiple consecutive points whether the spectral efficiency cease to further increase with the increase (or decrease) of the source rate, since the changes of discrete variable $T_{used}$ can lead to the local minimums of the function $\eta^{\text{fla}}(R_s)$. Its main steps are given by Algo 5.

## 4.3 Numerical results

In this chapter, we validate the proposed slow-link and fast-link adaptation algorithms by performing MC simulations. In all simulation scenarios we consider (3,3,1)-OMAMRC, with $T = 4$ and $\alpha = 0.5$. The "optimized" node selection strategy is assumed to be used in the second phase. The allocated rates are chosen from a discrete MCS family whose rates belong to the set {0.5,1,1.5,2,2.5,3,3.5} [b.c.u]. We assume independent Gaussian distributed channel inputs (with zero mean and unit variance), with $I_{a,b} = \log_2(1 + |h_{a,b}|^2)$. Note that again, just an noted in section 3.4 some other formulas could be used for calculating $I_{a,b}$.

Asymmetric link configuration is assumed, where the average SNR of each link is set as follows. First, the average SNR of each link is set to $\gamma$. Second, the average SNR of each link that includes source $s_2$ is reduced by 4dB. Third, the average SNR of each link that includes source $s_3$ is reduced by 7dB. Finally, the average SNR of the link between the sources $s_2$ and $s_3$ is set to $\gamma - 5$dB. In that way, we have set on purpose the source $s_1$ to be in the best propagation conditions, while the source $s_3$ is in the worst ones.

In the first part of simulations, we validate the performance of the slow-link adaptation algorithm under the constraint on the individual BLER target after $T$ retransmissions for each source set to $BLER^{(1)}_{\text{QoS}} = 1$. This kind of choice for the individual BLER targets corresponds to a pure maximization of the average spectral efficiency. Fig. 4.2 shows the average spectral efficiency that can be obtained using the allocated rates that result from different algorithms, as a function of $\gamma$. Five different algorithms are considered: the proposed slow-link adaptation algorithm for

**Algorithm 5** Iterative rate correction for the fast-link adaptation algorithm.

$t \leftarrow 0$. ▷ Counter of iterations.
Set the candidate rates: $\{\hat{R}_1, \ldots, \hat{R}_{n_{\text{MCS}}}\}$.
Rate initialization under GA assumption with the random node selection: $R_{s_1}(0), \ldots, R_{s_M}(0)$.
Calculate $\eta(R_{s_1}(0), \ldots, R_{s_M}(0))$.
$max\_throughput \leftarrow \eta(R_{s_1}(0), \ldots, R_{s_M}(0))$.
**while** $(|R_{s_i}(t) - R_{s_i}(t-1)| > 0$, for any $i \in \{1, \ldots, M\})$ **do** ▷ e.g. $R_{s_1}(-1) = 0$
  $t \leftarrow t + 1$.
  **for** $i \leftarrow 1$ **to** $M$ **do**
    $count\_SW \leftarrow 0$ ▷ Counter of adjacent rates that result in smaller $\eta$.
    $R_{s_i}(t) \leftarrow R_{s_i}(t-1)$. ▷ We start with the rate from the previous iteration.
    $finished\_increasing \leftarrow 0$. ▷ Aux. variable, to stop increasing the rate.
    $finished\_decreasing \leftarrow 0$. ▷ Aux. variable, to stop decreasing the rate.
    **while** $\Big((R_{s_i}(t) < \hat{R}_{n_{\text{MCS}}})$ **and** $(finished\_increasing = 0)\Big)$ **do**
      $R_{s_i}(t) \leftarrow R_{s_i}(t) + \Delta$. ▷ Increase to the first higher candidate rate.
      Calculate $\eta_{\text{current}} \leftarrow \eta(R_{s_1}(t), \ldots, R_{s_i}(t), R_{s_{i+1}}(t-1), \ldots, R_{s_M}(t-1))$.
      **if** $(\eta_{\text{current}} > max\_throughput)$ **then**
        $check\_lower\_rates \leftarrow 0$. ▷ No need to decrease the rates.
        $max\_throughput \leftarrow \eta_{\text{current}}$. ▷ Maximum throughput updated.
        $[R_1^{\text{opt}}, \ldots, R_M^{\text{opt}}] \leftarrow [R_{s_1}(t), \ldots, R_{s_i}(t), R_{s_{i+1}}(t-1), \ldots, R_{s_M}(t-1)]$.
      **else** ▷ If conditions are not met.
        $count\_SW \leftarrow count\_SW + 1$. ▷ We increase the counter.
        **if** $\Big((count\_SW = SW)$ **or** $(R_{s_i}(t) = \hat{R}_{n_{\text{MCS}}})\Big)$ **then**
          $R_{s_i}(t) \leftarrow R_{s_i}(t) - count\_SW \times \Delta$.
          $finished\_increasing \leftarrow 1$; ▷ We reverse $R_{s_i}$ to one which gives max $\eta$.
        **end if**
      **end if**
    **end while**
    **if** $(check\_lower\_rates = 0)$ **then**
      **continue** ▷ No need to decrease the rate.
    **end if**

31: $count\_SW \leftarrow 0$. ▷ We reset $count\_SW$.
32: **while** $\Big((R_{s_i}(t) > \hat{R}_1)$ **and** $(finished\_decreasing = 0)\Big)$ **do**
33: $R_{s_i}(t) \leftarrow R_{s_i}(t) - \Delta$. ▷ Decrease to the first lower candidate rate.
34: Calculate $\eta_{\text{current}} \leftarrow \eta(R_{s_1}(t), \ldots, R_{s_i}(t), R_{s_{i+1}}(t-1), \ldots, R_{s_M}(t-1))$.
35: **if** $(\eta_{\text{current}} > max\_throughput)$ **then**
36: $max\_throughput \leftarrow \eta_{\text{current}}$. ▷ Maximum throughput updated.
37: $[R_1^{\text{opt}}, \ldots, R_M^{\text{opt}}] \leftarrow [R_{s_1}(t), \ldots, R_{s_i}(t), R_{s_{i+1}}(t-1), \ldots, R_{s_M}(t-1)]$.
38: **else**
39: $count\_SW \leftarrow count\_SW + 1$. ▷ We increase the counter.
40: **if** $\Big((count\_SW = SW)$ **or** $(R_{s_i}(t) = \hat{R}_1)\Big)$ **then**
41: $R_{s_i}(t) \leftarrow R_{s_i}(t) + count\_SW \times \Delta$.
42: $finished\_decreasing \leftarrow 1$. ▷ We reverse $R_{s_i}$ to one which gives max $\eta$.
43: **end if**
44: **end if**
45: **end while**
46: **end for**
47: **end while**

the parameter $SW = 1$ (referred to as "GA+Iterative rate correction SW=1" on the figure), the algorithm based solely on GA assumption with random node selection (referred to as "Genie-Aided approach"), two trivial algorithms where the rates are predetermined and set to the minimum ("Min rates: $R_1 = 0.5, R_2 = 0.5, R_3 = 0.5$ [b.c.u.]") and the maximum ("Max rates: $R_1 = 3.5, R_2 = 3.5, R_3 = 3.5$ [b.c.u.]") possible ones, and the exhaustive search approach algorithm. We observe that the average spectral efficiency obtained by the proposed slow-link adaptation algorithm coincides with the one obtained by the exhaustive search approach algorithm, for each $\gamma$. The gain of those two algorithms compared with the one solely based on GA assumption (where no iterative rate correction is done) never exceeds 1dB. Still, even that simpler version of a slow-link adaptation algorithm provides the gain of approx. 1dB compared with the strategy of predetermined maximum possible allocated rates, the difference becoming lower as $\gamma$ grows (it converges to zero for $\gamma = 15$dB). The performance of the strategy of predetermined minimum possible allocated rates quickly becomes highly non-optimal starting already from $\gamma = -4$dB, as $\gamma$ grows.

Additionally, on Fig. 4.3 we show the allocated rates by the proposed slow-link adaptation algorithm, the algorithm based on GA assumption only, and the algorithm based on the exhaustive search approach. The other two algorithms where the rates are predetermined and fixed are not shown for the clarity of figure.

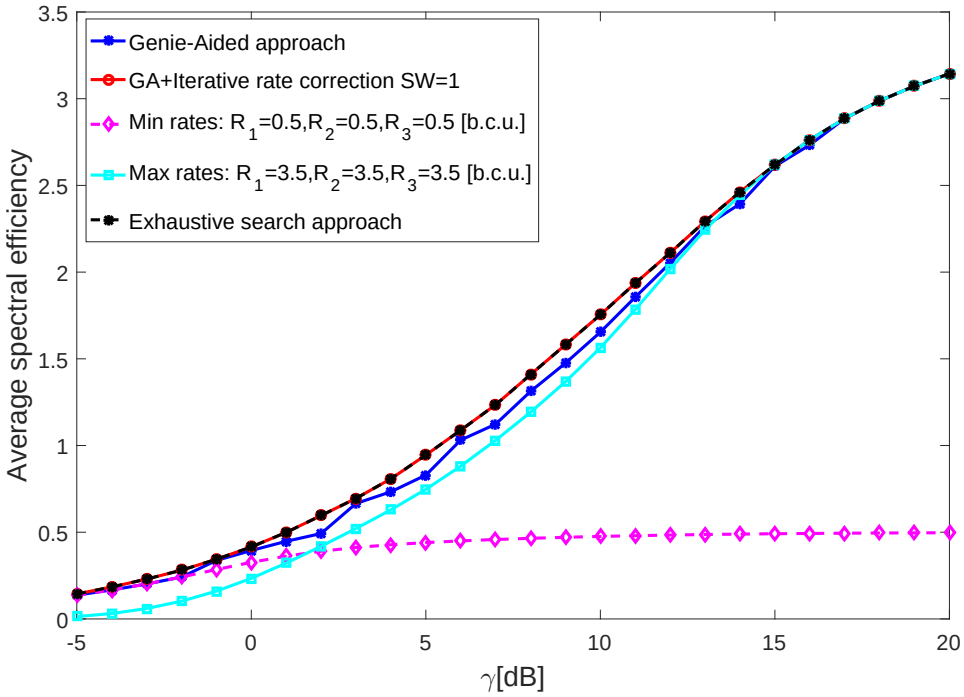


**Figure 4.2:** Average spectral efficiency that corresponds to different slow-link adaptation algorithms s.t. $BLER_{\mathrm{QoS}}^{(1)}$ target.

This figure confirms the optimality of the proposed slow-link adaptation algorithm, as the rates allocated by it are identical to the ones allocated by the algorithm based on the exhaustive search approach. It can be also observed that in general, for each $\gamma$, the rate allocated to source $s_1$ is the highest one, while the rate allocated to source $s_3$ is the lowest, which is in line with the assumed asymmetric link scenario. Finally, the rates allocated by the algorithm based solely on GA assumption are inaccurate and lower than the optimal ones. The main reason for that lies in the fact that not only the selected random node may be suboptimal from the perspective of decoding process at the destination, but may not even be beneficial at all.

On Fig. 4.4, we want to show the gain of using relaying compared with the case where no relaying is used for two different scenarios: (1) user co-operation is not present; (2) user co-operation is present. In the case (1), if the sources are not successfully decoded at the destination after the first transmission, they simply perform retransmissions of their own messages. They are scheduled by the destination which adopts the "optimized" node selection strategy (denoted by "independent retransmissions" on Fig. 4.4). In the case (2), the sources listen

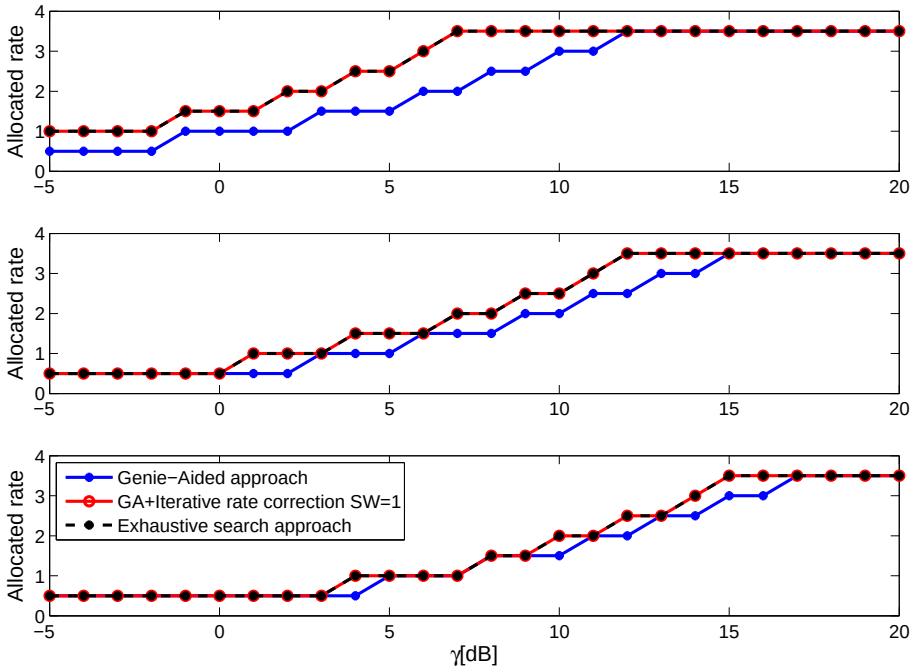


**Figure 4.3:** Allocated rates to sources for different slow-link adaptation algorithms s.t. $BLER^{(1)}_{\text{QoS}}$ target.

to other sources' messages and try to help the destination to decode all sources' messages. They are scheduled by the same node selection algorithm. For three defined scenarios, on Fig. 4.4 is shown the comparison of the average spectral efficiency obtained after adopting the rates that are the output of the proposed slow-link adaptation algorithm s.t. $BLER^{(1)}_{\text{QoS}} = 1$ target. In the case where no relays are used, the user co-operation brings up to 2dB of coding gain over the case where it is not used. The introduction of three relays brings at most an additional 1.5dB gain compared with the case where only user co-operation is used. Since in the user co-operation sources perform the functions of relays in the second phase, it can be understood as the advantage of using six relays over three.

Fig. 4.5 shows the convergence analysis of the proposed slow-link adaptation algorithm with respect to the number of channel outcomes generated within the Monte-Carlo simulations. It has been verified that 100000 MC iterations are sufficient for a convergence to the optimal average spectral efficiency. Hence, that result is used as a reference on the figure. Also, 1000, 100 and 10 number of MC iterations have been considered. We can see that in general, the less number of iterations are used, the less accurate the results are. However, even for 10 channel

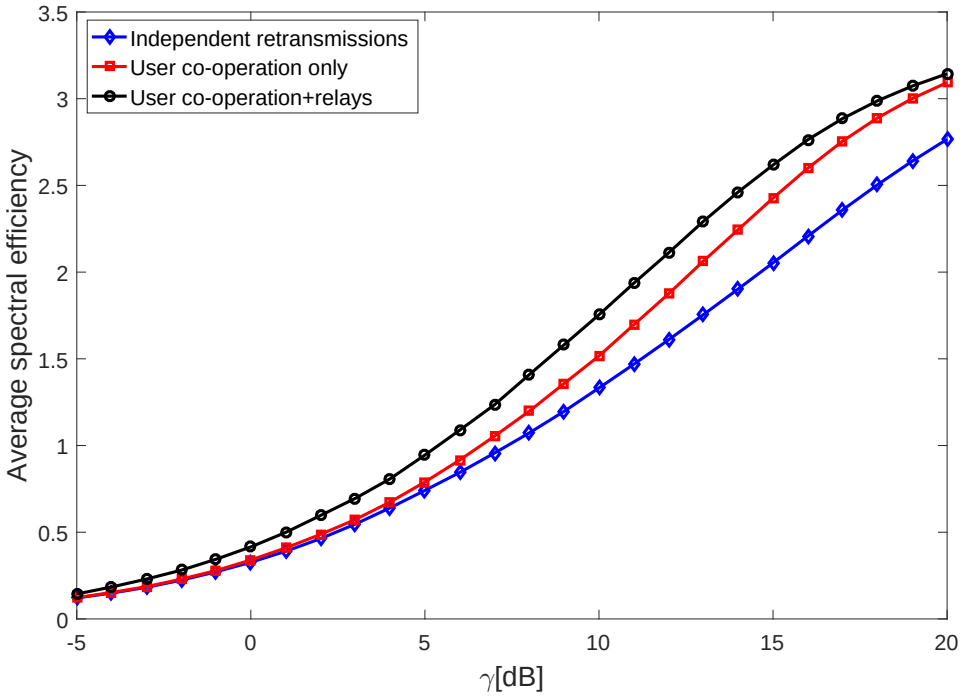


**Figure 4.4:** Average spectral efficiency that corresponds to the proposed slow-link adaptation algorithm for different scenarios s.t. $BLER^{(1)}_{\text{QoS}}$ target.

outcomes, the obtained average spectral efficiency is close to the optimal one, which means that the complexity of the algorithm could be even further reduced (substantially) with no great impact on the performance.

In the second part of simulations, we validate the performance of the slow-link adaptation algorithm under the constraint on the individual BLER target after $T$ retransmissions for each source set to $BLER^{(2)}_{\text{QoS}} = 10^{-3}$. Fig. 4.6 shows the comparison of the same five algorithms as on Fig. 4.2 in terms of the average spectral efficiency. Note that when the BLER target is not achieved for some source for a given value of $\gamma$, we set the average spectral efficiency to zero for that point. For each $\gamma <= 4$dB, even if the lowest possible candidate rates are allocated to all sources there is always at least one source whose individual BLER does not satisfy the constraint, which is understandable since the BLER target is rather severe. We observe that for some values of $\gamma$, the slow-link adaptation algorithm is not perfectly accurate, but still satisfyingly good, as the coding loss compared with the exhaustive search approach goes up to 1dB approximately. On the other hand, for the algorithm based on GA assumption with the random node selection the coding loss goes up to 5dB approximately. Allocation of the maximum possible candidate

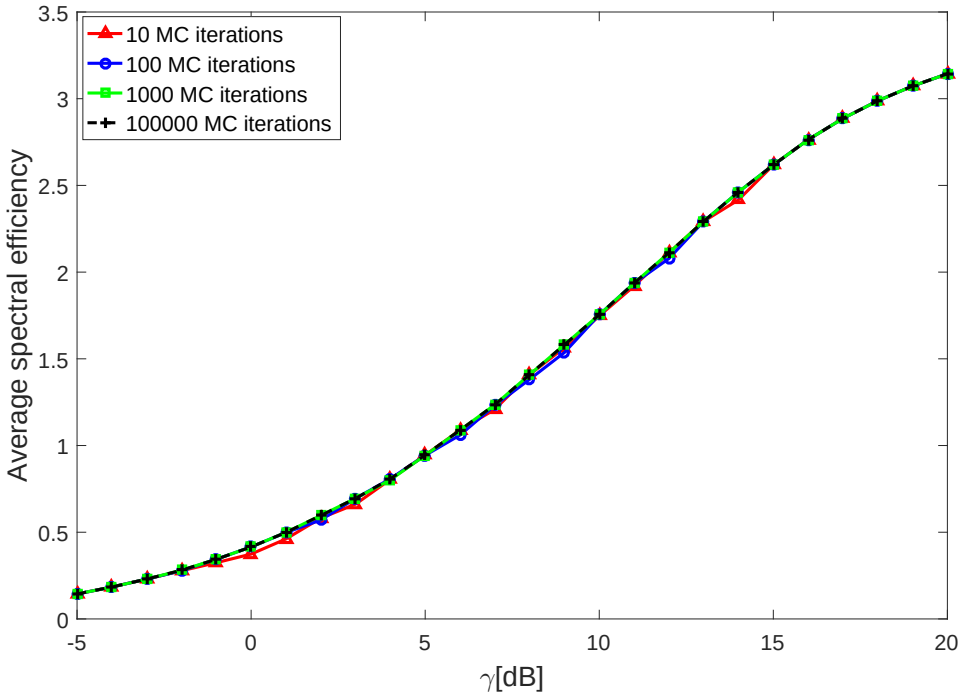


**Figure 4.5:** Convergence analysis of the proposed slow-link adaptation algorithm s.t. $BLER^{(1)}_{\text{QoS}}$ target.

rates only makes sense for the extremely high $\gamma$ in this scenario, so the use of a link adaptation algorithm is indispensable.

Just as on Fig. 4.3, we show the allocated rates to sources for the same three slow-link adaptation algorithms but under the $BLER^{(2)}_{\text{QoS}}$ target on Fig. 4.7. This time around, the allocated source rates by the proposed slow-link adaptation algorithm are not optimal, but still close to it, especially if their sum (the sum-rate) is observed. As expected, the rates allocated by the algorithm based on GA assumption only are even less accurate and lower than the optimal ones for each $\gamma$, for the same reason already explained for the Fig. 4.3.

Fig. 4.8 shows the highest individual BLER among all sources as a function of $\gamma$ for the same scenario. It validates our proposed slow-link adaptation algorithm, as the highest individual BLER is always lower or equal (and very close) to the $BLER^{(2)}_{\text{QoS}} = 10^{-3}$ target, just as in the case of the exhaustive search approach. The figure also reveals why the predetermined maximum possible allocated rates strategy cannot provide the valid rates, as the highest individual BLER in that case is higher than $10^{-3}$ for all $\gamma <= 17$dB. The highest individual BLER in the

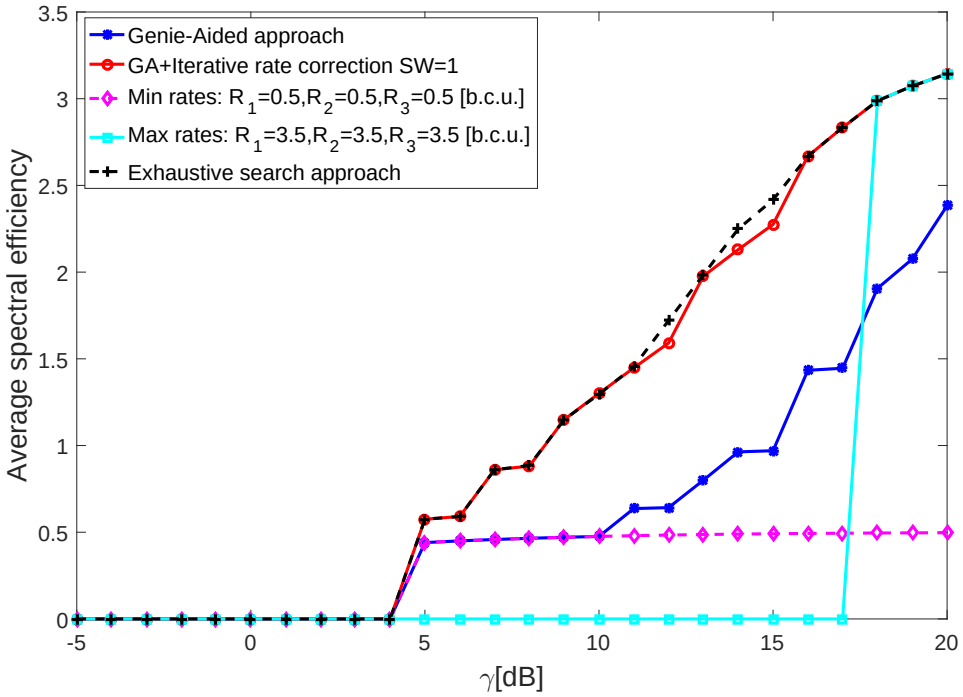


**Figure 4.6:** Average spectral efficiency that corresponds to different slow-link adaptation algorithms s.t. $BLER^{(2)}_{\text{QoS}}$ target.

case of the algorithm based on GA assumption with the random node selection continuously decreases, as the allocated rates are always lower or equal than the optimal ones, but not adequately adapted to the channel conditions and decoding capabilities of different nodes (just as for the minimum possible candidate rates).

Just as in the case of $BLER^{(1)}_{\text{QoS}}$ target, we show on Fig. 4.9 the gain of using relaying compared with the case where no relaying is used for $BLER^{(2)}_{\text{QoS}}$ target as well. In the case of independent retransmissions, even the lowest rates cannot provide the highest individual BLER to be below the target. User co-operation in combination with relays compared with the case where no relays are used brings at most 4dB of coding gain. Here, the gain is more pronounced compared with the configuration of no QoS constraint (i.e., $BLER^{(1)}_{\text{QoS}}$). Indeed, the QoS constraint is less costly to achieve in terms of average rates when the number of relaying nodes increases (increase diversity order or relaying path choices).

Finally, in the last part of the simulations, we validate the proposed fast-link adaptation algorithm, where we assume that the quality of each link changes after each frame (see Fig. 4.10). So, in each frame, the sources' rates are first allocated

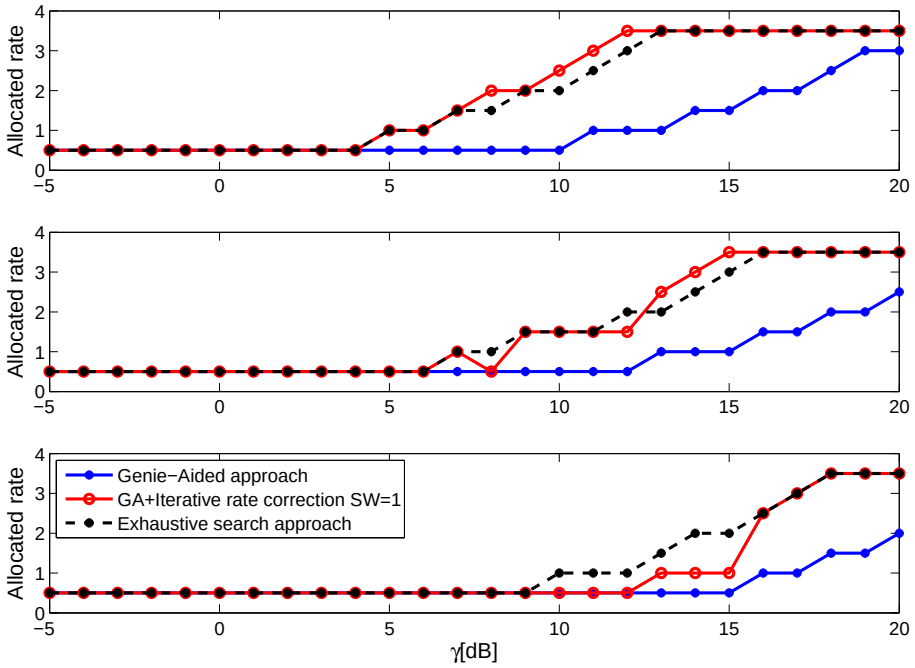


**Figure 4.7:** Allocated rates to sources for different slow-link adaptation algorithms s.t. $BLER^{(2)}_{\text{QoS}}$ target.

relying on the GA assumption, and than the proposed modified version of the iterative rate correction algorithm is applied. This time, we consider both the cases of "SW=1" and "SW=2", for the reason stated near the end of section 4.2.3. Also, we consider the algorithm based on exhaustive search approach (search is performed in each frame separately), the algorithm based on GA assumption with random node selection, and two trivial strategies where the rates are predetermined and set to the maximum and the minimum possible ones. Here, the proposed fast-link adaptation algorithm with parameter "SW=1" does not provide the optimal (average) spectral efficiency, but still it performs very close to it (coding loss is approx. 0.5dB). The same algorithm with parameter "SW=2" performs almost optimally, but with slightly higher complexity compared with the case of "SW=1". The algorithm based on GA assumption with random node selection has a coding loss that goes up to 2dB approximately, while the strategy of maximum possible rates has a loss which is at most 4dB approximately. As expected, the performance of the strategy of minimum possible rates is limited to 0.5 [b.c.u.]. We also remark that in general, by looking at the average spectral efficiency that is reached, we see that the algorithms based on fast-link adaptation perform better than their slow-

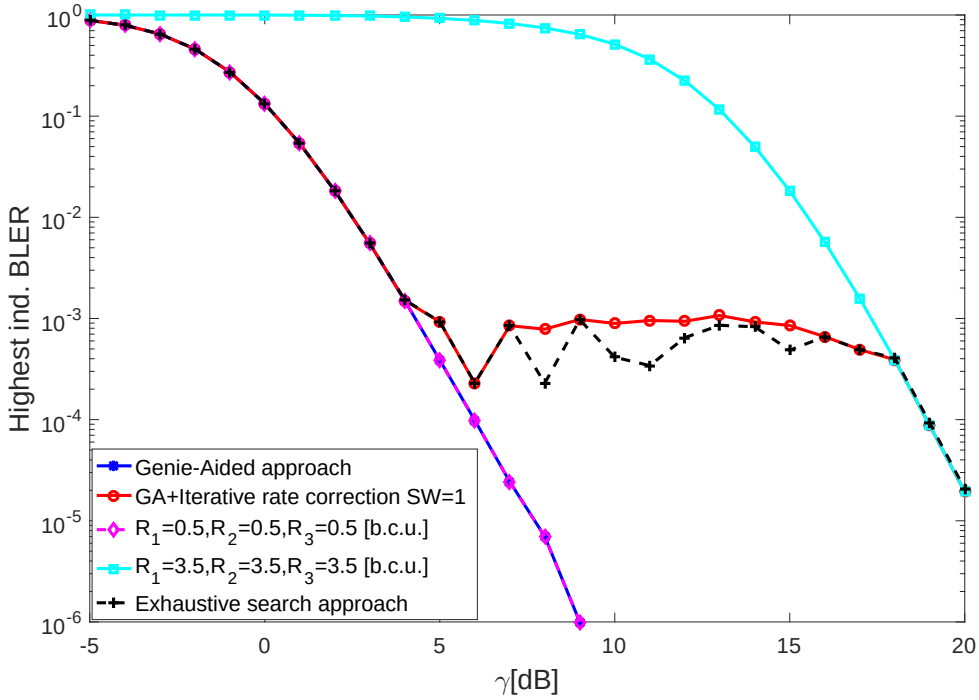


**Figure 4.8:** The highest individual BLER among sources for different slow-link adaptation algorithms s.t. $BLER_{\text{QoS}}^{(2)}$ target.

link adaptation counterparts, which of course comes at the price of the available knowledge of CSI of all the links in the network.

For the two same scenarios ("SW=1" and "SW=2") for fast-link adaptation, on Fig. 4.11 we show the average number of iterations needed by the proposed iterative rate correction algorithm to converge, using the initial rates calculated under GA assumption. We witness that for each $\gamma$, the average number of iterations performed under "SW=1" is higher than in the case of "SW=2", having the maximum value of approx. 2 (in the range 8dB <= $\gamma$ <= 11dB) compared with approx. 1.8 (in the range 3dB <= $\gamma$ <= 5dB). That is expected, since in the case of "SW=2", more comparisons of the spectral efficiency are performed in each iteration, but nonetheless we can conclude that in both cases the average number of iterations is relatively small.

On Fig. 4.12, we demonstrate the advantage of using relays for the proposed fast-link adaptation algorithm, by doing the same comparison as on Fig. 4.4 and Fig. 4.9. In this case, the coding loss of "independent retransmissions" scenario compared with "user co-operation only" scenario goes only up to 1dB approximately, just

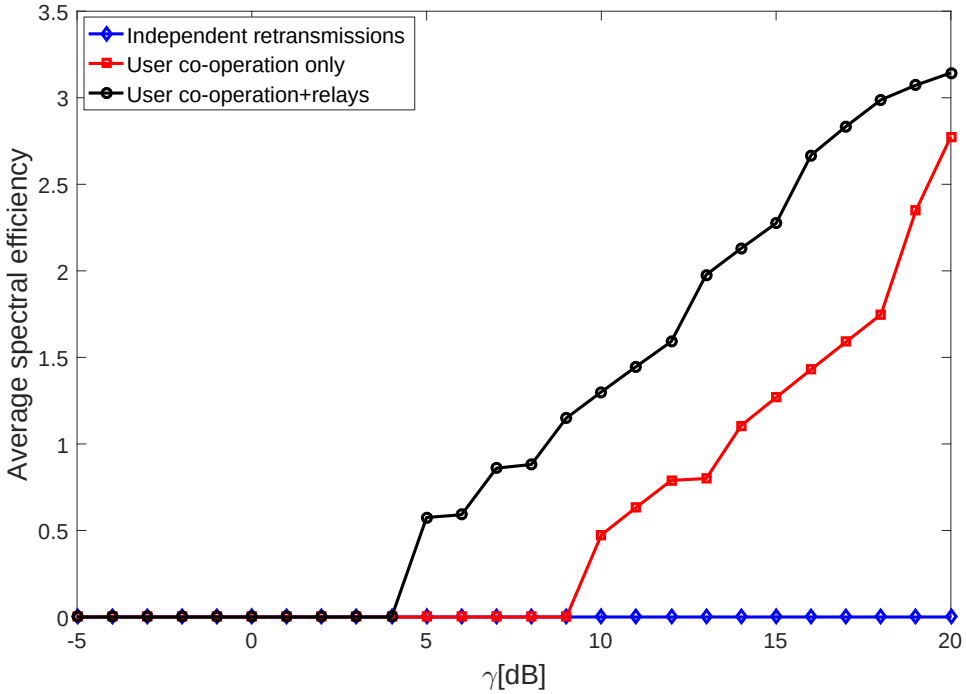


**Figure 4.9:** Average spectral efficiency that corresponds to the proposed slow-link adaptation algorithm for different scenarios s.t. $BLER^{(2)}_{\mathrm{QoS}}$ target.

as the coding loss of the later scenario compared with "user co-operation+relays" scenario. The possible explanation lies in the fact that in fast-link adaptation scenario, the rates are allocated optimally for any channel outcomes, while in the case of slow-link adaptation, the rates are adapted to the average conditions of those channels. So, when slow-link adaptation is used, in the cases where no relays are available a possible bad channel conditions of S-D links in certain frames can more easily lead to the individual outage of some sources due to a lack of diversity.

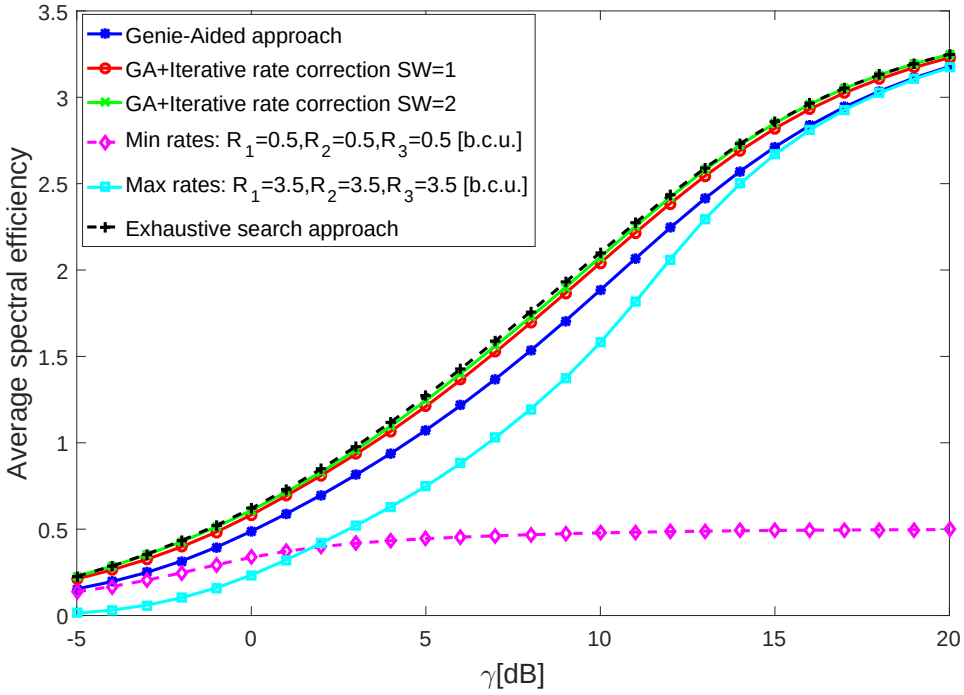


**Figure 4.10:** Average spectral efficiency that corresponds to different fast-link adaptation algorithms.

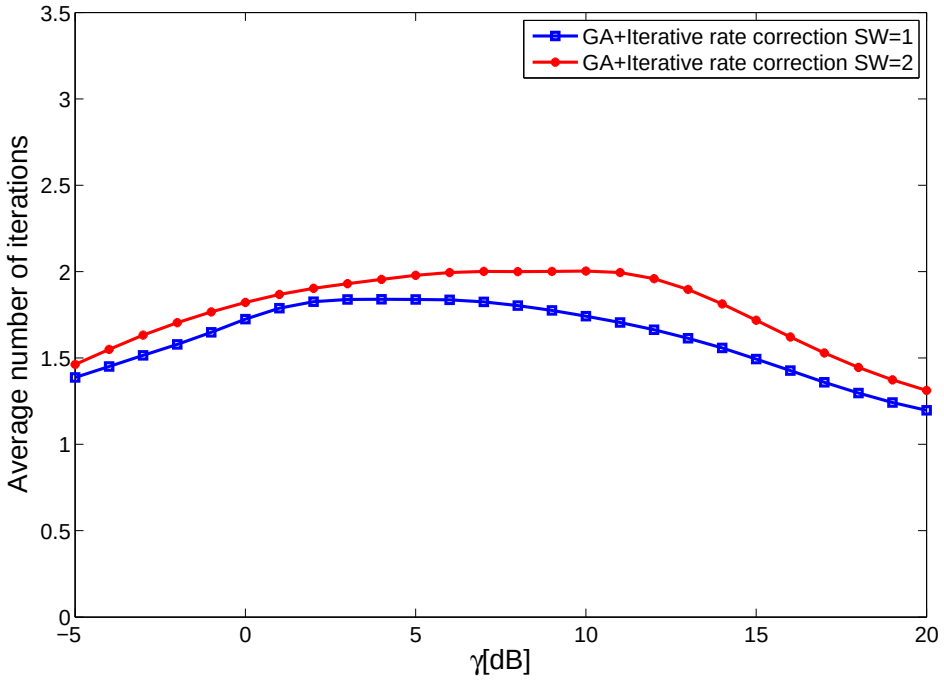


**Figure 4.11:** Average number of iterations needed by the iterative rate correction algorithm for fast-link adaptation to converge.

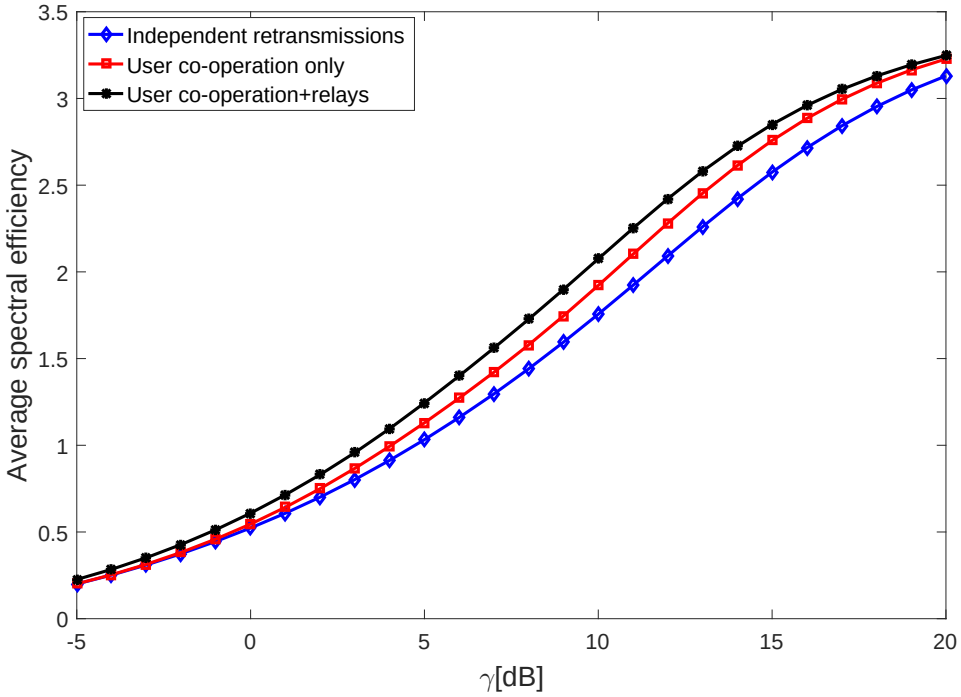


**Figure 4.12:** Average spectral efficiency that corresponds to the proposed fast-link adaptation algorithm for different scenarios.

# 5 | Cooperative HARQ Protocols

In the first part of this chapter, we evaluate the performance of three different Cooperative HARQ protocols for $(M, L, 1)$-MAMRC under the same system model assumptions as in previous chapters, with the goal to identify the one which offers the best trade-off between performance and complexity. The slow-link adaptation algorithm proposed in chapter 4 is performed before any transmission, while the node selection strategy 2 proposed in chapter 3 is used in the second phase, both adapted to specificities of considered cooperative HARQ protocols. Accordingly, the control exchange mechanism used at the beginning of each retransmission round in the second phase, adapted to the chosen node selection strategy, is the one proposed in section 3.3.

In the second part of this chapter, for the chosen cooperative HARQ protocol, we propose a practical encoding/decoding scheme based on capacity approaching turbo code, designed for a family of discrete Modulation and Coding Schemes. Circular buffer technique is used to obtain the codewords of desired coding rate.

## 5.1 Outage definitions of different cooperative HARQ protocols

### 5.1.1 IR-type of HARQ protocol with Multi-User encoding

For IR-type of HARQ protocol with Multi-User encoding, in given round $t$ of the second phase, the selected node $a_t$ sends incremental redundancies on all the messages in its decoding set. The definition of the common and individual outage events for this type of protocol have already been stated in chapter 3, but we recall them here for the sake of completeness.

If the set of non-successfully decoded sources at the destination is denoted by $\bar{\mathcal{S}}_{d,t-1}$, the common outage event for set $\mathcal{B} \subseteq \bar{\mathcal{S}}_{d,t-1}$ after round $t$ for the selected node $a_t$ is defined as:

$$\mathcal{E}_{t,\mathcal{B}}^{\mathrm{IR,MU}}(a_t, \mathcal{S}_{a_t,t-1}) = \bigcup_{\mathcal{U}\subseteq\mathcal{B}} \Big\{ \sum_{s\in\mathcal{U}} R_s > \sum_{s\in\mathcal{U}} I_{s,d} + \sum_{l=1}^{t-1} \alpha I_{\hat{a}_l,d}[\mathcal{C}_{\hat{a}_l}^{\mathrm{IR,MU}}] + \alpha I_{a_t,d}[\mathcal{C}_{a_t}^{\mathrm{IR,MU}}] \Big\}, \tag{5.1}$$

with $\mathcal{C}_{\hat{a}_l}^{\mathrm{IR,MU}}$ and $\mathcal{C}_{a_t}^{\mathrm{IR,MU}}$ defined as:

$$\begin{aligned} \mathcal{C}_{\hat{a}_l}^{\mathrm{IR,MU}} &= \Big\{ \{\mathcal{S}_{\hat{a}_l,l-1} \cap \mathcal{U} \neq \emptyset\} \wedge \{\mathcal{S}_{\hat{a}_l,l-1} \cap \mathcal{I} = \emptyset\} \Big\}, \\ \mathcal{C}_{a_t}^{\mathrm{IR,MU}} &= \Big\{ \{\mathcal{S}_{a_t,t-1} \cap \mathcal{U} \neq \emptyset\} \wedge \{\mathcal{S}_{a_t,t-1} \cap \mathcal{I} = \emptyset\} \Big\}, \end{aligned} \tag{5.2}$$

The individual outage event of the source $s$ after round $t$ is defined as:

$$\begin{aligned} \mathcal{O}_{s,t}^{\mathrm{IR,MU}}(a_t, \mathcal{S}_{a_t,t-1}) = \bigcap_{\mathcal{I}\subset\bar{\mathcal{S}}_{d,t-1}} \bigcup_{\mathcal{U}\subseteq\bar{\mathcal{I}}:s\in\mathcal{U}} \Big\{ \sum_{s\in\mathcal{U}} R_s > \sum_{s\in\mathcal{U}} I_{s,d} \\ + \sum_{l=1}^{t-1} \alpha I_{\hat{a}_l,d}[\mathcal{C}_{\hat{a}_l,s}] + \alpha I_{a_t,d}[\mathcal{C}_{a_t,s}] \Big\}, \end{aligned} \tag{5.3}$$

where $\bar{\mathcal{I}} = \bar{\mathcal{S}}_{d,t-1} \setminus \mathcal{I}$, and $\mathcal{C}_{\hat{a}_l,s}^{\mathrm{IR,MU}}$ and $\mathcal{C}_{a_t,s}^{\mathrm{IR,MU}}$ are defined as:

$$\begin{aligned} \mathcal{C}_{\hat{a}_l,s}^{\mathrm{IR,MU}} &= \Big\{ \{s \in \mathcal{S}_{\hat{a}_l,l-1} \cap \mathcal{U}\} \wedge \{\mathcal{S}_{\hat{a}_l,l-1} \cap \mathcal{I} = \emptyset\} \Big\}, \\ \mathcal{C}_{a_t,s}^{\mathrm{IR,MU}} &= \Big\{ \{s \in \mathcal{S}_{a_t,t-1} \cap \mathcal{U}\} \wedge \{\mathcal{S}_{a_t,t-1} \cap \mathcal{I} = \emptyset\} \Big\}, \end{aligned} \tag{5.4}$$

### 5.1.2 IR-type of HARQ protocol with Single User encoding

As stated in section 1.3, Single User encoding is particularly attractive since its implementation can reuse state-of-art rate compatible punctured codes such as low density parity check codes or turbo codes. Here, a selected node in retransmission round $t$ of the second phase cooperates with a single source from its decoding set, i.e., it transmits incremental redundancies for a single source. The choice of the source that the selected node will help is random, but among all sources which the destination has not successfully decoded up until that round. That information is available to each node in the network due to the control information exchange mechanism described in section 3.3.

Let us denote with $s_{\hat{a}_k}$ a randomly chosen source by the node $\hat{a}_k$ in round $k \in \{1, \ldots, T\}$ from its decoding set under the previously described condition. In this case, since the selected nodes during the second phase do not apply Multi-User encoding anymore and since the transmission is orthogonal in time, there is no need to use the MAC framework. The individual outage event of the source $s$ after round $t$ for the selected node $a_t$ which cooperates with the source $s_{a_t}$ can be simply defined as:

$$\mathcal{O}_{s,t}^{\mathrm{IR,SU}}(a_t, s_{a_t}) = \left\{ R_s > I_{s,d} + \sum_{l=1}^{t-1} \alpha I_{\hat{a}_l,d}[s = s_{\hat{a}_l}] + \alpha I_{a_t,d}[s = s_{a_t}] \right\}, \tag{5.5}$$

To find the common outage event of sources contained in the set $\mathcal{B} \subseteq \bar{\mathcal{S}}_{d,t-1}$ after round $t$, for the selected node $a_t$ which cooperates with the source $s_{a_t}$, we simply check if the individual outage event of any source $s$ contained in $\mathcal{B}$ is true:

$$\mathcal{E}_{t,\mathcal{B}}^{\mathrm{IR,SU}}(a_t, s_{a_t}) = \bigcup_{s \in \mathcal{B}} \mathcal{O}_{s,t}^{\mathrm{IR,SU}}(a_t, s_{a_t}). \tag{5.6}$$

### 5.1.3 CC-type of HARQ protocol

In this type of protocol, the selected node $a_t$ in round $t$ in the second phase apply the exact same MCS as source $s$ whose message is randomly selected from the decoding set of the destination $\bar{\mathcal{S}}_{d,t-1}$. It implies the constraint that $N_1 = N_2$ or $\alpha = 1$. At the destination, Maximum Ratio Combining (MRC) (at symbol or coded bit level) is used after each round in order to decode the message of a given source. By doing so, we obtain the highest achievable SNR, denoted $\gamma_{\mathrm{MRC}}$, for a given source at the destination which is equal to the summation of individual SNRs from the previous rounds. This kind of protocol offers less complexity in decoding then the protocol based on Multi-User encoding. The individual outage event of the source $s$ after round $t$ for the selected node $a_t$ which cooperates with the source $s_{a_t}$ is defined in this case as:

$$\mathcal{O}_{s,t}^{\mathrm{CC}}(a_t, s_{a_t}) = \left\{ R_s > I(\gamma_{\mathrm{MRC}}(a_t, s_{a_t})) \right\} \tag{5.7}$$

where

$$\gamma_{\mathrm{MRC}}(a_t, s_{a_t}) = |h_{s,d}|^2 + \sum_{l=1}^{t-1} |h_{\hat{a}_l,d}|^2 [s = s_{\hat{a}_l}] + |h_{a_t,d}|^2 [s = s_{a_t}] \tag{5.8}$$

The common outage event of sources contained in the set $\mathcal{B} \subseteq \bar{\mathcal{S}}_{d,t-1}$ after round $t$, for the selected node $a_t$ which cooperates with the source $s_{a_t}$ is, just as in the previous case, defined as:

$$\mathcal{E}_{t,\mathcal{B}}^{\mathrm{CC}}(a_t, s_{a_t}) = \bigcup_{s \in \mathcal{B}} \mathcal{O}_{s,t}^{\mathrm{CC}}(a_t, s_{a_t}). \tag{5.9}$$

**Table 5.1:** Average SNR of the links between all sources.

| $\gamma_{x,y}$[dB] | $s_1$ | $s_2$ | $s_3$ |
|---|---|---|---|
| $s_1$ | N.A. | $\gamma - 1$dB | $\gamma - 2$dB |
| $s_2$ | $\gamma - 1$dB | N.A. | $\gamma - 5$dB |
| $s_3$ | $\gamma - 2$dB | $\gamma - 5$dB | N.A. |

### 5.1.4 Numerical results

In this section, we want to evaluate the performance of the three types of HARQ protocols described in Sections 5.1.1, 5.1.2, 5.1.3 in terms of the average spectral efficiency by performing Monte-Carlo simulations. The node selection strategy 2 from chapter 3 is used in the second phase. Also, the optimal slow-link adaptation algorithm proposed in chapter 4 is used, which is conditional on the chosen node selection strategy. A discrete MCS family whose rates belong to {0.5,1,1.5,2,2.5,3,3.5} [b.c.u] is used for the initial rates. Independent Gaussian distributed channel inputs are assumed (with zero mean and unit variance), with $I_{a,b} = \log_2(1 + |h_{a,b}|^2)$.

In the first part of the simulations, we consider (3,3,1)-OMAMRC with $\alpha^{\mathrm{IR}} = 0.5$ and $T^{\mathrm{IR}} = 4$ for IR-types of HARQ protocol, and $\alpha^{\mathrm{CC}} = 1$ and $T^{\mathrm{CC}} = 2$ for CC-type of HARQ protocol. The asymmetric link configuration is assumed, where the average SNR of each link is in the range $\{-15\text{dB}, \ldots, 20\text{dB}\}$, where the source $s_1$ is set on purpose to be in the best propagation condition, while the source $s_3$ is in the worst one. Concretely, the network is configured as follows: (1) the average SNR of the links between source $s_1$ and each relay, as well as the link between source $s_1$ and the destination, is set to $\gamma$; (2) the average SNR of the links between source $s_2$ and each relay, as well as the link between source $s_2$ and the destination, is set to $\gamma - 4$dB; (3) the average SNR of the links between source $s_3$ and each relay, as well as the link between source $s_3$ and the destination, is set to $\gamma - 7$dB; (4) the average SNR of the links between all relays, as well as the links between each relay and the destination is set to $\gamma$; (5) the average SNR of the links between all sources are set according to the Tab. 5.1.

As a result, the initial rates associated to all sources are asymmetric. They are shown on Fig. 5.1 as a function of $\gamma$, which is the average SNR of the link between source $s_1$ and the destination. On that figure, IR-type of HARQ protocol with Multi-User encoding is labeled as “IR-HARQ MU”, IR-type of HARQ protocol with Single User encoding as “IR-HARQ SU” while CC-type of HARQ protocol is labelled as “CC-HARQ”. Fig. 5.2 shows the average spectral efficiency of the network as a function of $\gamma$. We observe that the IR-type of HARQ protocol with Multi-User encoding provides the highest average spectral efficiency. This result

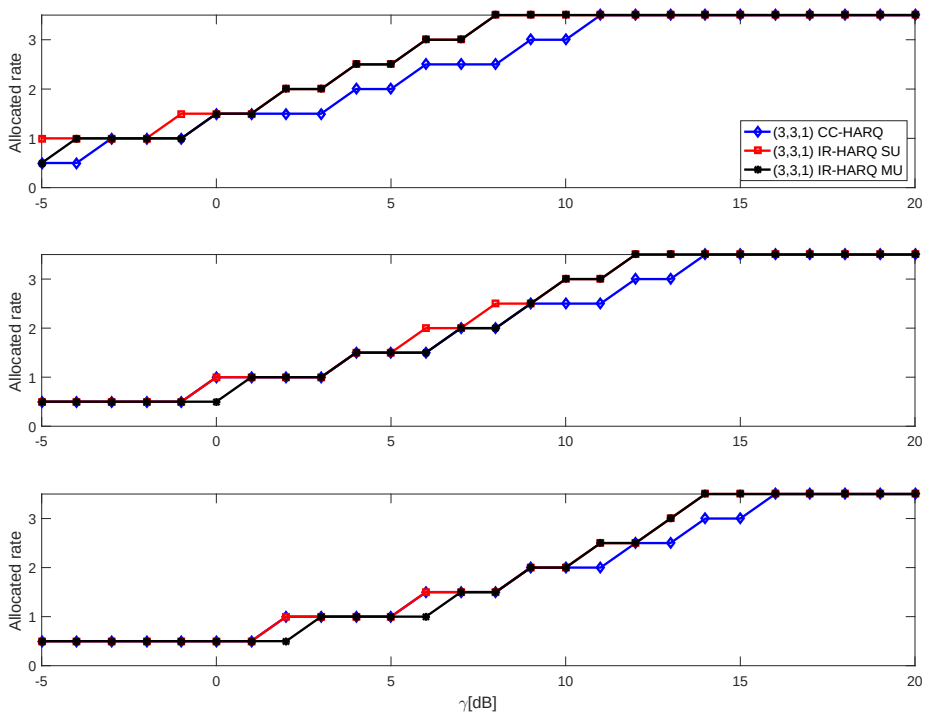


**Figure 5.1:** Allocated rates to sources for different HARQ protocols for asymmetric link configuration in (3,3,1)-OMAMRC.

was expected since the selected nodes in the second phase may help the decoding of multiple sources at the same time. IR-type of HARQ protocol with Single User encoding performance is not far behind, providing slightly lower average spectral efficiency. It can be explained by the fact that "only" three sources are present in the network, so there is often a case where the selected node in the second phase cooperates with exactly one source, even if Multi-User encoding is employed. Naturally, CC-type of HARQ has a noticeably worse performance compared with two IR based protocols.

Fig. 5.3 and Fig. 5.4 show the same comparison but for (4,3,1)-OMAMRC and (5,3,1)-OMAMRC, respectively. The average SNR of the links between source $s_4$ and each relay, as well as the link between source $s_4$ and the destination, is set to $\gamma - 9$dB, while the average SNR of the links between source $s_5$ and each relay, as well as the link between source $s_5$ and the destination, is set to $\gamma - 10$dB. The average SNR of the link between sources $s_4$ and $s_5$ is set to $\gamma - 9.5$dB, while the same parameter for the links between sources $s_4$ and $s_5$ and all other sources is set

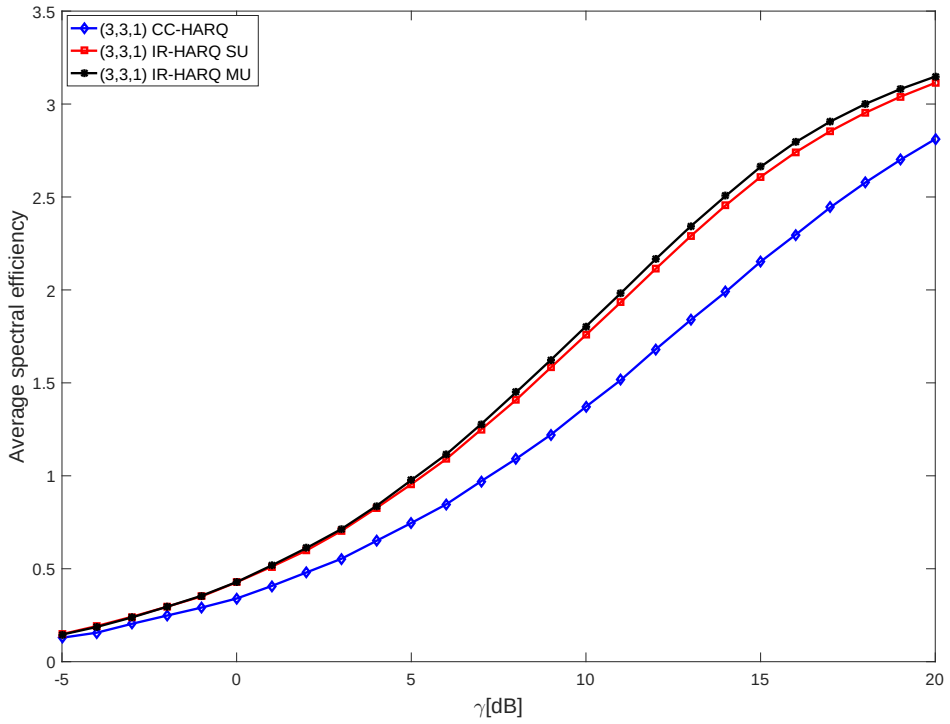


**Figure 5.2:** Average spectral efficiency obtained by using different HARQ protocols for asymmetric link configuration in (3,3,1)-OMAMRC.

to $\gamma$ reduced by a value from the set $[0\text{dB}, \ldots, 9\text{dB}]$, following the similar logic as in the case of (3,3,1)-OMAMRC. We observe that the performance ordering of the different protocols remains the same. But, as the number of sources in the network grows, we notice that for IR-type of HARQ the difference in performance between the Multi-User and Single User encoding slowly grows. Indeed, a scheduled node has all the more chances to have more than one source in its decoding set as the number of sources increases.

As a general conclusion, we can argument that for the OMAMRC with relatively small number of sources the IR-type of HARQ with Single User encoding offers the best compromise between performance and complexity.

It is also interesting to observe that the average spectral efficiency decreases for all three types of the HARQ protocol when the number of sources increases. There are two reasons from our understandings. The first one is that by adding more sources that are progressively in worse conditions than the previous ones, the probability that the added source will be successfully decoded decreases. The other reason is

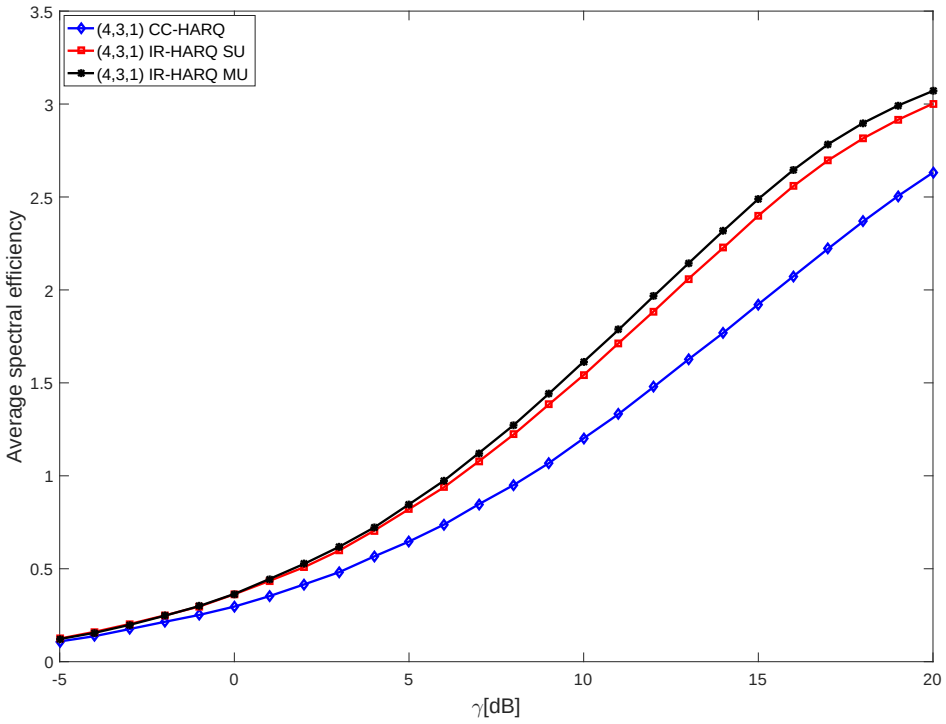


**Figure 5.3:** Average spectral efficiency obtained by using different HARQ protocols for asymmetric link configuration in (4,3,1)-OMAMRC.

that the number of retransmission rounds in the second phase is fixed to $T^{\mathrm{IR}} = 4$ and $T^{\mathrm{CC}} = 2$, so by adding more sources, even if they are all in the same conditions in average, it may happens that there are not enough available retransmissions for helping them all efficiently.

For that reason, in the last part of simulations, we consider the symmetric link configuration where the average SNR of each link is equal to $\gamma$, and where the number of possible retransmission rounds in the second phase varies with the number of sources. Namely, we try to keep a constant ratio between the number of time-slots in the first phase and the number of possible retransmissions in the second phase. Let $M_1 = 3$ be the number of sources in (3,3,1)-OMAMRC, with $T_1^{\mathrm{IR}} = 4$ the number of retransmissions in the second phase for IR-type of HARQ, and with $T_1^{\mathrm{CC}} = 2$ the same number, but for CC-type of HARQ. In (4,3,1)-OMAMRC, $M_2 = 4$, $T_2^{\mathrm{IR}} = \lceil \frac{T_1}{M_1} M_2 \rceil = 6$, and $T_2^{\mathrm{CC}} = \frac{T_2^{\mathrm{IR}}}{2} = 3$. In the case of (5,3,1)-OMAMRC, by similar reasoning and forcing the $T_3^{\mathrm{CC}}$ to be the round number, we choose $T_3^{\mathrm{IR}} = 8$ and $T_3^{\mathrm{CC}} = 4$. Fig. 5.5 shows the comparison of the average spectral

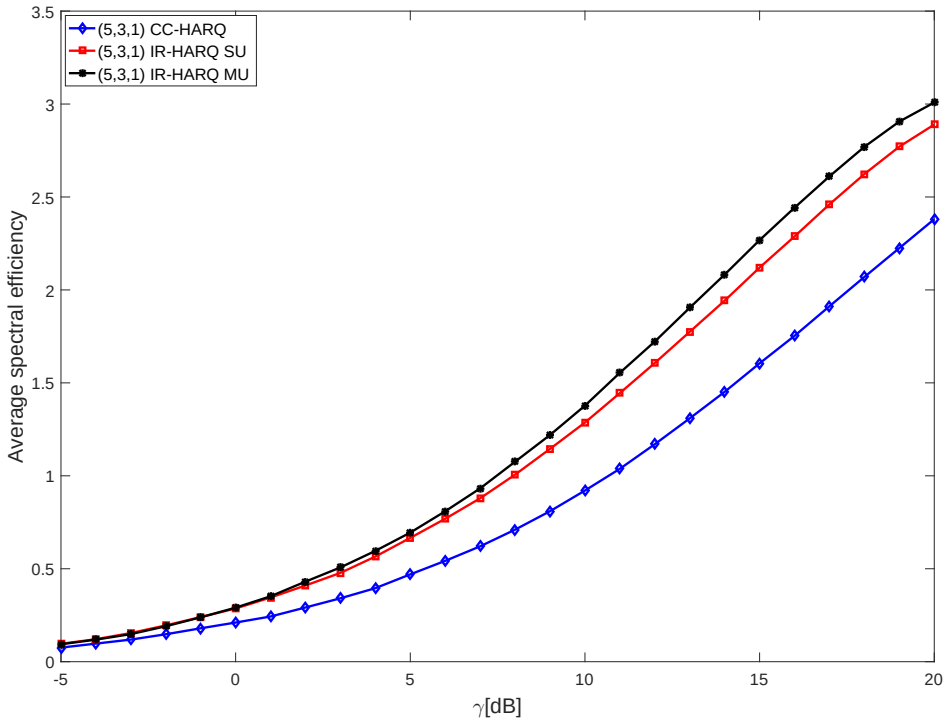


**Figure 5.4:** Average spectral efficiency obtained by using different HARQ protocols for asymmetric link configuration in (5,3,1)-OMAMRC.

efficiency for all $M_1$, $M_2$ and $M_3$ where we see that in this case the more sources there are in the network, the higher the average spectral efficiency is. For the clarity of the figure only the range $\gamma \in \{0\text{dB}, \ldots, 15\text{dB}\}$ is shown.

## 5.2 Practical coding scheme design

In 1993, Berrou et al. have proposed a class of convolutional codes which perform near to the Shannon limit in terms of BER while maintaining relatively modest decoding complexity for very long codewords, termed "turbo codes" [93, 143]. Turbo code encoding scheme consists of two Recursive Systematic Convolutional (RSC) codes concatenated in parallel, where the message sequence at the input of the second encoder is an interleaved version of the message sequence at the input of the first encoder. On the other hand two decoders, each adjusted for corresponding RSC encoder, operate in iterative decoding algorithm. There, each decoder takes

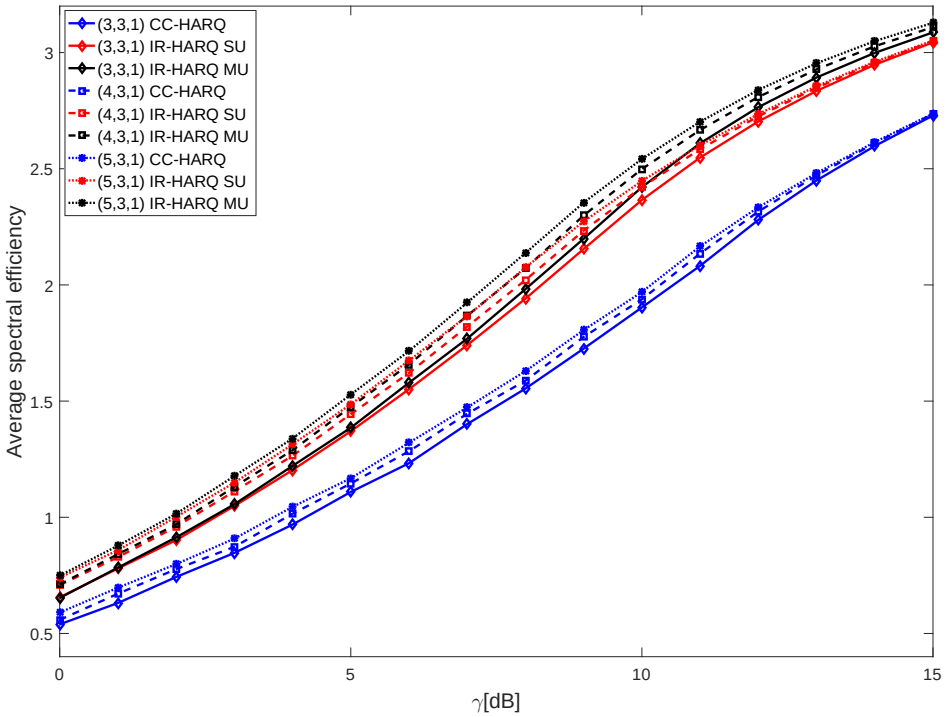


**Figure 5.5:** Average spectral efficiency obtained by using different HARQ protocols for symmetric link configuration and different OMAMRC.

turn to decode a part of the received sequence (originating from systematic bits and corresponding parity-check bits) using the estimated a priori probabilities of information bits provided by the other decoder. A modified version of Bahl Cocke Jeinek Raviv (BCJR) algorithm [144] is used at each decoder, which minimizes the bit error probability and yields the A Posteriori Probability (APP) for each decoded bit [93]. That soft information which is produced for the other decoder is also known as the extrinsic information, and the number of iterations performed where that information is passed in both directions can be in general greater than one (until the algorithm converges). The principle described above is reminiscent of turbo charging an automobile engine using engine-heated air at the air intake [143], and is the key for the very good performance of the decoding algorithm.

For that reason, turbo codes have found their place as the error correction code for certain transport channels in Release 14 of standard on “Multiplexing and channel coding” for Long-Term Evolution (LTE), the fourth generation of cellular networks [145]. Together with error detection, rate matching, interleaving and

mapping/splitting function between transport channel/control information and physical channels, error correction code builds a channel coding scheme for LTE. The coding scheme that we present in the rest of this section is inspired by the one described in the specification, with the main difference in rate matching (link adaptation) function, where in our work we apply the slow-link adaptation algorithm proposed in chapter 4, adapted to the network composed of multiple sources and multiple relays.

### 5.2.1 Encoding scheme

A turbo encoding scheme that is used is a Parallel Concatenated Convolutional Code (PCCC), shown on Fig. 5.6. It is made up of an internal interleaver and two identical constituent RSC encoders that have the following transfer function, just as in [145]:

$$G(D) = \left[1, \frac{1 + D + D^3}{1 + D^2 + D^3}\right]. \tag{5.10}$$

The number of memory elements (shift registers) is equal to 3, while the number of states is equal to 8 for each constituent encoder. Initially, the values of all shift registers are set to 0 at the beginning of encoding. Note that only systematic bits of first constituent encoder are being transmitted, so the total coding rate of the encoding scheme is equal to 1/3, when no puncturing is used. If the input block length is denoted by $K$, for the input sequence $u_0, u_1, \ldots, u_{K-1}$ the output stream of each branch is defined as follows:

$$\begin{aligned} d_k^{(0)} &= s_k, \\ d_k^{(1)} &= p_k^1, \\ d_k^{(2)} &= p_k^2, \end{aligned}$$

for $k = 0, \ldots, K-1$.

At the end of encoding of each input block, a trellis termination is being performed at each constituent encoder in order to set the value of each shift register to 0. The principle of trellis termination is to, starting from final state of the given encoder, provide at the input the feedback bit which is obtained from that state, and to repeat the procedure the same number of times as there are shift registers. To initiate the described function for given encoder, the corresponding switch is set to lower position (dotted lines on Fig. 5.6 are related to trellis termination).

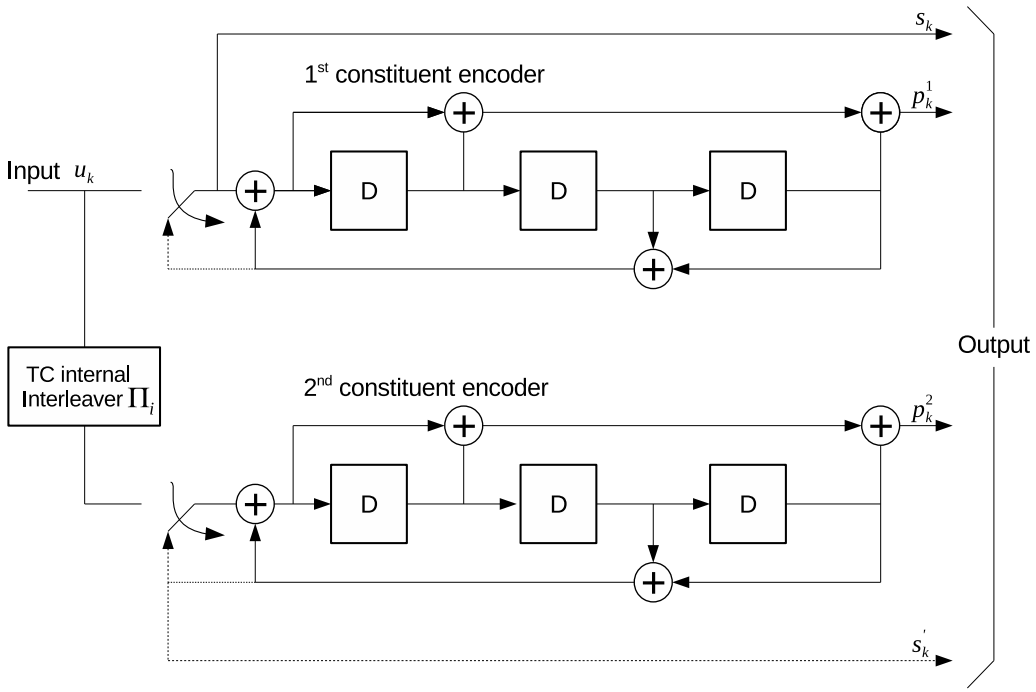


**Figure 5.6:** Turbo code encoding scheme.

The trellis of the first encoder is being terminated first, followed by the trellis termination of the second encoder, where the outputs of two encoders originating from tail bits are padded to the output sequences in the following way:

$$
\begin{aligned}
&d_K^{(0)} = s_K, d_{K+1}^{(0)} = p_{K+1}^1, d_{K+2}^{(0)} = s'_K, d_{K+3}^{(0)} = p_{K+1}^2, \\
&d_K^{(1)} = p_K^1, d_{K+1}^{(1)} = s_{K+2}, d_{K+2}^{(1)} = p_K^2, d_{K+3}^{(1)} = s'_{K+2}, \\
&d_K^{(2)} = s_{K+1}, d_{K+1}^{(2)} = p_{K+2}^1, d_{K+2}^{(2)} = s'_{K+1}, d_{K+3}^{(2)} = p_{K+2}^2.
\end{aligned}
$$

The internal turbo code interleaver is pure random, while without too much loss in accuracy we assume that CRC bits are transmitted without errors (we don't generate them), so the actual spectral efficiency of the given encoding scheme is a little bit smaller in practice.

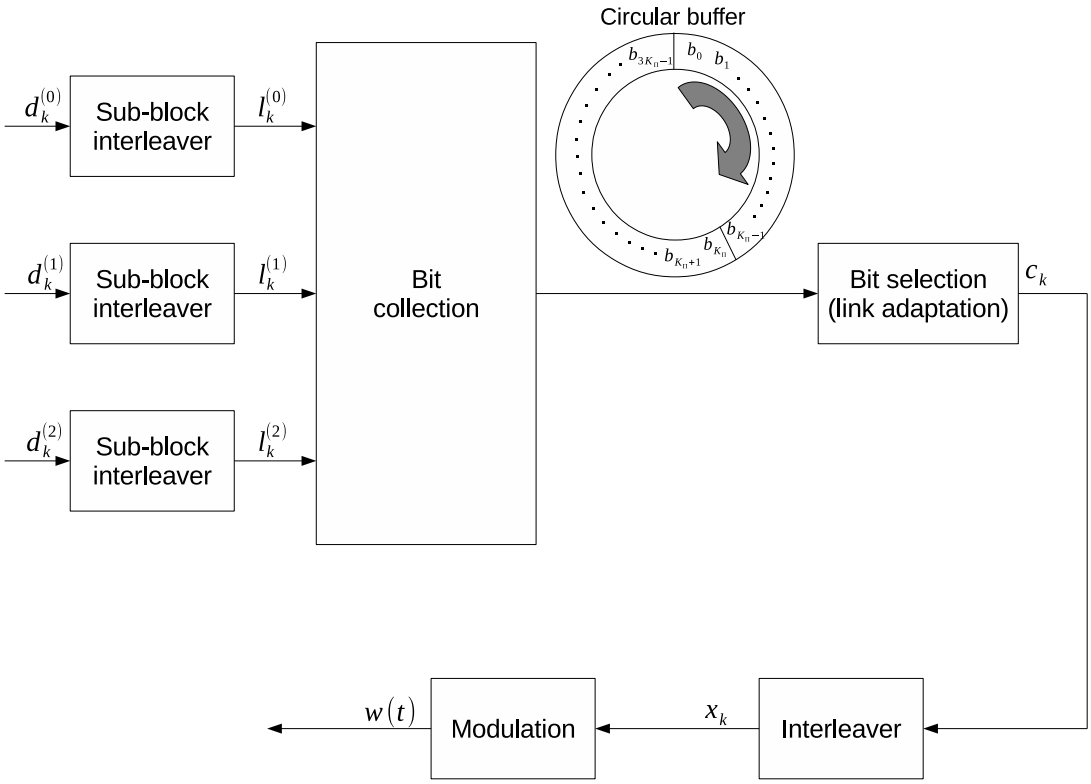


**Figure 5.7:** Link adaptation using circular buffer technique.

### 5.2.2 Link adaptation

For the purposes of the link adaptation algorithm (rate matching), a circular buffer is used in order to come up with different spectral efficiencies for the given family of MCSs, just as in [145]. The principle of circular buffer formation is depicted on Fig. 5.7.

First, all three output sequences $d_k^{(0)}$, $d_k^{(1)}$ and $d_k^{(2)}$ are interleaved according to the sub-block interleaver defined in Appendix A to obtain sequences $v_k^{(0)}$, $v_k^{(1)}$ and $v_k^{(2)}$:

$$
\begin{aligned}
d_k^{(0)} &\rightarrow v_0^{(0)}, v_1^{(0)}, \ldots, v_{K_\Pi-1}^{(0)} \\
d_k^{(1)} &\rightarrow v_0^{(1)}, v_1^{(1)}, \ldots, v_{K_\Pi-1}^{(1)} \\
d_k^{(2)} &\rightarrow v_0^{(2)}, v_1^{(2)}, \ldots, v_{K_\Pi-1}^{(2)}
\end{aligned}
$$

The parameter $K_\Pi$ is also defined in Appendix A. Starting from sequences $v_k^{(0)}$, $v_k^{(1)}$

and $v_k^{(2)}$, the sequence $b_k$ of circular buffer is formed in the following way:

$$
\begin{aligned}
b_k &= v_k^{(0)} \text{ for } k = 0, \ldots, K_\Pi - 1 \\
b_{K_\Pi + 2k} &= v_k^{(1)} \text{ for } k = 0, \ldots, K_\Pi - 1 \\
b_{K_\Pi + 2k + 1} &= v_k^{(2)} \text{ for } k = 0, \ldots, K_\Pi - 1
\end{aligned}
$$

Basically, the interleaved sequence of systematic bits (together with corresponding tail bits and eventually dummy bits) is first put into the circular buffer. Then, the sequences that include parity information for the first and second constituent encoder respectively are alternately added to the circular buffer. By using such a set-up, any desired coding rate can be relatively easily obtained by reading sufficient number of bits from the circular buffer to form the codeword. The first bit that is read corresponds to the first bit of interleaved sequence which includes systematic bits ($b_0$), sequentially followed by other bits $b_1, b_2, \ldots$. Once the end of the buffer is reached, the same bits $b_0, b_1, \ldots, b_{3K_\Pi - 1}$ are being read again starting from bit $b_0$. In that way, by sending some bits multiple times, even the rates that are lower than 1/3 can be obtained.

As before, we assume that $N_1$ channel uses are available for each time-slot during the first phase and $N_2$ during the second. Given the family of MCSs, slow-link adaptation algorithm presented in section 4.1 is applied to associate one MCS to each source. Since the number of channel uses per slot is fixed, the number of information bits $K_s$ is being adjusted for each source $s_i$, $i \in \{1, \ldots, M\}$, as a function of $N_1$, modulation order $q_i$ and coding rate $R_{c,i}$ of selected $\text{MCS}_{s_i}$. The total number of bits transmitted for source $s_i$ during the first phase is equal to $N_1 q_i R_{c,i}$. During the second phase, if the given source is being helped by a cooperating source or a relay in given time-slot, starting from the first following position in circular buffer with regard to last bit from previous transmission, $N_2 q_i R_{c,i}$ additional bits are transmitted. The node selection strategy being used is the one proposed in section 3.2.2.

Selected bits are first interleaved using random interleaver before being modulated for transmission over wireless medium. Note that since we deal with practical coding scheme design, for mutual information calculation we take into account discrete i.i.d. inputs instead of Gaussian i.i.d. inputs for both node selection strategy and slow-link adaptation algorithm, in order to gain in accuracy. In appendix B, we detail the calculation steps for mutual information with discrete i.i.d. inputs.

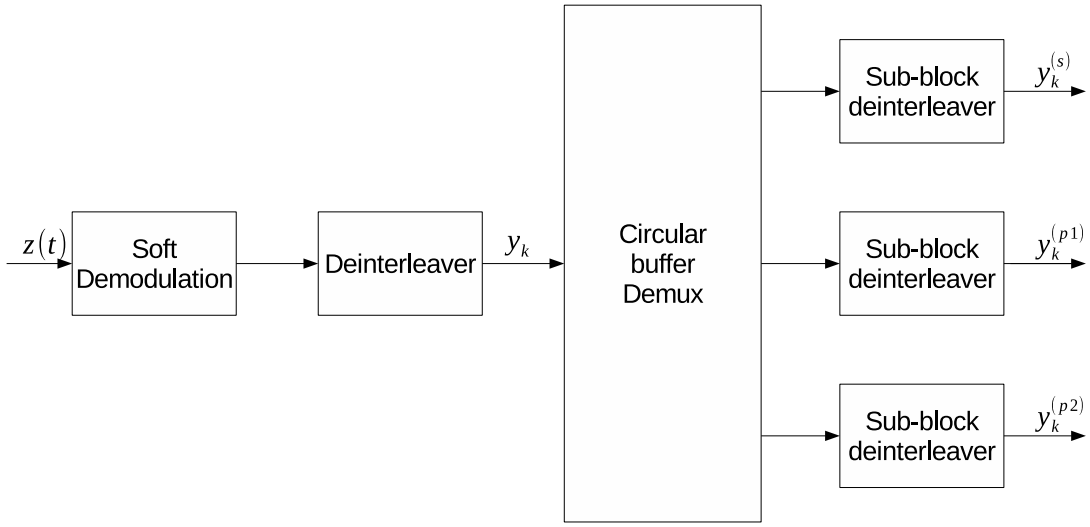


**Figure 5.8:** Demodulation, demultiplexing and deinterleaving at the receiver.

### 5.2.3 Demodulation and decoding scheme

After being passed through slowly Rayleigh fading channel with AWGN, inverse operations with regards to the transmitter scheme are applied to the received signal before performing the decoding (Fig. 5.8). If permutation pattern is given by $< P(j) >$, the deinterleaving is performed by $q_{P(j)}^{(P^{-1})} = q_j$.

BCJR algorithm, or Maximum a Posteriori (MAP) algorithm, is at the heart of the turbo decoding scheme. It is performed at each decoder, and its main purpose is to compute the *a posteriori* Log-Likelihood Ratio (LLR) $L(u_k|\mathbf{y})$ of the message bit sequence $u_k$ for the received symbol sequence $\mathbf{y}$ (each symbol being composed of $n$ bits if the number of outputs of corresponding convolutional encoder is equal to $n$), defined as:

$$L(u_k|\mathbf{y}) = \ln \frac{\Pr(u_k = +1|\mathbf{y})}{\Pr(u_k = -1|\mathbf{y})}. \tag{5.11}$$

That soft information can either be converted into a bit value through a hard decision, or passed to another decoder in order to be used as *a priori* LLR (actually, only part of the information is passed, called the *extrinsic* information). Nice and detailed tutorial on BCJR algorithm and its application to turbo decoding is done by Abrantes in [146], where in the following we are going to recall its main results only.

#### 5.2.3.1 Brief overview of BCJR algorithm

Let us denote the input sequence $\mathbf{u}$ of $N$ bits by $\mathbf{u} = u_1 u_2 \dots u_N$. The output sequence of the encoder of $Nn$ bits is denoted by $x_1 x_2 \dots x_N$, while the received sequence is denoted by $y_1 y_2 \dots y_N$. Following [146], it turns out that the a posteriori LLR of bit $u_k$ can be calculated as:

$$L(u_k|\mathbf{y}) = \ln \frac{\sum_{R_1} \alpha_{k-1}(s')\gamma_k(s',s)\beta_k(s)}{\sum_{R_0} \alpha_{k-1}(s')\gamma_k(s',s)\beta_k(s)}. \tag{5.12}$$

Probabilities $\alpha$, $\beta$ and $\gamma$ have the following definitions:

$$\begin{aligned}
\alpha_{k-1}(s') &= \Pr(s', y_1, \dots, y_{k-1}) \\
\beta_k(s) &= \Pr(y_{k+1}, \dots, y_N|s) \\
\gamma_k(s',s) &= \Pr(y_k, s|s')
\end{aligned}$$

where $s'$ is the encoder state at time $k-1$, and $s$ is the encoder state at time $k$.

If we plot the trellis of the convolutional code, we can see that probability $\gamma_k(s',s)$ is associated with branches or transitions between states, and can be calculated as follows:

$$\gamma_k(s',s) = C_k e^{u_k L(u_k)/2} \exp(\frac{L_c}{2} \sum_{l=1}^{n} x_{kl} y_{kl}),$$

where

$$C_k = \frac{e^{L(u_k)/2}}{1+e^{L(u_k)}} \frac{1}{\left(\sqrt{\pi N_0/E_c}\right)^n} \exp\left(-\frac{E_c}{N_0}\sum_{l=1}^{n} y_{kl}^2\right) \exp\left(-\frac{E_c}{N_0} a^2 \sum_{l=1}^{n} x_{kl}^2\right),$$

which is a constant that does not depend on bit $u_k$. $L(u_k) = \ln \frac{\Pr(u_k=+1)}{\Pr(u_k=-1)}$ is the a priori LLR of bit $u_k$, and $L_c = 4aR_c\frac{E_b}{N_0}$, with $a$ being the fading amplitude, $R_c$ the coding rate, $E_b$ energy per bit, and $N_0/2$ two-sided power spectral density of AWGN noise. Note that in the derivation for $\gamma_k(s',s)$, it is assumed that Binary Phase-Shift Keying (BPSK) modulation is being used.

Probabilities $\alpha$ and $\beta$ are associated with the encoder states and can be calculated recursively, based on all $\gamma$:

$$\begin{aligned}
\alpha_k(s) &= \sum_{s'} \alpha_{k-1}(s')\gamma_k(s',s), \text{ under initial conditions } \alpha_0(s) = \begin{cases} 1, & s=0 \\ 0, & s\neq 0 \end{cases} \\
\beta_{k-1}(s') &= \sum_{s} \beta_k(s)\gamma_k(s',s), \text{under initial conditions } \beta_N(s) = \begin{cases} 1, & s=0 \\ 0, & s\neq 0 \end{cases}
\end{aligned} \tag{5.13}$$

Note that in practice, variables $\alpha$, $\beta$, $\gamma$ as well as product $\alpha_{k-1}(s')\gamma_k(s',s)\beta_k(s)$ are always normalized before being further taken into account due to well known problems related to numerical instability that BCJR suffers from. Another problem of BCJR algorithm is its computational complexity because of the number of multiplications that is needed to be performed. There exist few simplified versions of BCJR algorithm with the goal to reduce it, one of the most widely used being "log-MAP algorithm" which offers the same performance as the original one.

In **log-MAP algorithm** the a posteriori LLR can be computed in the following way:

$$L(u_k|\mathbf{y}) = \max_{R_1}{}^{\star}\left[A_{k-1}(s') + \Gamma(s',s) + B_k(s)\right] - \max_{R_0}{}^{\star}\left[A_{k-1}(s') + \Gamma(s',s) + B_k(s)\right], \tag{5.14}$$

where function $\max^{\star}(a,b)$ is the Jacobian logarithm defined as:

$$\max{}^{\star}(a,b) = \ln(e^a + e^b) = \max(a,b) + \ln(1 + e^{-|a-b|}).$$

In (5.14), three new variables are used:

$$A_k(s) = \ln \alpha_k(s) = \max_{s'}{}^{\star}\left[A_{k-1}(s') + \Gamma(s',s)\right], \text{ with } A_0(s) = \begin{cases} 0, & s = 0 \\ -\infty, & s \neq 0 \end{cases}$$

$$B_{k-1}(s') = \ln \beta_{k-1}(s') = \max_{s}{}^{\star}\left[B_k(s) + \Gamma(s',s)\right], \text{ with } B_N(s) = \begin{cases} 0, & s = 0 \\ -\infty, & s \neq 0 \end{cases}$$

$$\Gamma_k(s',s) = \ln \gamma_k(s',s) = \ln C_k + \frac{u_k L(u_k)}{2} + \frac{L_c}{2}\sum_{l=1}^{n} x_{kl} y_{kl}$$

#### 5.2.3.2 LLR per bit calculation for multilevel modulations

In subsection 5.2.3.1 it was assumed that BPSK modulation is used, where the amplitude of transmitted signal is simply equal to $+\sqrt{E_c}$ or $-\sqrt{E_c}$.

In Release 14 of standard on "Physical layer procedures" for LTE [147], modulation schemes related to possible MCSs that can be used include Quadrature Phase Shift Keying (QPSK) and Quadrature Amplitude Modulation (QAM) (16-QAM, 64-QAM and 256-QAM), where QPSK modulation can be considered as 4-QAM. The signal space dimensionality of M-state QAM modulations is equal to two (unlike for BPSK modulation where it is equal to one), where the information is carried on two orthogonal (quadrature) carriers. Each constellation point of the M-QAM ($M = 2^m$) is represented with a pair of real-valued symbols $\{A_k, B_k\}$ (or alternatively with one complex symbol) at time $k$, and is coded by a set

$\{x_{k,i}\}, i = 1, \ldots, m$ of $m$ bits according to a Gray code [148]. For a coherent receiver, the in-phase and quadrature demodulator outputs $Y_k^{(I)}$ and $Y_k^{(Q)}$ are equal to [148]:

$$Y_k^{(I)} = h_k A_k + I_k$$
$$Y_k^{(Q)} = h_k B_k + Q_k$$

where $h_k$ is the fading amplitude that follows Rayleigh distribution, and $I_k$ and $Q_k$ are two uncorrelated gaussian noises, with zero mean and variance $\sigma_N^2$, which is independent of $h_k$.

Since the observation $\{Y_k^{(I)}, Y_k^{(Q)}\}$ is affected by two independent gaussian noises having the same variance $\sigma_N^2$, in the case where $m$ can be factorized as $m = 2p$ (which is the case for considered QAM modulations), we can find the a posteriori LLR $L(u_{k,i}|Y_k^{(I)}, Y_k^{(Q)})$ for bit $x_{k,i}$ by using Bayes' rule:

$$L(x_{k,i}|Y_k^{(I)}, Y_k^{(Q)}) = \ln \frac{\sum_{j=1}^{2^{p-1}} \exp\left\{-\frac{1}{2\sigma_N^2}(Y_k^{(I)} - h_k a_{1,j}^{(i)})^2\right\}}{\sum_{j=1}^{2^{p-1}} \exp\left\{-\frac{1}{2\sigma_N^2}(Y_k^{(I)} - h_k a_{0,j}^{(i)})^2\right\}}, \text{ for } i = 1, \ldots, p$$

$$L(x_{k,i}|Y_k^{(I)}, Y_k^{(Q)}) = \ln \frac{\sum_{j=1}^{2^{p-1}} \exp\left\{-\frac{1}{2\sigma_N^2}(Y_k^{(Q)} - h_k b_{1,j}^{(i-p)})^2\right\}}{\sum_{j=1}^{2^{p-1}} \exp\left\{-\frac{1}{2\sigma_N^2}(Y_k^{(Q)} - h_k b_{0,j}^{(i-p)})^2\right\}}, \text{ for } i = p+1, \ldots, 2p$$

where $a_{1,j}^{(i)}$ and $a_{0,j}^{(i)}$ represent the $j$-th out of $2^{p-1}$ symbols $A_k$ with 1 and 0 respectively on $i$-th position. Similarly, $b_{1,j}^{(i)}$ and $b_{0,j}^{(i)}$ represent the $j$-th out of $2^{p-1}$ symbols $B_k$ with 1 and 0 respectively on $i$-th position.

Due to the nature of QAM constellation diagram not all the bits $x_{k,i}$ have the same level of protection (thus they do not have the same variance $\sigma_{b,i}^2$). However, it is common in practice to approximate the variance of each bit to the same value $\hat{\sigma}_b^2$ by using an estimation technique. Starting from well known relationship between observation $y_k$ of variable $x_k$ and its LLR for Rayleigh channel with fading amplitude $h_k$ and AWGN $L(x_k) = \frac{2h_k y_k}{\sigma^2}$, if we take the mathematical expectation of absolute value squared of both sides of equality (assuming that average energy per symbol is equal to one):

$$\mathbb{E}\{|L(x_k)|^2\} = \frac{1}{N_{xk}} \sum_{k=1}^{N_{xk}} |L(x_k)|^2 = \left(\frac{2}{\sigma^2}\right)^2 (1 + \sigma^2)$$

where $N_{xk} = N_1 q_i R_{c,i}$ if the transmission occurs during the first phase, and $N_{xk} = N_2 q_i R_{c,i}$ during the second (for $\text{MCS}_i$ being used). Finally, we obtain:

$$\hat{\sigma}_b^2 = \frac{2}{\sqrt{1 + \frac{1}{N_{xk}} \sum_{k=1}^{N_{xk}} |L(x_k)|^2} - 1}$$

#### 5.2.3.3 BCJR algorithm with retransmissions originating from different nodes

In subsection 5.2.3.1, it was assumed that all transmitted symbols experience the identical channel conditions, having constant fading amplitude $a$ and ratio $\frac{E_c}{N_0}$. Such an assumption suits a scenario of point-to-point channel with slowly Rayleigh fading and AWGN where the channel conditions remain constant (fading amplitude and noise variance) even after the initial transmission time-slot, i.e. during all retransmission time-slots.

However, in MAMRC a retransmission may be performed by a node other than the one which performed the initial transmission (ex. a relay sending additional parity bits to the destination for the codeword of a source). In that case, probability $\gamma_k(s', s)$ should be calculated as:

$$\gamma_k(s', s) = C'_k e^{u_k L(u_k)/2} \frac{1}{\sqrt{\pi^n \prod_{l=1}^{n} \{N_0/E_c\}^{(l)}}} \exp\left(-\sum_{l=1}^{n} \left\{\frac{E_c}{N_0}\right\}^{(l)} y_{kl}^2\right)$$
$$\exp\left(-a^2 \sum_{l=1}^{n} \left\{\frac{E_c}{N_0}\right\}^{(l)} x_{kl}^2\right) \exp(2a \sum_{l=1}^{n} \left\{\frac{E_c}{N_0}\right\}^{(l)} x_{kl} y_{kl}),$$

where $\left\{\frac{E_c}{N_0}\right\}^{(l)} = \frac{1}{2\sigma_l^2}$ is $\frac{E_c}{N_0}$ ratio which bit $l$ experiences having variance $\sigma_l^2$, and:

$$C'_k = \frac{e^{L(u_k)/2}}{1 + e^{L(u_k)}}.$$

Circular buffer principle implies that after all $3K_\Pi$ bits are transmitted, in the case of need those same bits are starting to be retransmitted sequentially (starting from the beginning of circular buffer), where in theory, for sufficient number of retransmission time-slots and bad enough channel conditions, certain bits can even be transmitted more than two times. We use MRC technique to combine the identical information originating from different time-slots and possibly different nodes, which is the optimal diversity combining scheme for AWGN channel with flat fading. Classically, that technique is used to combine the signal received by multiple antennas at the receiver. Its main principle consists in co-phasing and weighting up signals originating from different branches with coefficients proportional to their own SNR before summing them up, in order to maximize the output SNR.

Let us consider the case where signals $y_1$ and $y_2$ from two branches need to be combined in order to detect transmitted symbol $x$, where $h_1$ and $h_2$ are fading coefficients and $n_1$ and $n_2$ are gaussian noises in the first and the second branch,

respectively. The problem consists in finding the optimal coefficients $w_1$ and $w_2$ in order to maximize the output SNR:

$$\begin{aligned} y_1 &= h_1 x + n_1 \\ y_2 &= h_2 x + n_2 \\ \widetilde{y} &= w_1 y_1 + w_2 y_2 \end{aligned}$$

In the case where $n_1$ and $n_2$ have the same variance $\sigma^2$ (which is most often the case when signals are combined from two receiving antennas), the solution for $w_1$ and $w_2$ is well-known to be:

$$w_1 = \frac{h_1^\star}{\sqrt{|h_1|^2 + |h_2|^2}}, \qquad w_2 = \frac{h_2^\star}{\sqrt{|h_1|^2 + |h_2|^2}}$$

In that way, the equivalent SNR is equal to the addition of two individual SNRs:

$$\mathrm{SNR}_{eq} = \mathrm{SNR}_1 + \mathrm{SNR}_2.$$

If $n_1$ and $n_2$ have variances $\sigma_1^2$ and $\sigma_2^2$ that are not the same, we find that the optimal coefficients are:

$$w_1 = \frac{\frac{h_1^\star}{\sigma_1^2}}{\sqrt{\frac{|h_1|^2}{\sigma_1^4} + \frac{|h_2|^2}{\sigma_2^4}}}, \qquad w_2 = \frac{\frac{h_2^\star}{\sigma_2^2}}{\sqrt{\frac{|h_1|^2}{\sigma_1^4} + \frac{|h_2|^2}{\sigma_2^4}}}$$

This solution can be easily extended for the case of $L$ branches, where the optimal coefficient $w_k$ is equal to:

$$w_k = \frac{\frac{h_k^\star}{\sigma_k^2}}{\sqrt{\frac{|h_1|^2}{\sigma_1^4} + \frac{|h_2|^2}{\sigma_2^4} + \cdots + \frac{|h_L|^2}{\sigma_L^4}}}$$

#### 5.2.3.4 Iterative turbo decoding

At each decoder BCJR algorithm is applied in order to calculate the a posteriori LLR $L(u_k|\mathbf{y})$ of bit $u_k$ based on received sequence $\mathbf{y}$. This probability can be decomposed in the following way [146]:

$$L(u_k|\mathbf{y}) = L(u_k) + L_c y_k^{(s)} + L_e(u_k). \tag{5.15}$$

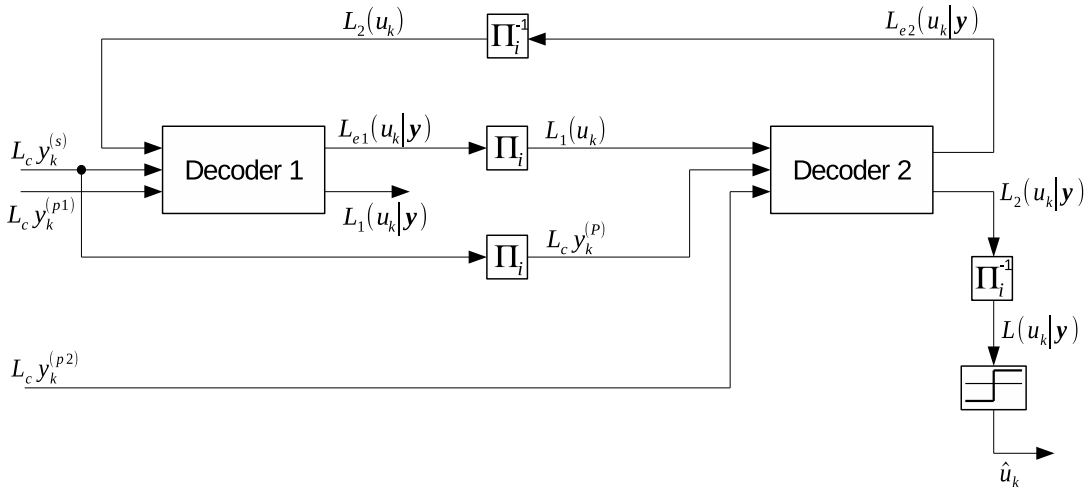


**Figure 5.9:** Turbo code decoding scheme.

In (5.15), the first two terms are related to information bits, while the third one, the extrinsic information $L_e(u_k)$, is related to parity-check bits produced by the corresponding encoder. The structure of turbo decoder is depicted on 5.9. The extrinsic information is passed from one decoder to another (after appropriate interleaving/deinterleaving), and used as a new and more accurate value of a priori LLR $L(u_k)$. Using new information received from the other decoder the a posteriori LLR $L(u_k|\mathbf{y})$ is again calculated, and the extrinsic information is calculated anew and passed to the other decoder. The described procedure of a back and forth exchange of extrinsic information is repeated until the stopping criterion is fulfilled or if the specified number of iterations is reached. In the end, the hard decision on value of bit $u_k$ is made after deinterleaving the a posteriori LLR of the second decoder, by checking out the sign of the obtained value [146]:

$$\hat{u}_k = sign[L(u_k|\mathbf{y})] = sign\{P^{-1}[L_2(u_k|\mathbf{y})]\}.$$

### 5.2.4 Numerical results

In order to evaluate the performance of designed practical coding scheme for HARQ protocol with Single User encoding/decoding, we perform MC simulations to compare the average spectral efficiency that can be obtained by using it with the

**Table 5.2:** Candidate MCSs.

| Nb. | Modulation | Coding rate (approx.) | Spectral eff. (approx.) |
|---|---|---|---|
| 0 | QPSK | 0.3 | 0.6 |
| 1 | QPSK | 0.44 | 0.88 |
| 2 | QPSK | 0.59 | 1.18 |
| 3 | 16-QAM | 0.33 | 1.32 |
| 4 | 16-QAM | 0.42 | 1.68 |
| 5 | 16-QAM | 0.54 | 2.16 |
| 6 | 16-QAM | 0.64 | 2.56 |
| 7 | 64-QAM | 0.46 | 2.76 |
| 8 | 64-QAM | 0.55 | 3.3 |
| 9 | 64-QAM | 0.65 | 3.9 |

theoretical upper-bound defined in subsection 5.1.2 where the capacity achieving coding scheme is implicitly assumed.

We assume that the number of channel uses being used in each time-slot of the first phase is equal to $N_1 = 512$, while during the second phase $N_2 = 256$ ($\alpha = 0.5$). A discrete family of 10 MCSs given in tab. 5.2 is available to slow-link adaptation algorithm, which represents a subset of the set of MCSs given in [147]. In order to easily refer to different MCSs, a number is assigned to each MCS in the first column of tab. 5.2, so e.g. $\text{MCS}_i$ corresponds to MCS in row $i$. Since the number of channel uses is fixed during each time-slot in the first phase, different input block sizes are used for different MCSs, going from 280 for $\text{MCS}_0$ to 1952 for $\text{MCS}_9$. The maximum number of iterations of turbo decoder is set to 10.

First, we verify our turbo encoding and decoding scheme for point-to-point channel for two different MCSs: $\text{MCS}_1$ where QPSK modulation is used, and $\text{MCS}_8$ where 16-QAM modulation is used. We consider two scenarios: (i) the slowly Rayleigh fading channel with AWGN; and (ii) the AWGN only channel (fading amplitude $a = 1$). Maximum number of retransmissions is set to 3 in all cases, and on Fig. 5.10 we plot Bit Error Rate (BER) as a function of average SNR of the channel after the initial transmission (referred to as "MCSx AWGN/Rayleigh f. t=0",$x \in \{1, 8\}$), as well as after each one of three retransmissions (referred to as "MCSx AWGN/Rayleigh f. t=y", $x \in \{1, 8\}, y \in \{1, 2, 3\}$). For the case of AWGN channel (no fading) we can recognize the well-known "waterfall region" for each curve, where its slope is very steep in a certain SNR region. For both considered MCSs, bigger the number of retransmissions being used, bigger the shift of that region in negative direction of SNR-axis, as expected (the probability of error decreases with each additional retransmission). Also, the BER curves

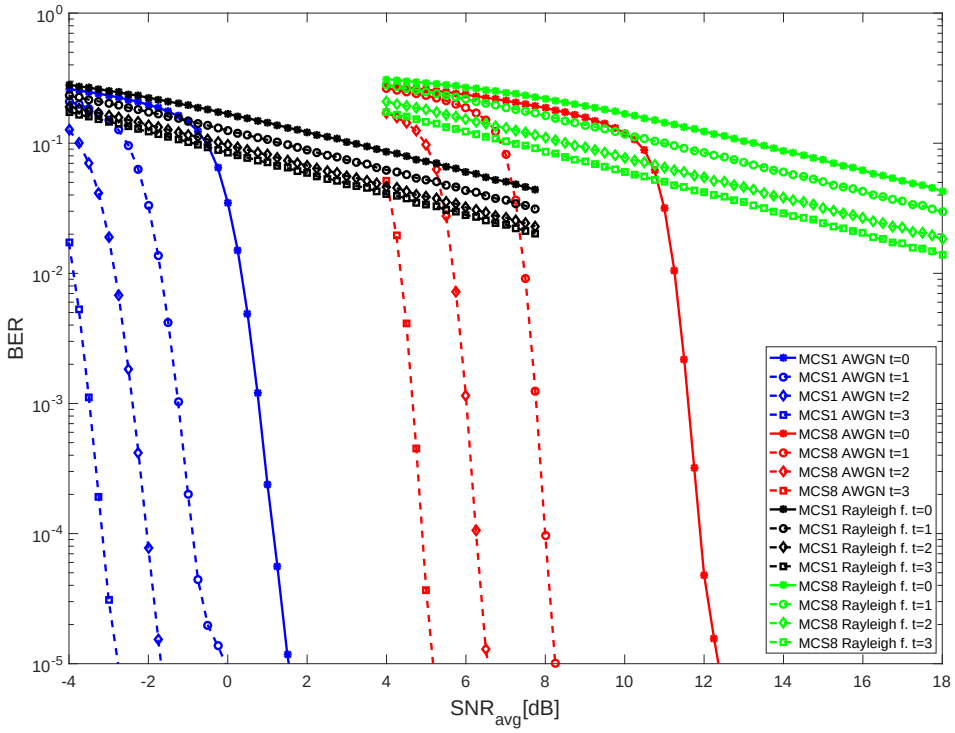


**Figure 5.10:** BER performance of proposed turbo coding scheme for $MCS_1$ and $MCS_8$.

for $MCS_8$ have a coding loss of about 10dB compared with $MCS_1$ since although 64-QAM modulation is more spectrally efficient than QPSK modulation, it is less robust to AWGN. For the same curves, we can observe that the coding gain of first retransmission compared with the initial transmission is bigger than the coding gain between any of the two consecutive retransmissions. One possible reason for that is the fact that in first retransmission, the amount of additional parity-check bits transmitted (which were not transmitted during the initial transmission) is higher than the same amount in the second retransmission and beyond (we have already discussed the advantage of IR-HARQ compared with CC-HARQ). Finally, we observe that corresponding slopes of curves related to slowly Rayleigh fading channel are much less steep compared with the case of AWGN channel. The realizations of small value of fading amplitude makes it much more difficult to decode even after 3 retransmissions and high average SNR. Conclusions concerning the performance comparison between $MCS_1$ and $MCS_8$, as well as between different transmission time-slots remain the same as for the case of AWGN channel.

Finally, we evaluate the total average spectral efficiency that can be obtained in the

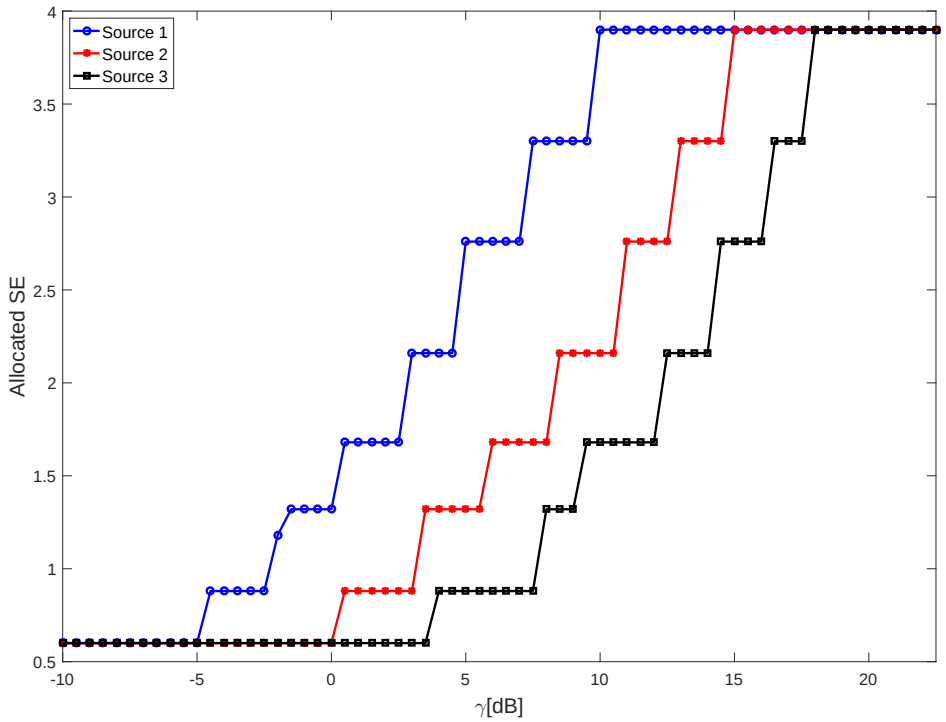


**Figure 5.11:** Allocated MCSs to different sources as a function of $\gamma$, in terms of corresponding spectral efficiencies.

network composed of 3 sources, 3 relays and one destination, where user co-operation is not used (without loss of generality). Maximum number of retransmissions remains equal to 3. Node selection strategy 2 proposed in subsec. 3.2.2 and slow-link adaptation algorithm under no QoS constraint ($BLER_{\text{QoS}} = 1$ for each source) proposed in sec. 4.1 are used, both being adapted to Single User encoding described in 5.1.2. Discrete i.i.d. inputs are taken into account in both cases for calculation of different mutual informations (see Appendix B). The same asymmetric link configuration as described in sec. 4.3 is used, with source $s_1$ being in the best propagation conditions, and source $s_3$ in the worst. Parameter $\gamma$ has the same definition as in 4.3. This time around, only slowly Rayleigh fading channel with AWGN is considered. First, on Fig. 5.11 we plot the allocated spectral efficiencies (which is equivalent to term "allocated rates" that we have used in theoretic outage analysis) to sources (unambiguously determined by allocated MCSs) as a function of $\gamma$. As expected, in the biggest part of the range of interest, $-4.5\text{dB} \leq \gamma \leq 17.5\text{dB}$, source $s_1$ is being allocated by more spectrally efficient MCS compared with other sources, source $s_3$ having the least spectral efficient MCS of them all. Finally, on

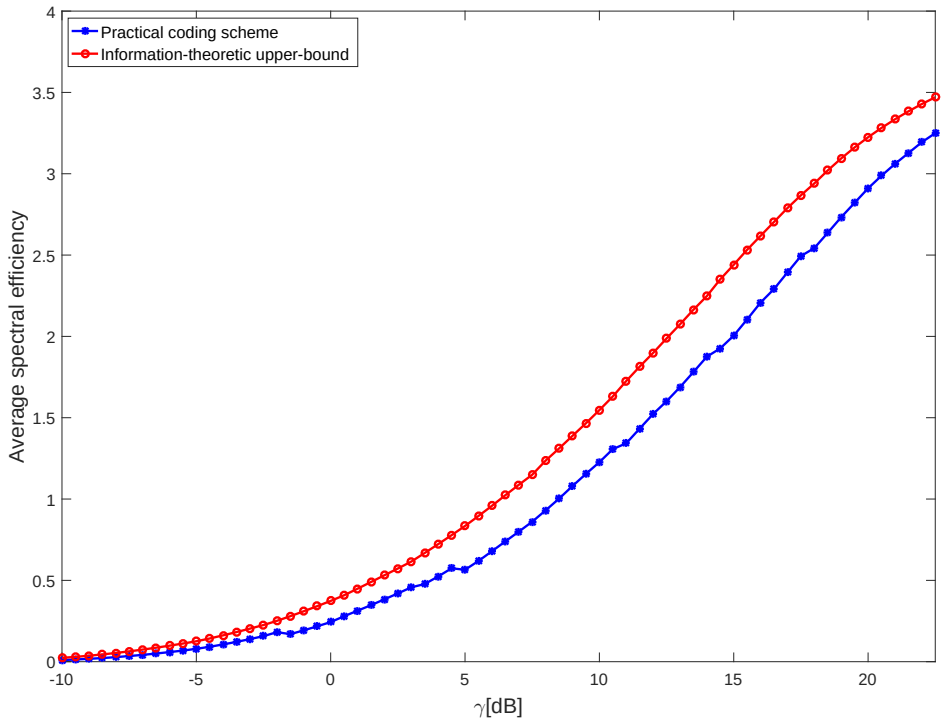


**Figure 5.12:** Total average spectral efficiency obtained for (3,3,1)-MAMRC with 3 retransmissions and no user co-operation.

Fig. 5.12 we compare the total average spectral efficiency of our practical coding scheme with the theoretical bound obtained as described in sec. 5.1.2, but for the network parameters defined at the beginning of this paragraph. For that curve, we also take discrete i.i.d. inputs into account for mutual information calculation. We observe that the coding loss of practical coding scheme compared with the theoretical upper-bound is not bigger than 3dB for each $\gamma$, which confirms the validity of our practical coding scheme design. The difference can be further reduced by increasing the number of available channel uses in both phases, which would increase the processing complexity, especially at the receiver, due to increased input block sizes for considered MCSs for turbo code.

# 6 | Conclusion and Perspective

## 6.1 Conclusion

An innovative concept such as cooperative communications allows the enhancement of total throughput and coverage of multi-terminal wireless networks. The focus of this thesis is set on three important aspects of multiple access multiple relay networks with time division multiplexing: design of node selection strategies, design of link-adaptation algorithms and evaluation of different cooperative HARQ protocols, as well as the design of a practical encoding/decoding scheme.

In chapter 3, we have proposed three centralized scheduling strategies for cooperative IR retransmissions in the slow-fading half-duplex time-slotted $(M, L, 1)$-MAMRC, that are applicable both to symmetric and asymmetric source rate scenarios. During the first phase, the sources transmit in turn. During the second phase, a scheduled node (relay or source) transmits incremental redundancies on its correctly decoded source messages. The first proposed strategy is based on the exhaustive search of the node which maximizes the cardinality of the decoding set at the destination after each time-slot. The other two proceed from intuitive approaches and are less computationally expensive: (i) the first one consists of node selection based on the highest mutual information; (ii) the second one consists of node selection based on the highest product of mutual information and the cardinality of the decoding set. A scheduled node uses Multi-User Encoding (Joint Network and Channel Coding) on its decoded source set. Using Monte-Carlo simulations we show that all the proposed strategies perform close to each other in terms or the average spectral efficiency. Additionally, our strategies perform close to the average spectral efficiency upper bound (under the given fairness constraint) obtained by an exhaustive search over all possible node sequence activations. Finally, it is demonstrated that the proposed strategies always perform better than the state-of-the-art strategy based on the minimization of the common outage event probability after each time-slot.

In chapter 4, we propose a slow-link adaptation algorithm for the $(M, L, 1)$-MAMRC under the same system model assumptions. Typically, the acquisition of the CSI of each link in the network at the destination is too costly in terms of feedback overhead for a fluctuating environment. So the Channel Distribution Information is reported to the destination in order to derive the rates allocated to the sources on a long-term basis. The proposed slow-link adaptation algorithm aims at maximizing the average spectral efficiency under individual QoS targets for a given modulation and coding scheme family. We also propose a fast-link adaptation algorithm where the rates are allocated with respect to CSI of all the links in the network, which can be a suitable solution for a scenario where radio conditions do not change too quickly. Its goal is to maximize the spectral efficiency in each frame. To reduce the complexity of proposed algorithms, the discrete rates are first determined by using the "Genie-Aided" assumption which consists in considering for a given source that all the other ones are known to the relaying nodes and the destination. In a second step, an iterative rate correction algorithm is applied similar to the well known iterative water filling algorithm. The resulting scheduling and link adaptation algorithms offer a tractable complexity for both scenarios of the available knowledge on channel qualities, where MC simulations demonstrate that the proposed algorithms offer performance close to corresponding exhaustive search approaches. In addition, it is shown that adopting some form of cooperation between the nodes (user cooperation, relays) is crucial for the slow link adaptation case when tight reliability constraint, e.g., low BLER targets at the destination, must be complied with the sources.

In chapter 5, we have compared the performance of three different cooperative HARQ protocols for the same $(M, L, 1)$-MAMRC as studied in previous chapters. Among the three proposed HARQ protocols, two follow the Incremental Redundancy (IR) approach. One consists in sending incremental redundancies on all the source messages decoded correctly by the scheduled node (Multi-User encoding) while the other one helps a single source (Single User encoding) chosen randomly. The third one is of the Chase Combining (CC) type, where the selected node repeats the transmission (including modulation and coding scheme) of one source chosen randomly in its correctly decoded source message set (its decoding set). It allows MRC at the destination of all the transmissions related to a given source. Single User encoding and decoding is well mastered in terms of code construction (state of the art rate compatible punctured codes) and, clearly, less complex than Multi-User encoding and iterative joint decoding. On the other hand, the Chase Combining approach can be considered as having a similar complexity to Single User IR-HARQ. To identify the most efficient cooperative HARQ protocol, i.e., the one that achieves the best complexity-performance tradeoff, we resort to information theory outage based average spectral efficiency performance comparison by performing MC simulations. We conclude that IR-type of HARQ with Single User encoding

offers the best trade-off between performance and complexity for a small number of sources in our setting. In the second part of this chapter, we have designed the practical encoding/decoding scheme with the slow-link adaptation algorithm proposed in chapter 4 which operates with the family of discrete Modulation and Coding Schemes, and the node selection strategy proposed in chapter 3. The encoding and decoding schemes are based on capacity approaching turbo codes with Circular Buffer technique used to form the codewords of desired coding rates. Finally, we have evaluated and compared the performance of the proposed coding scheme by performing MC simulations with the information theoretic upper-bound obtained as described in the first part. The coding loss of practical coding scheme compared with the theoretical upper-bound of at most 3dB in terms of average spectral efficiency validates its design.

## 6.2 Perspectives

In this section, we mention some of the possible directions for future research.

We have analysed in detail the performance of (static) SDF under Multi and Single User (JNCC/JNCD) encoding schemes at relying nodes for the slow $(M, L, 1)$-OMAMRC with limited feedback from the destination to the sources and the relays [137, 149, 150]. On another side, D-SDF/JNCC/JNCD for $(M, L, 1)$-NOMAMRC without limited feedback has been proposed in [82]. We know that D-SDF is more efficient than static SDF. Therefore, a natural research direction is to extend our work to D-SDF/JNCC/JNCD for $(M, L, 1)$-NOMAMRC. If limited feedback is available from the destination to the sources and the relays, then the destination could (i) decode at the end of each time slot; and (ii) estimate the level of coded cooperation required by each source to be correctly decoded. If the destination successfully decodes a set of sources, then it can ask these sources and the relays which were specifically helping them to stay idle. Such a strategy would allow to save power, decrease the level of interference in the network, and, in some cases, increase the spectral efficiency, e.g., when the destination can decode before the end of the frame. We could also imagine that, at the end of each time slot, the relays inform the destination of their decoding sets, and, in return, receive the instruction to continue listening or start transmitting.

Another interesting avenue of research could be to take into account the aspects of spatial multiplexing, by assuming multiple antennas at nodes which perform relaying functions and the destination, together with link adaptation and scheduling for $(M, L, 1)$-MAMRC. Obviously, multiple antennas allow for non-orthogonal multiple access. Additionally, either in combination with previous extensions or

independently, the effect of non-perfect broadcast feedback control channel and/or unicast forward coordination control channels could be evaluated.

Unlike half-duplex relays, in-band full-duplex relays can *simultaneously transmit and receive* data signals in the same frequency band. The basic advantages are numerous: in-band full duplex can double the (ergodic) capacity, reduce feedback delay, reduce end-to-end delay, increase spectrum usage flexibility, etc. On the other side, the main limitation is the presence of unavoidable Self-Interference (SI) when the transmitted signal couples back to the receiver in the in-band full-duplex transceiver. Even though the transmitted signal is perfectly known in the digital baseband, eliminating the SI it generates at the receiver has always been considered as a difficult, if not impossible, task. The reasons essentially come from the considerable difference in power between the transmitted and received signals (the direct SI signal is typically 100 dB more powerful than the intended received signal in Wi-Fi systems and 130 dB more powerful than the intended received signal in cellular systems) and the multiple sources of distortion (nonlinear effects of amplifiers or mixers) and RF imperfections (in-phase/quantization imbalance, phase noise of the local oscillator, analog-to-digital quantization noise, thermal noise, etc.) in the transceiver chain than must be accounted for when subtracting the transmitted signal from the received signal. If the latest advances on the subject of Self-Interference Cancellation (SIC) techniques tend to nuance this negative belief, achieving a sufficient amount of SI attenuation calls for multiple sophisticated measures. Passive isolation, analog/RF cancellation and Digital SIC are the techniques which can be applied independently, where recent experimentations [151 – 153] have proved that the aforementioned cancellation techniques, when combined all at once, could achieve up to $70 - 110$ dB aggregate attenuation levels of SI, i.e., below the noise floor. Thus, in-band full-duplex radios remain a promising feature for relay-assisted cooperative communications, which could potentially have a widespread use in the future.

Hence, full-duplex radios could be an alternative solution for the "switching problem" propounded in section 1.2. For instance, if we assume that each source has $B$ packets to transmit, the idea is to allow the sources to implement regular block Markov encoding [4] and to decompose each block in a given number of time slots, say $T$. Within a given block $b$, at the end of a given time slot $t$, any relay tries to decode the sources' packets and starts cooperating with the successfully decoded ones by means of JNCC until the end of the block duration (and even beyond). But, contrary to half-duplex case, the relay, while transmitting extra parity bits, has still the opportunity to listen and try to decode the non-successfully decoded sources in the subsequent time slots $t + 1$, $t + 2$, etc. Normally, a relay in a given block helps the sources' packets indexed for that block. However, as long as the relay is not able to decode successfully a particular source in a given block, it can

still produce extra parity bits calculated from the source's packets successfully decoded in previous blocks.

# Appendices

## A Sub-block interleaver

In this appendix we detail the sub-block interleaver defined in [145]. Let the input sequence to the sub-block interleaver be $d_0^{(i)}, d_1^{(i)}, \ldots, d_{D-1}^{(i)}$, where $D$ is the length of the sequence. The output sequence is obtained as follows:

1. Form the matrix of dimensions $R_{sb} \times C_{sb}$, where $C_{sb} = 32$ is number of columns of the matrix, and $R_{sb}$ is number of rows of matrix. $R_{sb}$ is obtained by finding the minimum integer which satisfies the following inequality:

$$D \leq (R_{sb} \times C_{sb}) \tag{1}$$

   Matrix columns are numbered $0, \ldots, C_{sb} - 1$ from left to right, while matrix rows are numbered $0, \ldots, R_{sb} - 1$ from top to bottom.

2. If $(R_{sb} \times C_{sb}) > D$, then add $N_D = R_{sb} \times C_{sb} - D$ dummy bits to the beginning of sequence $v_k$, i.e. $v_k =< NULL >$ for $k \in \{0, \ldots, N_D - 1\}$. Remainder of the sequence $v_k$ is directly obtained from the input sequence: $v_{k+N_D} = d_k^{(i)}$, for $k = 0, \ldots, D - 1$. Then, sequence $v_k$ is put row by row into the defined matrix starting from column 0 and row 0:

$$\begin{bmatrix} v_0 & v_1 & v_2 & \cdots & v_{C_{sb}-1} \\ v_{C_{sb}} & v_{C_{sb}+1} & v_{C_{sb}+2} & \cdots & v_{2C_{sb}-1} \\ \vdots & \vdots & \vdots & \ddots & \vdots \\ v_{(R_{sb}-1)\times C_{sb}} & v_{(R_{sb}-1)\times C_{sb}+1} & v_{(R_{sb}-1)\times C_{sb}+2} & \cdots & v_{(R_{sb}\times C_{sb}-1)} \end{bmatrix}$$

**For sequences $d_k^{(0)}$ and $d_k^{(1)}$:**

**Table A.1:** Inter-column permutation pattern for sub-block interleaver.

| **Number of columns** $C_{sb}$ | **Inter-column permutation pattern** $< P(0), P(1), \ldots, P(C_{sb}-1) >$ |
|---|---|
| 32 | $< 0, 16, 8, 24, 4, 20, 12, 28, 2, 18, 10, 26, 6, 22, 14, 30,$ $1, 17, 9, 25, 5, 21, 13, 29, 3, 19, 11, 27, 7, 23, 15, 31 >$ |

3. Inter-column permutation of the matrix is performed based on the pattern $< P(j) >_{j\in\{0,1,\ldots,C_{sb}-1\}}$ defined in table A.1, where $P(j)$ represents the original column position of the $j$-th permuted column ($m_j^{(P)} = m_{P(j)}$). After permutation of the columns, the inter-column permuted matrix is equal to:

$$\begin{bmatrix} v_{P(0)} & v_{P(1)} & \cdots & v_{P(C_{sb}-1)} \\ v_{P(0)+C_{sb}} & v_{P(1)+C_{sb}} & \cdots & v_{P(C_{sb}-1)+C_{sb}} \\ \vdots & \vdots & \ddots & \vdots \\ v_{P(0)+(R_{sb}-1)\times C_{sb}} & v_{P(1)+(R_{sb}-1)\times C_{sb}} & \cdots & v_{P(C_{sb}-1)+(R_{sb}-1)\times C_{sb}} \end{bmatrix}$$

4. The output sequence $l_0^{(i)}, l_1^{(i)}, \ldots, l_{K_\Pi-1}^{(i)}$ is obtained by reading column by column the inter-column permuted $(R_{sb}\times C_{sb})$ matrix. $l_0^{(i)}$ corresponds to $v_{P(0)}$, $l_1^{(i)}$ to $v_{P(0)} + C_{sb}$, etc. until $l_{K_\Pi-1}^{(i)}$ which corresponds to $v_{P(C_{sb}-1)+(R_{sb}-1)\times C_{sb}}$, where $K_\Pi = (R_{sb} \times C_{sb})$.

**For sequence** $d_k^{(2)}$:

3. The output sequence $l_0^{(i)}, l_1^{(i)}, \ldots, l_{K_\Pi-1}^{(i)}$ is obtained from sequence $v_k^{(2)}$ by $l_k^{(2)} = v_{\pi(k)}$, where

$$\pi(k) = \left( P\left( \left\lfloor \frac{k}{R_{sb}} \right\rfloor \right) + C_{sb} \times (k \bmod R_{sb}) + 1 \right) \bmod K_\Pi.$$

Permutation function $P(j)$ is defined in the table A.1.

# B Mutual information calculation for discrete i.i.d. inputs

Let $X$ be a discrete random variable (r.v.) which can take any of $M = 2^q$ possible values from set $\mathcal{X}$ with equal probability, i.e. its Probability Mass Function (PMF)

$P_X(x)$ is defined as:

$$P_X(x) = \Pr(X = x) = \frac{1}{2^q} = \frac{1}{M}, \text{ for } x \in \mathcal{X}.$$

Let $Y$ be a r.v. with support set $\mathcal{Y}$, which is a function of r.v. $X \sim P_X$ and gaussian r.v. $N \sim \mathcal{N}(0, \sigma^2)$:

$$Y = hX + N,$$

where $h$ is known fading amplitude.

Mutual information between random variables $X$ and $Y$ is defined as:

$$I(X;Y|h) = H(X) - H(X|Y,h).$$

The entropy $H(X)$ of r.v. $X$ can be calculated as:

$$H(X) = \mathbb{E}\{-\log_2(P(X))\} = -\sum_{i=1}^{M} p(x_i)\log_2 p(x_i) = -\frac{1}{M}\sum_{i=1}^{M}\log_2 2^{-q} = q.$$

The conditional entropy $H(X|Y,h)$ is defined as:

$$H(X|Y,h) = -\sum_{x\in\mathcal{X}}\sum_{y\in\mathcal{Y}} p(x,y|h)\log_2\frac{p(x,y|h)}{p(y|h)}.$$

It follows that the mutual information $I(X;Y|h)$ can be expressed as:

$$\begin{aligned} I(X;Y|h) &= q + \sum_{x\in\mathcal{X}}\sum_{y\in\mathcal{Y}} p(x,y|h)\log_2\frac{p(x,y|h)}{p(y|h)} \\ &= q + \sum_{k=1}^{M}\sum_{y\in\mathcal{Y}} p(y|x_k,h)p(x_k)\log_2\frac{p(y|x_k,h)p(x_k)}{\sum_{i=1}^{M} p(y|x_i,h)p(x_i)} \\ &= q - \frac{1}{M}\sum_{k=1}^{M}\sum_{y\in\mathcal{Y}} p(y|x_k,h)\left(\log_2(\sum_{i=1}^{M} p(y|x_i,h)) - \log_2(p(y|x_k,h))\right) \end{aligned} \tag{2}$$

Since $p(y|x_k,h)$ is a conditional probability density function for given $x_k$, and the second summation in (2) is performed over all values $y$ in its supporting set, we can replace it with the mathematical expectation with respect to $p(y|x_k,h)$ in the following way:

$$I(X;Y|h) = q - \frac{1}{M}\sum_{k=1}^{M}\mathbb{E}_{\{p(y|x_k,h)\}}\left(\log_2(\sum_{i=1}^{M} p(y|x_i,h)) - \log_2(p(y|x_k,h))\right)$$

Finally, the expectation in previous eq. can be replaced with its Monte Carlo estimate:

$$I(X;Y|h) = q - \frac{1}{M}\sum_{k=1}^{M}\frac{1}{n}\sum_{l=1}^{n}\left(\log_2(\sum_{i=1}^{M}p(y_l|x_i,h)) - \log_2(p(y_l|x_k,h))\right)$$

where $y_l$ is generated following the distribution $p(y_l|x_k,h)$:

$$\Pr(Y = y_l|x_k,h) = \frac{1}{\sqrt{2\pi\sigma^2}}e^{-\frac{(y_l - hx_k)^2}{2\sigma^2}}$$

# List of Publications

## Journal Papers

1. S. Cerovic, R. Visoz, "Slow-link adaptation algorithm for Multi-Source Multi-Relay Wireless Networks with Cooperative Retransmissions", *to be submitted*.

## Conference Papers

1. S. Cerovic, R. Visoz, L. Madier, A. O. Berthet, "Centralized scheduling strategies for cooperative harq retransmissions in multi-source multi-relay wireless networks", in *Proc. IEEE ICC'18*, Kansas City, MO, USA, May 2018.

2. S. Cerovic, R. Visoz, L. Madier, "Efficient Cooperative HARQ for Multi-Source Multi-Relay Wireless Networks", *2018 14th International Conference on Wireless and Mobile Computing, Networking and Communications (WiMob)*, Limassol, Greece, Oct. 2018.

## Patents

1. S. Cerovic, A. Mohamad, R. Visoz, "Centralized scheduling and user cooperation for improved Incremental Retransmission in the uplink", *Patent n:201362FR01*, France, 2017.

2. S. Cerovic, R. Visoz, "Iterative Rate Allocation for Slow-Link Adaptation with Cooperative HARQ Retransmissions in Multi-Source Multi-Relay Wireless Networks", *Patent n:201534FR01*, France, 2018.

3. S. Cerovic, R. Visoz, "Optimized control channel design for Orthogonal Multiple Access Multiple Relay Channel", *Patent n:201564FR01*, France, 2018.

# Bibliography


[1] E. C. Van Der Meulen, "Transmission of information in a t-terminal discrete memoryless channel," Ph.D. dissertation, Dept. of Statistics, University of California, Berkeley, 1968.

[2] ———, "Three-terminal communication channels," *Adv. Appl. Probab.*, vol. 3, no. 1, pp. 120–154, 1971.

[3] H. Satō and U. of Hawaii (Honolulu), *Information Transmission Through a Channel with Relay*, ser. Aloha system technical report B. University of HAWAII, 1976. [Online]. Available: https://books.google.rs/books?id=3KabPgAACAAJ

[4] T. Cover and A. E. Gamal, "Capacity theorems for the relay channel," *IEEE Trans. Inf. Theory*, vol. 25, no. 5, pp. 572–584, Sep. 1979.

[5] L. R Ford Jr and D. R. Fulkerson, "Maximal flow through a network," *Canadian Journal of Mathematics*, vol. 8, pp. 399–404, 01 1956.

[6] A. El Gamal, "On information flow in relay networks," in *NTC '81; National Telecommunications Conference, Volume 2*, vol. 2, 1981, pp. D4.1.1–D4.1.4.

[7] A. El Gamal and T. M. Cover, "Multiple user information theory," *Proceedings of the IEEE*, vol. 68, no. 12, pp. 1466–1483, Dec 1980.

[8] J. N. Laneman, "Cooperative diversity in wireless networks: Algorithms and architectures," Ph.D. dissertation, Massachusetts Institute of Technology, Cambridge, MA, 2002.

[9] M. A. A. Khojastepour, A. Sabharwal, and B. Aazhang, "Lower bounds on the capacity of gaussian relay channel," in *38th Annu. Conf. Information Sciences and Systems (CISS)*, Mar. 2004.

[10] A. Wyner, "On source coding with side information at the decoder," *IEEE Trans. Inf. Theory*, vol. 21, no. 3, pp. 294–300, May 1975.

[11] A. Wyner and J. Ziv, "The rate-distortion function for source coding with side information at the decoder," *IEEE Trans. Inf. Theory*, vol. 22, no. 1, pp. 1 – 10, January 1976.

[12] S. H. Lim, Y. H. Kim, A. E. Gamal, and S. Y. Chung, "Noisy network coding," *IEEE Trans. Inf. Theory*, vol. 57, no. 5, pp. 3132 – 3152, May 2011.

[13] A. El Gamal and M. Aref, "The capacity of the semideterministic relay channel." *IEEE Trans. Inf. Theory*, vol. 28, pp. 536 – , 01 1982.

[14] B. Nazer and M. Gastpar, "Lattice coding increases multicast rates for gaussian multiple-access networks," 01 2007.

[15] – – –, "Compute-and-forward: Harnessing interference through structured codes," *IEEE Trans. Inf. Theory*, vol. 57, no. 10, pp. 6463 – 6486, Oct. 2011.

[16] L. Wei and W. Chen, "Compute-and-forward network coding design over multi-source multi-relay channels," *IEEE Trans. Wireless Commun.*, vol. 11, no. 9, pp. 3348 – 3357, Sept. 2012.

[17] A. S. Avestimehr, S. N. Diggavi, and D. N. C. Tse, "Wireless network information flow: A deterministic approach," *IEEE Trans. Inf. Theory*, vol. 57, no. 4, pp. 1872 – 1905, Apr. 2011.

[18] G. Kramer, M. Gastpar, and P. Gupta, "Cooperative strategies and capacity theorems for relay networks," *IEEE Trans. Inf. Theory*, vol. 51, no. 9, pp. 3037 – 3063, Sept. 2005.

[19] A. Host-Madsen and J. Zhang, "Capacity bounds and power allocation for wireless relay channels," *IEEE Trans. Inf. Theory*, vol. 51, no. 6, pp. 2020 – 2040, June 2005.

[20] A. El Gamal and S. Zahedi, "Capacity of a class of relay channels with orthogonal components," *IEEE Trans. Inf. Theory*, vol. 51, no. 5, pp. 1815 – 1817, May 2005.

[21] Y. Liang and V. V. Veeravalli, "Gaussian orthogonal relay channels: optimal resource allocation and capacity," *IEEE Trans. Inf. Theory*, vol. 51, no. 9, pp. 3284 – 3289, Sep. 2005.

[22] A. El Gamal, M. Mohseni, and S. Zahedi, "Bounds on capacity and minimum energy-per-bit for awgn relay channels," *IEEE Trans. Inf. Theory*, vol. 52, no. 4, pp. 1545 – 1561, April 2006.

[23] M. R. Aref, "Information flow in relay networks," Ph.D. dissertation, Stanford Univ., CA., 1980.

[24] K. Azarian, H. El Gamal, and P. Schniter, "On the achievable diversity-multiplexing tradeoff in half-duplex cooperative channels," *IEEE Trans. Inf. Theory*, vol. 51, no. 12, pp. 4152 – 4172, Dec 2005.

[25] M. Khojastepour, "Distributed cooperative communications in wireless networks," Ph.D. dissertation, Rice University, 2004.

[26] G. Kramer, "Distributed and layered codes for relaying," in *Conference Record of the Thirty-Ninth Asilomar Conference onSignals, Systems and Computers, 2005.*, Oct 2005, pp. 1752 – 1756.

[27] H. F. Chong, M. Motani, and H. K. Garg, "New coding strategies for the relay channel," in *Proceedings. International Symposium on Information Theory, 2005. ISIT 2005.*, Sep. 2005, pp. 1086 – 1090.

[28] A. Bletsas, A. Khisti, D. P. Reed, and A. Lippman, "A simple cooperative diversity method based on network path selection," *IEEE J. Sel. Areas Commun.*, vol. 24, no. 3, pp. 659 – 672, March 2006.

[29] M. Gastpar and M. Vetterli, "On the capacity of large gaussian relay networks," *IEEE Trans. Inf. Theory*, vol. 51, no. 3, pp. 765 – 779, March 2005.

[30] A. F. Dana and B. Hassibi, "On the power efficiency of sensory and ad hoc wireless networks," *IEEE Trans. Inf. Theory*, vol. 52, no. 7, pp. 2890 – 2914, July 2006.

[31] A. d. Coso Sánchez, "Transmission of information in a t-terminal discrete memoryless channel," Ph.D. dissertation, Universitat Politècnica de Catalunya, 2008.

[32] J. N. Laneman, D. N. C. Tse, and G. W. Wornell, "Cooperative diversity in wireless networks: Efficient protocols and outage behavior," *IEEE Transactions on Information Theory*, vol. 50, no. 12, pp. 3062 – 3080, Dec 2004.

[33] J. N. Laneman and G. W. Wornell, "Distributed space-time-coded protocols for exploiting cooperative diversity in wireless networks," *IEEE Trans. Inf. Theory*, vol. 49, no. 10, pp. 2415 – 2425, Oct. 2003.

[34] Lizhong Zheng and D. N. C. Tse, "Diversity and multiplexing: a fundamental tradeoff in multiple-antenna channels," *IEEE Transactions on Information Theory*, vol. 49, no. 5, pp. 1073 – 1096, May 2003.

[35] A. Sendonaris, E. Erkip, and B. Aazhang, "User cooperation diversity. part i. system description," *IEEE Transactions on Communications*, vol. 51, no. 11, pp. 1927 – 1938, Nov 2003.

[36] – – –, "User cooperation diversity. part ii. implementation aspects and performance analysis," *IEEE Transactions on Communications*, vol. 51, no. 11, pp. 1939 – 1948, Nov 2003.

[37] L. H. Ozarow, S. Shamai, and A. D. Wyner, "Information theoretic considerations for cellular mobile radio," *IEEE Transactions on Vehicular Technology*, vol. 43, no. 2, pp. 359 – 378, May 1994.

[38] M. Effros, A. Goldsmith, and Y. Liang, "Generalizing capacity: New definitions and capacity theorems for composite channels," *IEEE Transactions on Information Theory*, vol. 56, no. 7, pp. 3069 – 3087, July 2010.

[39] T. E. Hunter and A. Nosratinia, "Cooperation diversity through coding," in *Proceedings IEEE International Symposium on Information Theory,*, June 2002, pp. 220 –.

[40] A. Nosratinia, T. E. Hunter, and A. Hedayat, "Cooperative communication in wireless networks," *IEEE Communications Magazine*, vol. 42, no. 10, pp. 74 – 80, Oct 2004.

[41] M. Janani, A. Hedayat, T. E. Hunter, and A. Nosratinia, "Coded cooperation in wireless communications: space-time transmission and iterative decoding," *IEEE Trans. Signal Process.*, vol. 52, no. 2, pp. 362 – 371, Feb. 2004.

[42] T. E. Hunter and A. Nosratinia, "Diversity through coded cooperation," *IEEE Transactions on Wireless Communications*, vol. 5, no. 2, pp. 283 – 289, Feb 2006.

[43] T. E. Hunter, S. Sanayei, and A. Nosratinia, "Outage analysis of coded cooperation," *IEEE Transactions on Information Theory*, vol. 52, no. 2, pp. 375 – 391, Feb 2006.

[44] G. Kramer and A. J. van Wijngaarden, "On the white gaussian multiple-access relay channel," in *Proc. IEEE ISIT'00*, Sorrento, Italy, June 2000.

[45] L. Sankaranarayanan, G. Kramer, and N. B. Mandayam, "Capacity theorems for the multiple-access relay channel," in *In Allerton Conference on Communications, Control and Computing*, 2004, pp. 1782 – 1791.

[46] L. Sankaranarayanan, G. Kramer, and N. B. Mandayam, "Hierarchical sensor networks: capacity bounds and cooperative strategies using the multiple-access relay channel model," in *2004 First Annual IEEE Communications Society Conference on Sensor and Ad Hoc Communications and Networks, 2004. IEEE SECON 2004.*, Oct 2004, pp. 191 – 199.

[47] P. Mitran, H. Ochiai, and V. Tarokh, "Space-time diversity enhancements using collaborative communications," *IEEE Transactions on Information Theory*, vol. 51, no. 6, pp. 2041 – 2057, June 2005.

[48] D. Chen and J. N. Laneman, "The diversity-multiplexing tradeoff for the multiaccess relay channel," in *2006 40th Annual Conference on Information Sciences and Systems*, March 2006, pp. 1324 – 1328.

[49] C. Lee and H. Su, "Dynamic decode and forward for the multi-access relay channel with finite block length," in *2011 IEEE 22nd International Symposium on Personal, Indoor and Mobile Radio Communications*, Sep. 2011, pp. 1825 – 1829.

[50] Y. Liang and V. V. Veeravalli, "The impact of relaying on the capacity of broadcast channels," in *International Symposium onInformation Theory, 2004. ISIT 2004. Proceedings.*, June 2004, pp. 403 – .

[51] R. Dabora and S. Servetto, "Broadcast channels with cooperating receivers: a downlink for the sensor reachback problem," in *International Symposium onInformation Theory, 2004. ISIT 2004. Proceedings.*, June 2004, pp. 176 – .

[52] Y. Liang and V. V. Veeravalli, "Cooperative relay broadcast channels," in *2005 International Conference on Wireless Networks, Communications and Mobile Computing*, vol. 2, June 2005, pp. 1449 – 1454 vol.2.

[53] – – –, "Cooperative relay broadcast channels," *IEEE Transactions on Information Theory*, vol. 53, no. 3, pp. 900 – 928, March 2007.

[54] A. Reznik, S. R. Kulkarni, and S. Verdu, "Broadcast-relay channel: capacity region bounds," in *Proceedings. International Symposium on Information Theory, 2005. ISIT 2005.*, Sep. 2005, pp. 820 – 824.

[55] S. I. Bross, "On the discrete memoryless partially cooperative relay broadcast channel and the broadcast channel with cooperating decoders," *IEEE Transactions on Information Theory*, vol. 55, no. 5, pp. 2161 – 2182, May 2009.

[56] S. A. Jafar, K. S. Gomadam, and C. Huang, "Duality and rate optimization for multiple access and broadcast channels with amplify-and-forward relays," *IEEE Transactions on Information Theory*, vol. 53, no. 10, pp. 3350 – 3370, Oct 2007.

[57] R. Ahlswede, N. Cai, S. Y. R. Li, and R. W. Yeung, "Network information flow," *IEEE Trans. Inf. Theory*, vol. 46, no. 4, pp. 1204 – 1216, July 2000.

[58] S. . R. Li, R. W. Yeung, and Ning Cai, "Linear network coding," *IEEE Transactions on Information Theory*, vol. 49, no. 2, pp. 371 – 381, Feb 2003.

[59] R. Koetter and M. Medard, "An algebraic approach to network coding," *IEEE/ACM Trans. Netw.*, vol. 11, no. 5, pp. 782 – 795, Oct. 2003.

[60] R. Dougherty, C. Freiling, and K. Zeger, "Insufficiency of linear coding in network information flow," *IEEE Transactions on Information Theory*, vol. 51, no. 8, pp. 2745 – 2759, Aug 2005.

[61] T. Ho, M. Médard, J. Shi, M. Effros, and D. R. Karger, "On randomized network coding," in *2003 41st Annual Allerton Conference on Communication, Control, and Computing (Allerton)*, Oct. 2003.

[62] T. Ho, M. Medard, R. Koetter, D. R. Karger, M. Effros, J. Shi, and B. Leong, "A random linear network coding approach to multicast," *IEEE Transactions on Information Theory*, vol. 52, no. 10, pp. 4413 – 4430, Oct 2006.

[63] S. Zhang, S. C. Liew, and P. P. Lam, "Hot topic: Physical-layer network coding," in *Proceedings of the 12th Annual International Conference on Mobile Computing and Networking*, ser. MobiCom '06. New York, NY, USA: ACM, 2006, pp. 358 – 365. [Online]. Available: http://doi.acm.org/10.1145/1161089.1161129

[64] S. Zhang and S. C. Liew, "Channel coding and decoding in a relay system operated with physical-layer network coding," *IEEE J. Sel. Areas Commun.*, vol. 27, no. 5, pp. 788 – 796, June 2009.

[65] Y. Wu, P. A. Chou, and S.-Y. Kung, "Information exchange in wireless networks with network coding and physical-layer broadcast," in *Conference on Information Sciences and Systems*, Baltimore, MD, USA, March 2005.

[66] B. Rankov and A. Wittneben, "Achievable rate regions for the two-way relay channel," in *2006 IEEE International Symposium on Information Theory*, July 2006, pp. 1668 – 1672.

[67] L. Xie, "Network coding and random binning for multi-user channels," in *2007 10th Canadian Workshop on Information Theory (CWIT)*, June 2007, pp. 85 – 88.

[68] Y. Song and N. Devroye, "List decoding for nested lattices and applications to relay channels," in *2010 48th Annual Allerton Conference on Communication, Control, and Computing (Allerton)*, Sep. 2010, pp. 1038 – 1045.

[69] P. Larsson, N. Johansson, and K. . Sunell, "Coded bi-directional relaying," in *2006 IEEE 63rd Vehicular Technology Conference*, vol. 2, May 2006, pp. 851 – 855.

[70] Z. Ding, I. Krikidis, B. Rong, J. S. Thompson, C. Wang, and S. Yang, "On combating the half-duplex constraint in modern cooperative networks: protocols and techniques," *IEEE Wireless Communications*, vol. 19, no. 6, pp. 20 – 27, December 2012.

[71] T. J. Oechtering, C. Schnurr, I. Bjelakovic, and H. Boche, "Achievable rate region of a two phase bidirectional relay channel," in *2007 41st Annual Conference on Information Sciences and Systems*, March 2007, pp. 408 – 413.

[72] – – –, "Broadcast capacity region of two-phase bidirectional relaying," *IEEE Transactions on Information Theory*, vol. 54, no. 1, pp. 454 – 458, Jan 2008.

[73] C. Schnurr, T. J. Oechtering, and S. Stanczak, "Achievable rates for the restricted half-duplex two-way relay channel," in *2007 Conference Record of the Forty-First Asilomar Conference on Signals, Systems and Computers*, Nov 2007, pp. 1468 – 1472.

[74] – – –, "On coding for the broadcast phase in the two-way relay channel," in *2007 41st Annual Conference on Information Sciences and Systems*, March 2007, pp. 271 – 276.

[75] B. Rankov and A. Wittneben, "Spectral efficient protocols for half-duplex fading relay channels," *IEEE Journal on Selected Areas in Communications*, vol. 25, no. 2, pp. 379 – 389, February 2007.

[76] M. P. Wilson, K. Narayanan, H. D. Pfister, and A. Sprintson, "Joint physical layer coding and network coding for bidirectional relaying," *IEEE Transactions on Information Theory*, vol. 56, no. 11, pp. 5641 – 5654, Nov 2010.

[77] S. J. Kim, P. Mitran, and V. Tarokh, "Performance bounds for bidirectional coded cooperation protocols," *IEEE Transactions on Information Theory*, vol. 54, no. 11, pp. 5235 – 5241, Nov 2008.

[78] S. J. Kim, N. Devroye, P. Mitran, and V. Tarokh, "Achievable rate regions and performance comparison of half duplex bi-directional relaying protocols," *IEEE Transactions on Information Theory*, vol. 57, no. 10, pp. 6405 – 6418, Oct 2011.

[79] P. Popovski and H. Yomo, "Physical network coding in two-way wireless relay channels," in *2007 IEEE International Conference on Communications*, June 2007, pp. 707 – 712.

[80] S. Deb, M. Effros, T. Ho, D. R. Karger, R. Koetter, D. S. Lun, M. Médard, and N. Ratnakar, "Network coding for wireless applications: A brief tutorial," in *In IWWAN*, 2005.

[81] Y. Saito, Y. Kishiyama, A. Benjebbour, T. Nakamura, A. Li, and K. Higuchi, "Non-orthogonal multiple access (noma) for cellular future radio access," in *2013 IEEE 77th Vehicular Technology Conference (VTC Spring)*, June 2013, pp. 1 – 5.

[82] A. Mohamad, R. Visoz, and A. O. Berthet, "Dynamic selective decode and forward in wireless relay networks," in *2015 7th International Congress on Ultra Modern Telecommunications and Control Systems and Workshops (ICUMT)*, Oct 2015, pp. 189 – 195.

[83] – – –, "Outage achievable rate analysis for the non orthogonal multiple access multiple relay channel," in *2013 IEEE Wireless Communications and Networking Conference Workshops (WCNCW)*, April 2013, pp. 160 – 165.

[84] – – –, "Practical joint network-channel coding schemes for slow-fading orthogonal multiple-access multiple-relay channels," in *2014 IEEE Globecom Workshops (GC Wkshps)*, Dec 2014, pp. 936 – 941.

[85] A. Mohamad, R. Visoz, and A. O. Berthet, "Code design for multiple-access multiple-relay wireless channels with non-orthogonal transmission," in *Proc. IEEE ICC'15*, London, UK, June 2015.

[86] D. H. Woldegebreal and H. Karl, "Multiple-access relay channel with network coding and non-ideal source-relay channels," in *2007 4th International Symposium on Wireless Communication Systems*, Oct 2007, pp. 732 – 736.

[87] A. Mohamad, R. Visoz, and A. O. Berthet, "Outage analysis of various cooperative strategies for the multiple access multiple relay channel," in *2013 IEEE 24th Annual International Symposium on Personal, Indoor, and Mobile Radio Communications (PIMRC)*, Sep. 2013, pp. 1321 – 1326.

[88] J. Li, J. Yuan, R. Malaney, and M. Xiao, "Binary field network coding design for multiple-source multiple-relay networks," in *2011 IEEE International Conference on Communications (ICC)*, Jun. 2011, pp. 1–6.

[89] Z. Guo, J. Huang, B. Wang, S. Zhou, J. Cui, and P. Willett, "A practical joint network-channel coding scheme for reliable communication in wireless networks," *IEEE Transactions on Wireless Communications*, vol. 11, no. 6, pp. 2084–2094, Jun. 2012.

[90] M. Xiao, J. Kliewer, and M. Skoglund, "Design of network codes for multiple-user multiple-relay wireless networks," *IEEE Transactions on Communications*, vol. 60, no. 12, pp. 3755–3766, Dec. 2012.

[91] C. Hausl, F. Schreckenbach, I. Oikonomidis, and G. Bauch, "Iterative network and channel decoding on a tanner," *Proc. Allerton Conf. on Commun. Control and Computing*, Sep. 2005.

[92] C. Hausl and P. Dupraz, "Joint network-channel coding for the multiple access relay channel," in *Proc. IEEE SECON'06*, Reston, VA, USA, Sept. 2006.

[93] C. Berrou, A. Glavieux, and P. Thitimajshima, "Near shannon limit error-correcting coding and decoding: Turbo-codes. 1," in *Proceedings of ICC '93 - IEEE International Conference on Communications*, vol. 2, May 1993, pp. 1064–1070 vol.2.

[94] B. Zhao and M. C. Valenti, "Distributed turbo coded diversity for relay channel," *Electronics Letters*, vol. 39, no. 10, pp. 786–787, May 2003.

[95] L. Xiao, T. E. Fuja, J. Kliewer, and D. J. Costello, "A network coding approach to cooperative diversity," *IEEE Trans. Inf. Theory*, vol. 53, no. 10, pp. 3714–3722, Oct. 2007.

[96] D. Duyck, D. Capirone, J. J. Boutros, and M. Moeneclaey, "Analysis and construction of full-diversity joint network-ldpc codes for cooperative communications," *EURASIP J. Wirel. Commun. Netw.*, vol. 2010, pp. 9:1–9:16, Jan. 2010. [Online]. Available: http://dx.doi.org/10.1155/2010/805216

[97] J. J. Boutros, A. Guillen i Fabregas, E. Biglieri, and G. Zemor, "Low-density parity-check codes for nonergodic block-fading channels," *IEEE Transactions on Information Theory*, vol. 56, no. 9, pp. 4286–4300, Sep. 2010.

[98] A. Hatefi, R. Visoz, and A. O. Berthet, "Joint channel-network turbo coding for the non-orthogonal multiple access relay channel," in *21st Annual IEEE*

*International Symposium on Personal, Indoor and Mobile Radio Communications*, Sep. 2010, pp. 408–413.

[99] A. Mohamad, R. Visoz, and A. O. Berthet, "Practical joint network-channel coding schemes for slow-fading orthogonal multiple-access multiple-relay channels," in *2014 IEEE Globecom Workshops (GC Wkshps)*, Dec 2014, pp. 936–941.

[100] D. Divsalar and F. Pollara, "Multiple turbo codes," in *Proceedings of MILCOM '95*, vol. 1, Nov 1995, pp. 279–285 vol.1.

[101] F. R. Kschischang, B. J. Frey, and H. . Loeliger, "Factor graphs and the sum-product algorithm," *IEEE Transactions on Information Theory*, vol. 47, no. 2, pp. 498–519, Feb 2001.

[102] M. Luby, "Lt codes," in *The 43rd Annual IEEE Symposium on Foundations of Computer Science, 2002. Proceedings.*, Nov 2002, pp. 271–280.

[103] A. Shokrollahi, "Raptor codes," in *2007 IEEE Information Theory Workshop on Information Theory for Wireless Networks*, July 2007, pp. 1–1.

[104] C. Gong, G. Yue, and X. Wang, "Analysis and optimization of a rateless coded joint relay system," *IEEE Transactions on Wireless Communications*, vol. 9, no. 3, pp. 1175–1185, March 2010.

[105] J. Hagenauer, "Rate-compatible punctured convolutional codes (rcpc codes) and their applications," *IEEE Transactions on Communications*, vol. 36, no. 4, pp. 389–400, April 1988.

[106] A. S. Barbulescu and S. S. Pietrobon, "Rate compatible turbo codes," *Electronics Letters*, vol. 31, no. 7, pp. 535–536, March 1995.

[107] D. N. Rowitch and L. B. Milstein, "On the performance of hybrid fec/arq systems using rate compatible punctured turbo (rcpt) codes," *IEEE Transactions on Communications*, vol. 48, no. 6, pp. 948–959, June 2000.

[108] F. Babich, G. Montorsi, and F. Vatta, "Some notes on rate-compatible punctured turbo codes (rcptc) design," *IEEE Transactions on Communications*, vol. 52, no. 5, pp. 681–684, May 2004.

[109] Jeongseok Ha, Jaehong Kim, and S. W. McLaughlin, "Rate-compatible puncturing of low-density parity-check codes," *IEEE Transactions on Information Theory*, vol. 50, no. 11, pp. 2824–2836, Nov 2004.

[110] H. Seo and B. G. Lee, "Optimal transmission power for single- and multi-hop links in wireless packet networks with arq capability," *IEEE Transactions on Communications*, vol. 55, no. 5, pp. 996 – 1006, May 2007.

[111] R. Comroe and D. Costello, "Arq schemes for data transmission in mobile radio systems," *IEEE Journal on Selected Areas in Communications*, vol. 2, no. 4, pp. 472 – 481, July 1984.

[112] D. Chase, "Code combining - a maximum-likelihood decoding approach for combining an arbitrary number of noisy packets," *IEEE Transactions on Communications*, vol. 33, no. 5, pp. 385 – 393, May 1985.

[113] P. Frenger, S. Parkvall, and E. Dahlman, "Performance comparison of harq with chase combining and incremental redundancy for hsdpa," in *IEEE 54th Vehicular Technology Conference. VTC Fall 2001. Proceedings (Cat. No.01CH37211)*, vol. 3, Oct 2001, pp. 1829 – 1833 vol.3.

[114] B. Makki, T. Eriksson, and T. Svensson, "On the performance of the relay-arq networks," *IEEE Trans. Veh. Technol.*, vol. 65, no. 4, pp. 2078 – 2096, Apr. 2016.

[115] A. Chelli and M. Alouini, "On the performance of hybrid-arq with incremental redundancy and with code combining over relay channels," *IEEE Trans. Wireless Commun.*, vol. 12, no. 8, pp. 3860 – 3871, Aug. 2013.

[116] N. Abuzainab and A. Ephremides, "Energy efficiency of cooperative relaying over a wireless link," *IEEE Transactions on Wireless Communications*, vol. 11, no. 6, pp. 2076 – 2083, June 2012.

[117] J. Choi, D. To, Y. Wu, and S. Xu, "Energy-delay tradeoff for wireless relay systems using harq with incremental redundancy," *IEEE Transactions on Wireless Communications*, vol. 12, no. 2, pp. 561 – 573, February 2013.

[118] Y. Qi, R. Hoshyar, M. A. Imran, and R. Tafazolli, "H2-arq-relaying: Spectrum and energy efficiency perspectives," *IEEE Journal on Selected Areas in Communications*, vol. 29, no. 8, pp. 1547 – 1558, Sep. 2011.

[119] G. Yu, Z. Zhang, and P. Qiu, "Cooperative arq in wireless networks: Protocols description and performance analysis," in *2006 IEEE International Conference on Communications*, vol. 8, June 2006, pp. 3608 – 3614.

[120] I. Stanojev, O. Simeone, Y. Bar-Ness, and D. H. Kim, "Energy efficiency of non-collaborative and collaborative hybrid-arq protocols," *IEEE Transactions on Wireless Communications*, vol. 8, no. 1, pp. 326 – 335, Jan 2009.

[121] R. Narasimhan, "Throughput-delay performance of half-duplex hybrid-arq relay channels," in *2008 IEEE International Conference on Communications*, May 2008, pp. 986–990.

[122] J. S. Harsini and M. Zorzi, "Effective capacity for multi-rate relay channels with delay constraint exploiting adaptive cooperative diversity," *IEEE Transactions on Wireless Communications*, vol. 11, no. 9, pp. 3136–3147, Sep. 2012.

[123] S. Lee, W. Su, D. A. Pados, and J. D. Matyjas, "The average total power consumption of cooperative hybrid-arq on quasi-static rayleigh fading links," in *2010 IEEE Global Telecommunications Conference GLOBECOM 2010*, Dec 2010, pp. 1–5.

[124] ———, "The optimal power assignment for cooperative hybrid-arq relaying protocol," in *2011 IEEE Global Telecommunications Conference - GLOBECOM 2011*, Dec 2011, pp. 1–6.

[125] Ilmu Byun, Duho Rhee, Young Jin Sang, Mingyu Kang, and Kwang Soon Kim, "Performance analysis of a decode-and-forward based hybrid-arq protocol," in *MILCOM 2008 - 2008 IEEE Military Communications Conference*, Nov 2008, pp. 1–5.

[126] E. Beres and R. Adve, "On selection cooperation in distributed networks," in *Proc. CISS'06*, Princeton, NJ, USA, Mar. 2006.

[127] E. Beres and R. Adve, "Selection cooperation in multi-source cooperative networks," *IEEE Transactions on Wireless Communications*, vol. 7, no. 1, pp. 118–127, Jan 2008.

[128] B. Maham, A. Behnad, and M. Debbah, "Analysis of outage probability and throughput for half-duplex hybrid-arq relay channels," *IEEE Trans. Veh. Technol.*, vol. 61, no. 7, pp. 3061–3070, Sept. 2012.

[129] Y. Sun, Y. Li, and X. Wang, "Cooperative hybrid-arq protocol with network coding," in *Proc. ChinaCom'09*, Xi'an, China, Aug. 2009.

[130] P. Zhang, Y. Wang, Z. Feng, R. Li, Z. Wei, and S. Chen, "Joint power allocation and relay selection for multi-hop cognitive network with arq," in *2012 IEEE 23rd International Symposium on Personal, Indoor and Mobile Radio Communications - (PIMRC)*, Sep. 2012, pp. 1220–1225.

[131] 3GPP, "NR; Study on integrated access and backhaul," 3rd Generation Partnership Project (3GPP), Technical report (TR) 38.874, 12 2018, version

16.0.0. [Online]. Available: https://portal.3gpp.org/desktopmodules/Specifications/SpecificationDetails.aspx?specificationId=3232

[132] L. Sun, T. Zhang, L. Lu, and H. Niu, "On the combination of cooperative diversity and multiuser diversity in multi-source multi-relay wireless networks," *IEEE Signal Processing Letters*, vol. 17, no. 6, pp. 535–538, June 2010.

[133] Z. Zhang, T. Lv, and X. Su, "Combining cooperative diversity and multiuser diversity: A fair scheduling scheme for multi-source multi-relay networks," *IEEE Communications Letters*, vol. 15, no. 12, pp. 1353–1355, December 2011.

[134] W. Guo, J. Liu, Y. Liu, L. Zheng, and D. Zheng, "Performance analysis of incremental relaying based on partial selection in multi-source multi-relay networks," in *2011 International Conference on Wireless Communications and Signal Processing (WCSP)*, Nov 2011, pp. 1–6.

[135] L. Wang, X. Zhang, and Y. Dong, "User scheduling and relay selection with fairness concerns in multi-source cooperative networks," in *Proc. WiOpt'13*, May 2013, pp. 588–592.

[136] Y. Cheng and L. Yang, "Joint relay ordering and linear finite field network coding for multiple-source multiple-relay wireless sensor networks," *Int. J. Distrib. Sensor Netw.*, vol. 9, no. 10, pp. 1–12, Sept. 2013.

[137] A. Mohamad, R. Visoz, and A. O. Berthet, "Cooperative incremental redundancy hybrid automatic repeat request strategies for multi-source multi-relay wireless networks," *IEEE Commun. Lett.*, vol. 20, no. 9, pp. 1808–1811, Sep. 2016.

[138] H. Alves, G. Brante, and R. D. Souza, "Throughput performance of incremental decode-and-forward using infra-structured relays and rate allocation," in *Proc. ISWCS'11*, Aachen, Germany, Nov. 2011.

[139] S. H. Kim, S. J. Lee, D. K. Sung, H. Nishiyama, and N. Kato, "Optimal rate selection scheme in a two-hop relay network adopting chase combining harq in rayleigh block-fading channels," in *Proc. IEEE WCNC'12*, Paris, France, Apr. 2012.

[140] S. R. Khosravirad, L. Szczecinski, and F. Labeau, "Rate adaptation for cooperative harq," *IEEE Trans. Commun.*, vol. 62, no. 5, pp. 1469–1479, May 2014.

[141] S. H. Kim and B. C. Jung, "On the optimal link adaptation in linear relay networks with incremental redundancy harq," *IEEE Commun. Lett.*, vol. 18, no. 8, pp. 1411 – 1414, Aug. 2014.

[142] Y. Polyanskiy, H. V. Poor, and S. Verdu, "Channel coding rate in the finite blocklength regime," *IEEE Transactions on Information Theory*, vol. 56, no. 5, pp. 2307 – 2359, May 2010.

[143] T. K. Moon, *Error Correction Coding: Mathematical Methods and Algorithms*. New York, NY, USA: Wiley-Interscience, 2005.

[144] L. Bahl, J. Cocke, F. Jelinek, and J. Raviv, "Optimal decoding of linear codes for minimizing symbol error rate (corresp.)," *IEEE Transactions on Information Theory*, vol. 20, no. 2, pp. 284 – 287, March 1974.

[145] 3GPP, "Evolved Universal Terrestrial Radio Access (E-UTRA); Multiplexing and channel coding," 3rd Generation Partnership Project (3GPP), Technical Specification (TS) 36.212, 06 2019, version 14.10.0. [Online]. Available: https://portal.3gpp.org/desktopmodules/Specifications/SpecificationDetails.aspx?specificationId=2426

[146] S. A. Abrantes, "From bcjr to turbo decoding: Map algorithms made easier," Jan. 2004.

[147] 3GPP, "Evolved Universal Terrestrial Radio Access (E-UTRA); Physical layer procedures," 3rd Generation Partnership Project (3GPP), Technical Specification (TS) 36.213, 06 2019, version 14.11.0. [Online]. Available: https://portal.3gpp.org/desktopmodules/Specifications/SpecificationDetails.aspx?specificationId=2427

[148] S. Le Goff, A. Glavieux, and C. Berrou, "Turbo-codes and high spectral efficiency modulation," in *Proceedings of ICC/SUPERCOMM'94 - 1994 International Conference on Communications*, May 1994, pp. 645 – 649 vol.2.

[149] S. Cerovic, R. Visoz, L. Madier, and A. O. Berthet, "Centralized scheduling strategies for cooperative harq retransmissions in multi-source multi-relay wireless networks," in *Proc. IEEE ICC'18*, Kansas City, MO, USA, May 2018.

[150] S. Cerović, R. Visoz, and L. Madier, "Efficient cooperative harq for multi-source multi-relay wireless networks," in *2018 14th International Conference on Wireless and Mobile Computing, Networking and Communications (WiMob)*, Oct 2018, pp. 61 – 68.

[151] D. Kim, H. Lee, and D. Hong, "A survey of in-band full-duplex transmission: From the perspective of phy and mac layers," *IEEE Communications Surveys Tutorials*, vol. 17, no. 4, pp. 2017–2046, Fourthquarter 2015.

[152] M. Heino, D. Korpi, T. Huusari, E. Antonio-Rodriguez, S. Venkatasubramanian, T. Riihonen, L. Anttila, C. Icheln, K. Haneda, R. Wichman, and M. Valkama, "Recent advances in antenna design and interference cancellation algorithms for in-band full duplex relays," *IEEE Communications Magazine*, vol. 53, no. 5, pp. 91–101, May 2015.

[153] Z. Zhang, X. Chai, K. Long, A. V. Vasilakos, and L. Hanzo, "Full duplex techniques for 5g networks: self-interference cancellation, protocol design, and relay selection," *IEEE Communications Magazine*, vol. 53, no. 5, pp. 128–137, May 2015.

université PARIS-SACLAY
ÉCOLE DOCTORALE
Sciences et technologies de l'information et de la communication (STIC)

**Titre :** Communications sans fil coopératives en présence de voies de retour à débit limité

**Mots clés :** Ordonnancement centralisé, sélection de nœud, adaptation de lien lente, correction itérative du débit, réseaux sans-fil multi-source multi-relais, efficacité spectrale, chase combining, redondance incrémentale, HARQ, code turbo.

**Résumé :** Dans cette thèse, les techniques de coopération ont été étudiées pour un canal multi-accès multi-relais composé d'au moins deux sources qui communiquent avec une seule destination à l'aide d'au moins deux nœuds de relayage en mode semi-duplex. Le multiplexage par répartition dans le temps est supposé. Tout d'abord, l'algorithme d'adaptation de lien est exécuté par l'ordonnanceur centralisé. Durant la première phase de transmission, les sources transmettent chacune à leur tour leur message respectif pendant des intervalles de temps consécutifs. Dans chaque intervalle de temps dans la deuxième phase, la destination planifie un nœud pour transmettre les redondances, mettant en œuvre un protocole coopératif d'Hybrid Automatic Repeat reQuest (HARQ), où les canaux de contrôle limités bidirectionnels sont disponibles depuis les sources et les relais vers la destination. Dans la première partie de la thèse, les stratégies de sélection des nœuds centralisé sont proposées pour la deuxième phase de transmission. Les décisions d'ordonnancement sont prises en fonction de la connaissance des ensembles de sources correctement décodées par chaque noeud et ayant comme objectif de maximiser l'efficacité spectrale moyenne. L'analyse de la probabilité de coupure de l'information ainsi que les simulations Monte-Carlo (MC) sont effectués afin de valider ces stratégies. Dans la seconde partie, un algorithme d'adaptation de lien lent est proposé afin de maximiser l'efficacité spectrale moyenne sous contrainte de vérification d'une qualité de service individuelle cible pour une famille donnée de schémas de modulation et de codage, réposant sur l'information sur la distribution des canaux signalée. Les débits des sources discrets sont déterminés en utilisant l'approche "Genie-Aided" suivie d'un algorithme itératif de correction de débit. Les simulations MC montrent que l'algorithme d'adaptation de lien proposé offre des performances proches de celles de la recherche exhaustive. Dans la troisième partie, les performances de protocole HARQ à redondance incrémentale (IR) avec codage mono et multi-utilisateur, ainsi que l'HARQ de type Chase Combining avec codage mono-utilisateur sont comparées. Les simulations MC montrent que l'IR-HARQ avec codage mono-utilisateur offre le meilleur compromis entre performance et complexité pour le scénario de petit nombre de sources. Un schéma de codage pratique est proposé et validé à l'aide de simulations MC.

**Title :** Cooperative wireless communications in the presence of limited feedback

**Keywords :** Centralized scheduling, node selection, slow-link adaptation, iterative rate correction, Multi-Source Multi-Relay Wireless Network, spectral efficiency, chase combining, incremental redundancy, HARQ, turbo code.

**Abstract :** In this thesis, cooperation techniques have been studied for Multiple Access Multiple Relay Channel, consisted of at least two sources which communicate with a single destination with the help of at least two half-duplex relaying nodes. Time Division Multiplexing is assumed. First, the link adaptation algorithm is performed at the centralised scheduler. Sources transmit in turns in consecutive time slots during the first transmission phase. In each time slot of the second phase, the destination schedules a node to transmit redundancies, implementing a cooperative Hybrid Automatic Repeat reQuest (HARQ) protocol, where bidirectional limited control channels are available from sources and relays towards the destination. In the first part of the thesis, centralized node selection strategies are proposed for the second phase. The scheduling decisions are made based on the knowledge of the correctly decoded source sets of each node, with the goal to maximize the average spectral efficiency. An information outage analysis is conducted and Monte-Carlo (MC) simulations are performed to evaluate their performance. In the second part, a slow-link adaptation algorithm is proposed which aims at maximizing the average spectral efficiency under individual QoS targets for a given modulation and coding scheme family relying on the reported Channel Distribution Information of all channels. Discrete source rates are first determined using the "Genie-Aided" assumption, which is followed by an iterative rate correction algorithm. The resulting link adaptation algorithm yields performance close to the exhaustive search approach as demonstrated by MC simulations. In the third part, performances of Incremental Redundancy (IR) HARQ with Single and Multi User encoding, as well as the Chase Combining HARQ with Single User encoding are compared. MC simulations demonstrate that IR-HARQ with Single User encoding offers the best trade-off between performance and complexity for a small number of sources in our setting. Practical coding scheme is proposed and validated using MC simulations.

**Université Paris-Saclay**
Espace Technologique / Immeuble Discovery
Route de l'Orme aux Merisiers RD 128 / 91190 Saint-Aubin, France